CDF/ANAL/TOP/CDFR/7536
Version 3.2
July 13, 2005

Measurement of Top Pair Production Cross Section in Lepton Plus Jets Events with `SecVtx` Tags using 318.5 pb^{-1} of $\mathrm{p\bar{p}}$ Data

Andrew Foland [1], Melissa Franklin [2], João Guimarães da Costa [3], Salvatore Rappoccio [4], Daniel Sherman [5],

Harvard University

Abstract

We present the optimization of the $\mathrm{t\bar{t}}$ cross section in the lepton plus jets channel with ≥ 1 and ≥ 2 `SecVtx` tags. We use the scalar sum of transverse energies of the event (H_T) to discriminate $\mathrm{t\bar{t}}$ from the other backgrounds. We also use the transverse mass of the leptonic W-boson (M_T^W) to further reduce the Non-W backgrounds. We use the "Method 2" technique to estimate the backgrounds, where a combination of data and Monte Carlo is used to estimate the backgrounds from electroweak processes, single top, fake leptons, fake tags, and real $W+$ Heavy Flavor production.

For the optimized measurement, we obtain a value of $\sigma_{\geq 1} = 8.7^{+0.9}_{-0.9}(stat)^{+1.2}_{-0.9}(sys)$ pb for the ≥ 1 tag cross section, and $\sigma_{\geq 2} = 8.7^{+1.8}_{-1.6}(stat)^{+1.9}_{-1.3}(sys)$ pb for the ≥ 2 tag cross section.

For the unoptimized measurement, we measure a $\mathrm{t\bar{t}}$ cross section of $\sigma_{\geq 1} = 8.9^{+1.0}_{-0.9}(stat)^{+1.2}_{-1.0}(sys)$ pb for the ≥ 1 tag cross section and $\sigma_{\geq 2} = 8.2^{+1.7}_{-1.5}(stat)^{+2.0}_{-1.5}(sys)$ pb for the ≥ 2 tag cross section.

We also present a measurement of the $\mathrm{t\bar{t}}$ cross section by fitting the N_{jet} spectrum. We combine the $= 1$ and ≥ 2 tag cross sections to obtain $\sigma_{t\bar{t}} = 8.9^{+0.9}_{-0.9}(stat)^{+1.4}_{-1.3}(syst) pb$.

[1] adf@fnal.gov
[2] franklin@fnal.gov
[3] guima@fnal.gov
[4] rappocc@fnal.gov
[5] dsherman@fnal.gov

Contents

0 Changes since Blessing **3**

1 Unoptimized Analysis **3**
1.1 Signal Estimate . . . 3
1.1.1 Pretag Acceptance × Efficiency . . . 4
1.1.2 $t\bar{t}$ Event Tagging Efficiency . . . 4
1.2 Backgrounds . . . 8
1.3 Unoptimized Results . . . 8

2 Optimization **13**
2.1 Improvement of S/B with Analysis Cuts . . . 14
2.2 Non-W Background Reduction . . . 23

3 Optimized Analysis **25**
3.1 Signal Estimate . . . 25
3.1.1 Pretag Acceptance × Efficiency . . . 25
3.1.2 $t\bar{t}$ Event Tagging Efficiency . . . 25
3.2 Background Estimate . . . 26
3.2.1 W+HF . . . 26
3.2.2 Non-W Background . . . 27
3.3 Systematic Uncertainties . . . 27
3.4 Optimized Results . . . 29
3.5 *A priori* Expectation . . . 30
3.6 Top Mass Dependence . . . 32
3.7 Comparison with Gen4 Results . . . 32

4 Improvement of Background Uncertainties with N_{jet} Spectrum Fitting **40**
4.1 Likelihood . . . 40
4.1.1 Simple Example: Only Fit W+HF . . . 40
4.1.2 Full Likelihood . . . 41

5 Conclusions **49**

A Electron Versus Muon Cross-Check **50**

B 162 pb^{-1} Cross-Check **53**

C Cross Check Using Muon χ^2 Probability Cut **53**

D Cross Check: $W \to l\nu$ Cross Section **81**

0 Changes since Blessing

We have updated our mistag estimate. Previously, we were double counting our light flavor tags from top and other backgrounds. We now correct the mistag estimate for light flavor tags counted elsewhere. Now, the mistag estimate is an estimate of the $W+$ light flavor component. To do this, we updated the equation for the double mistag calculation. We have also included a factor to correct α_{LF} to reflect the true light-flavor asymmetry. We now also use a $\sum E_T$ dependent α_{LF}.

Just correcting for $\mathrm{t\bar{t}}$ induces a change of $+0.5$ pb in the ≥ 1 optimized cross section. Improving the correction for the other backgrounds induces a further $+0.2$ pb change. We have also included a factor to correct α_{LF} to reflect the true light-flavor asymmetry. This has a negligible effect on the ≥ 1 tag cross section. Using the $\sum E_T$ dependent α_{LF} results in an additional -0.1 pb change.

There was a small change in the $W + HF$ calculation. Previously, we were taking light flavor tags from the Monte Carlo. Now, we run the mistag matrix over the light flavor jets in the Monte Carlo as in the other backgrounds.

There was also a small change in the weighting of the Non-W backgrounds. Instead of assuming the errors on R_B and F_{Non-W} are correlated, we assume they are uncorrelated because the former is a tag rate, and the latter is a fraction of events in the signal region. A statistical fluctuation in Region B will show up in F_{Non-W}, but not in R_B. In addition, we previously (incorrectly) took the weighted average of the pretag and tag methods using the errors to the first power, when it should be squared. These two modifications result in a change of $+0.1$ pb in the cross section.

We have also fixed two errors in the $\mathrm{t\bar{t}}$ pretag efficiency. The efficiency was incorrectly calculated due to a type-o, inducing a change of 1.3% on the pretag efficiency. This results in a change of $+0.1$ pb in the cross section. The event scale factor Φ_E was using the mistag matrix prediction in both the numerator and the denominator, whereas the denominator should have the light quark tagging efficiency in the Monte Carlo. This does not affect the ≥ 1 tag cross section, but does affect the ≥ 2 tag cross section.

The total change in $\sigma_{\mathrm{t\bar{t}}}$ is 0.8 pb. Table 1 shows the changes for both the ≥ 1 and ≥ 2

1 Unoptimized Analysis

1.1 Signal Estimate

We measure the top cross section using the formula

$$\sigma_{t\bar{t}} = \frac{N_{obs} - N_{bkg}}{(\epsilon_{tag} * \Phi_e)\left(\epsilon_{pretag} \int \mathcal{L}dt\right)} \tag{1}$$

where N_{obs} is the number of observed tagged events in the $W+ \geq 3$ jet sample, N_{bkg} is the number of expected background events, ϵ_{tag} is the event tag rate in $t\bar{t}$ Monte Carlo,

	≥ 1	≥ 2
0. Blessed	7.9	8.7
1. Correct $t\bar{t}$ only	8.4	8.7
2. Correct $t\bar{t}$, MC and W+HF, change ≥ 2 mistag equation	8.6	8.7
3. Change denominator of Φ_E to ϵ_p instead of M_p	8.6	8.5
4. Fix $t\bar{t}$ acceptance type-o	8.7	8.7
5. Change $W + HF$ calculation, to include mistag matrix pred.	8.7	8.7
6. Fix Non-W error weighting and correlations	8.8	8.7
7. Use $\sum E_T$ dependent α_{LF}	8.7	8.7
Total Change	+0.9 -0.1	+0.3 -0.2

Table 1: Sequential changes since blessing for the optimized cross section results.

Φ_e is an "effective event scale factor" described in Section 1.1.2, ϵ_{pretag} is the pretag efficiency for $t\bar{t}$, and $\int \mathcal{L}dt$ is the integrated luminosity.

1.1.1 Pretag Acceptance × Efficiency

The pretag efficiency was estimated using the `ttopel` PYTHIA $t\bar{t}$ sample with $m_{top} = 178\ GeV/c^2$. Table 3 shows the acceptance times efficiencies for each lepton trigger type.

The lepton ID scale factors and trigger efficiencies, along with common systematics not evaluated in this note, are given in Table 2. The pretag acceptance times efficiency is given in Table 3.

We obtain a luminosity weighted pretag efficiency of

$$\epsilon^{t\bar{t}}_{pretag} \int \mathcal{L}dt = 23.6 \pm 2.1 \quad (2)$$

1.1.2 $t\bar{t}$ Event Tagging Efficiency

Recall from [1] the equation for tag rates derived from the binomial expression for tagging N jets, given inputs from the b and c quark tagging efficiencies, and the mistag rate. The full expression for the combinatoric combination of tagging exactly N_{jet} jets

	Lepton ID and Trigger Quantities		
	CEM	CMUP	CMX
Lepton ID Eff SF	0.996 ± 0.005	0.874 ± 0.009	0.989 ± 0.006
Trigger Eff	0.962 ± 0.006	0.908 ± 0.005	0.965 ± 0.004
Total	0.959 ± 0.015	0.794 ± 0.015	0.954 ± 0.016
Luminosity (pb^{-1})	318.5 ± 19.1	318.5 ± 19.1	305.2 ± 18.3
z_0 Eff		0.951 ± 0.003	
Lepton Isolation Modelling		1.000 ± 0.050	

Table 2: Lepton ID scale factors and trigger efficiencies, plus z_0 efficiency and lepton isolation modelling systematic (to account for the extrapolation from isolated Z-samples to samples with jets).

$t\bar{t}$ Pretag Efficiency in ≥ 3 jets (ϵ_{pretag}) (%)					
Jet Multiplicity	1 jet	2 jets	3 jets	4 jets	≥ 5 jets
CEM (No SF)	0.21 ± 0.00	1.10 ± 0.01	2.14 ± 0.01	1.94 ± 0.01	0.60 ± 0.01
				4.68 ± 0.02	
CEM Acc * SF				4.27 ± 0.29	
CMUP (No SF)	0.13 ± 0.00	0.71 ± 0.01	1.39 ± 0.01	1.22 ± 0.01	0.37 0.01
				2.98 ± 0.02	
CMUP Acc * SF				2.25 ± 0.15	
CMX (No SF)	0.04 ± 0.00	0.24 ± 0.00	0.47 ± 0.01	0.41 ± 0.01	0.13 ± 0.00
				1.00 ± 0.01	
CMX Acc * SF				0.91 ± 0.06	
$t\bar{t}$ Luminosity Weighted Denominator in ≥ 3 jets ($\epsilon_{pretag} \int \mathcal{L}dt$) (%)					
Total				23.6 ± 2.1 pb^{-1}	

Table 3: $t\bar{t}$ pretag efficiencies for the different trigger types. Lepton ID scale factors have been applied where indicated. Numbers are given in percentage. Also shown is the luminosity weighted pretag denominator.

N_{tag} times is

$$\begin{aligned}
\epsilon_{ev} = \sum_{n_b=0}^{N_{jet}} \sum_{n_c=0}^{N_{jet}} \sum_{n_p=0}^{N_{jet}} \Big\{ F_{n_b n_c n_p} \times \sum_{n_b^+=0}^{n_b} \sum_{n_c^+=0}^{n_c} \sum_{n_c^+=0}^{n_c} & \Big[\binom{n_b}{n_b^+} & (\epsilon_b SF_b)^{n_b^+} (1-\epsilon_b SF_b)^{(n_b-n_b^+)} \\
\times & \binom{n_c}{n_c^+} & (\epsilon_c SF_c)^{n_c^+} (1-\epsilon_c SF_c)^{(n_c-n_c^+)} \\
\times & \binom{n_p}{n_p^+} & (M_p SF_p)^{n_p^+} (1-M_p SF_p)^{(n_p-n_p^+)} \Big] \Big\} \qquad (3)
\end{aligned}$$

$$n_b + n_c + n_p = N_{jet} \tag{4}$$

$$n_b^+ + n_c^+ + n_p^+ = N_{tag} \tag{5}$$

$$\tbinom{r}{k} = \frac{r!}{(r-k)!k!} \tag{6}$$

where F_{bcp} is the fraction of events with b b-jet, c c-jets, and p p-jets, ϵ_b and ϵ_c are the Monte Carlo efficiencies for jets matched to B- and C-hadrons at HEPG level, M_p is the per-jet prediction of the mistag matrix applied to light quark jets in $t\bar{t}$ Monte Carlo, SF_b and SF_c are the scale factors for b and c-jets, and SF_p is the ratio of predicted tag rates in data and Monte Carlo in JET50 events, multiplied by the light flavor asymmetry (1.37 ± 0.23) as described in Ref [2].

The event tagging efficiency for $\mathrm{t\bar{t}}$ is done as is described in Ref [1]. That is, we multiply the efficiency in the Monte Carlo by the *event scale factor*

$$\Phi_E = \frac{\epsilon_{ev}(\epsilon_b SF_b, \epsilon_c SF_c, M_p SF_p)}{\epsilon_{ev}(\epsilon_b, \epsilon_c, \epsilon_p)} \tag{7}$$

where ϵ_{ev} is given in Equation 3. Thus, we obtain

$$\epsilon_{DATA} = \epsilon_{MC} \times \Phi_E \tag{8}$$

The heavy quark tagging efficiencies in $\mathrm{t\bar{t}}$ are flat as a function of the number of jets. However, due to the different $\sum E_T$ in the different jet bins, the mistag matrix will predict a non-constant rate for the per-jet mistag rate in each jet bin, so the inputs to Equation 3 reflect that accordingly. The inputs we use are shown in Table 4. The calculation details are shown in Table 5, and the results are shown in Table 7.

Quantity	1-jet	2-jet	3-jet	4-jet	$\geq$ 5-jet	SF
ε_b	0.450	0.450	0.450	0.450	0.450	0.909 ± 0.060
ε_c	0.098	0.098	0.098	0.098	0.098	0.909 ± 0.120
M_p	0.004	0.005	0.006	0.006	0.007	$(0.88 \pm 0.26)\times(1.37 \pm 0.23)$

Table 4: The inputs to the event efficiency calculation.

Njet = 1						
N_b	N_c	N_p	F_{bcp}	1-tag	2-tag	3-tag
0	0	1	0.1512	0.0003 ± 0.0001		
0	1	0	0.0322	0.0031 ± 0.0000		
1	0	0	0.8166	0.3648 ± 0.0008		
Total				0.3683 ± 0.0010		
Njet = 2						
N_b	N_c	N_p	F_{bcp}	1-tag	2-tag	3-tag
0	0	2	0.0320	0.0002 ± 0.0000	0.0000 ± 0.0000	
0	1	1	0.0213	0.0021 ± 0.0000	0.0000 ± 0.0000	
0	2	0	0.0008	0.0001 ± 0.0000	0.0000 ± 0.0000	
1	0	1	0.3608	0.1613 ± 0.0004	0.0004 ± 0.0000	
1	1	0	0.0910	0.0416 ± 0.0002	0.0040 ± 0.0001	
2	0	0	0.4941	0.2442 ± 0.0001	0.0986 ± 0.0005	
Total				0.4495 ± 0.0006	0.1030 ± 0.0005	
Njet = 3						
N_b	N_c	N_p	F_{bcp}	1-tag	2-tag	3-tag
0	0	3	0.0081	0.0001 ± 0.0000	0.0000 ± 0.0000	0.0000 ± 0.0000
0	1	2	0.0077	0.0008 ± 0.0000	0.0000 ± 0.0000	0.0000 ± 0.0000
0	2	1	0.0006	0.0001 ± 0.0000	0.0000 ± 0.0000	0.0000 ± 0.0000
0	3	0	0.0000	0.0000 ± 0.0000	0.0000 ± 0.0000	0.0000 ± 0.0000
1	0	2	0.1896	0.0848 ± 0.0002	0.0005 ± 0.0000	0.0000 ± 0.0000
1	1	1	0.1350	0.0617 ± 0.0003	0.0060 ± 0.0001	0.0000 ± 0.0000
1	2	0	0.0022	0.0010 ± 0.0000	0.0002 ± 0.0000	0.0000 ± 0.0000
2	0	1	0.5181	0.2558 ± 0.0001	0.1038 ± 0.0005	0.0003 ± 0.0000
2	1	0	0.1369	0.0652 ± 0.0002	0.0312 ± 0.0002	0.0027 ± 0.0000
3	0	0	0.0019	0.0008 ± 0.0000	0.0006 ± 0.0000	0.0002 ± 0.0000
Total				0.4702 ± 0.0005	0.1424 ± 0.0007	0.0032 ± 0.0000
Njet = 4						
N_b	N_c	N_p	F_{bcp}	1-tag	2-tag	3-tag
0	0	4	0.0024	0.0000 ± 0.0000	0.0000 ± 0.0000	0.0000 ± 0.0000
0	1	3	0.0025	0.0003 ± 0.0000	0.0000 ± 0.0000	0.0000 ± 0.0000
0	2	2	0.0002	0.0000 ± 0.0000	0.0000 ± 0.0000	0.0000 ± 0.0000
0	3	1	0.0000	0.0000 ± 0.0000	0.0000 ± 0.0000	0.0000 ± 0.0000
0	4	0	0.0000	0.0000 ± 0.0000	0.0000 ± 0.0000	0.0000 ± 0.0000
1	0	3	0.0719	0.0322 ± 0.0001	0.0003 ± 0.0000	0.0000 ± 0.0000
1	1	2	0.0644	0.0295 ± 0.0001	0.0030 ± 0.0000	0.0000 ± 0.0000
1	2	1	0.0046	0.0021 ± 0.0000	0.0004 ± 0.0000	0.0000 ± 0.0000
1	3	0	0.0002	0.0001 ± 0.0000	0.0000 ± 0.0000	0.0000 ± 0.0000
2	0	2	0.4839	0.2386 ± 0.0001	0.0974 ± 0.0005	0.0006 ± 0.0000
2	1	1	0.3608	0.1715 ± 0.0004	0.0826 ± 0.0006	0.0072 ± 0.0001
2	2	0	0.0036	0.0016 ± 0.0000	0.0009 ± 0.0000	0.0001 ± 0.0000
3	0	1	0.0039	0.0016 ± 0.0000	0.0013 ± 0.0000	0.0003 ± 0.0000
3	1	0	0.0012	0.0005 ± 0.0000	0.0004 ± 0.0000	0.0001 ± 0.0000
4	0	0	0.0002	0.0001 ± 0.0000	0.0001 ± 0.0000	0.0000 ± 0.0000
Total				0.4782 ± 0.0003	0.1864 ± 0.0008	0.0085 ± 0.0001
Njet = 5						
Total				0.3833 ± 0.0003	0.1584 ± 0.0007	0.0097 ± 0.0001

Table 5: Calculation of event tagging efficiency for $t\bar{t}$ Monte Carlo.

$t\bar{t}$ Event Tagging Efficiency in MC (%)					
	1 jet	2 jets	3 jets	4 jets	$\geq$ 5 jets
$\epsilon_{\geq 1}$	36.81 ± 0.07	54.88 ± 0.31	61.34 ± 0.22	66.41 ± 0.22	67.00 ± 0.40
				64.15 ± 0.15	
$\epsilon_{\geq 2}$	-	11.28 ± 0.20	15.55 ± 0.16	20.75 ± 0.19	21.83 ± 0.35
				18.49 ± 0.12	

Table 6: Event tagging efficiencies in *Monte Carlo*. Calculated from Equation 3 with inputs from Table 4. See Table 5 for details on the calculation. Note: Scale factor *has not* been applied.

$t\bar{t}$ Event Tagging Efficiency in Data (%)					
	1 jet	2 jets	3 jets	4 jets	$\geq$ 5 jets
$\epsilon_{\geq 1} * \Phi_e$ (%)	33.51 ± 2.34	50.85 ± 2.88	57.19 ± 3.09	62.27 ± 3.17	63.07 ± 3.22
				60.06 ± 3.13	
$\epsilon_{\geq 2} * \Phi_e$(%)	0.00 ± 0.00	9.38 ± 1.30	13.12 ± 1.80	17.66 ± 2.38	18.85 ± 2.52
				15.73 ± 2.13	
$t\bar{t}$ Event Φ_E Factors (%)					
$\Phi_e^{\geq 1}$(%)	91.04 ± 6.13	92.65 ± 5.23	93.23 ± 5.03	93.76 ± 4.77	94.13 ± 4.78
				93.62 ± 4.87	
$\Phi_e^{\geq 2}$(%)	0.00 ± 0.00	83.20 ± 11.40	84.35 ± 11.56	85.13 ± 11.44	86.36 ± 11.45
				85.10 ± 11.48	

Table 7: Event tagging efficiencies in *data*. Calculated from Equation 3 with inputs from Table 4. See Table 5 for details on the calculation. Note: Scale factor *has* been applied. The values for Φ_E are also shown.

1.2 Backgrounds

The background calculation for the unoptimized results is given in Ref [1], as backup material for Ref [3].

1.3 Unoptimized Results

The luminosity weighted pretag efficiency in ≥ 3 jets is

$$\epsilon^{t\bar{t}}_{pretag} \int \mathcal{L} dt = 23.6 \pm 2.1 \; pb^{-1} \tag{9}$$

The tag rate in ≥ 3 jets is

$$\epsilon^{t\bar{t}}_{\geq 1 \; tag} = 60.06 \pm 3.13\% \tag{10}$$
$$\epsilon^{t\bar{t}}_{\geq 2 \; tag} = 15.73 \pm 2.13\% \tag{11}$$

To obtain the cross section, we start the analysis assuming $\sigma = 6.1$ pb. We then iterate until the results are stable to $< 1\%$. The number of observed events is 171 for the single tags and 36 for the double tags. After iteration, the number of background events is

$$N_{bkg}^{\geq 1\ tag} = 51.70 \pm 9.11 \quad (12)$$
$$N_{bkg}^{\geq 2\ tag} = 5.61 \pm 3.98 \quad (13)$$

This gives unoptimized cross sections of

$$\sigma_{\geq 1} = 8.9 \pm 0.9(stat) \pm 1.1(sys)\ pb \quad (14)$$
$$\sigma_{\geq 2} = 8.2 \pm 1.6(stat) \pm 1.7(sys)\ pb \quad (15)$$

The asymmetric errors of these cross sections are

$$\sigma_{\geq 1} = 8.9^{+1.0}_{-0.9}(stat)^{+1.2}_{-1.0}(sys)\ pb \quad (16)$$
$$\sigma_{\geq 2} = 8.2^{+1.7}_{-1.5}(stat)^{+2.0}_{-1.5}(sys)\ pb \quad (17)$$

Figures 3 and 4 show the likelihood curves with statistical error bands.

Summary					
Jet Multiplicity	1 jet	2 jets	3 jets	4 jets	$\geq$ 5 jets
Pretags					
Data	30628	4791	769	179	36
$t\bar{t}$ (8.9 pb)	9.20 $\pm$ 0.82	49.55 $\pm$ 4.40	96.66 $\pm$ 8.58	86.37 $\pm$ 7.67	26.63 $\pm$ 2.38
$\geq$ 1 Tags					
EW	4.47 $\pm$ 0.69	8.47 $\pm$ 1.25	2.10 $\pm$ 0.34	0.39 $\pm$ 0.08	0.10 $\pm$ 0.03
Single Top	6.86 $\pm$ 1.71	11.55 $\pm$ 2.42	2.50 $\pm$ 0.53	0.41 $\pm$ 0.09	0.06 $\pm$ 0.01
Non-W	42.25 $\pm$ 10.05	19.34 $\pm$ 4.77	6.70 $\pm$ 1.92	3.07 $\pm$ 1.06	0.61 $\pm$ 0.39
W + LF Mistags	94.05 $\pm$ 19.28	39.12 $\pm$ 7.86	11.05 $\pm$ 2.24	2.27 $\pm$ 0.45	0.22 $\pm$ 0.05
$W + c$	99.23 $\pm$ 26.61	21.06 $\pm$ 6.03	3.22 $\pm$ 0.98	0.51 $\pm$ 0.23	0.02 $\pm$ 0.02
$W + c\bar{c}$	33.52 $\pm$ 10.17	20.13 $\pm$ 6.60	4.88 $\pm$ 1.70	0.81 $\pm$ 0.40	0.02 $\pm$ 0.02
$W + b\bar{b}$	98.74 $\pm$ 32.37	55.13 $\pm$ 17.85	10.94 $\pm$ 3.44	1.70 $\pm$ 0.79	0.12 $\pm$ 0.12
$t\bar{t}$ (8.9 pb)	3.08 $\pm$ 0.35	25.19 $\pm$ 2.66	55.28 $\pm$ 5.74	53.78 $\pm$ 5.50	16.80 $\pm$ 1.73
Bkg	379.12 $\pm$ 72.53	174.80 $\pm$ 32.04	41.39 $\pm$ 6.84	9.16 $\pm$ 1.83	1.15 $\pm$ 0.43
Bkg + $t\bar{t}$ (8.9 pb)	382.20 $\pm$ 72.53	199.99 $\pm$ 32.15	96.67 $\pm$ 8.93	62.94 $\pm$ 5.80	17.95 $\pm$ 1.78
Data	432	242	95	63	19
$\geq$ 2 Tags					
EW	-	0.42 $\pm$ 0.09	0.14 $\pm$ 0.04	0.02 $\pm$ 0.01	0.01 $\pm$ 0.01
Single Top	-	1.52 $\pm$ 0.29	0.53 $\pm$ 0.13	0.09 $\pm$ 0.03	0.02 $\pm$ 0.01
Non-W	-	0.29 $\pm$ 0.17	0.90 $\pm$ 0.50	0.78 $\pm$ 0.49	0.34 $\pm$ 2.64
W + LF Mistags	-	0.55 $\pm$ 0.12	0.30 $\pm$ 0.06	0.20 $\pm$ 0.04	0.08 $\pm$ 0.05
$W + HF$	-	8.39 $\pm$ 2.93	1.84 $\pm$ 0.62	0.34 $\pm$ 0.16	0.03 $\pm$ 0.02
$t\bar{t}$ (8.2 pb)	-	4.28 $\pm$ 0.70	11.68 $\pm$ 1.91	14.06 $\pm$ 2.27	4.63 $\pm$ 0.74
Bkg	-	11.17 $\pm$ 2.96	3.71 $\pm$ 0.82	1.42 $\pm$ 0.52	0.48 $\pm$ 2.64
Bkg + $t\bar{t}$ (8.2 pb)	-	15.46 $\pm$ 3.04	15.39 $\pm$ 2.08	15.48 $\pm$ 2.33	5.11 $\pm$ 2.74
Data	-	15	17	16	3

Table 8: Method 2 background calculation summary for 318.5 pb^{-1} for the *unoptimized* analysis. Here the $t\bar{t}$ prediction is show for the measured cross sections of 8.9 pb and 8.2 pb for ≥ 1 and ≥ 2 tags, respectively.

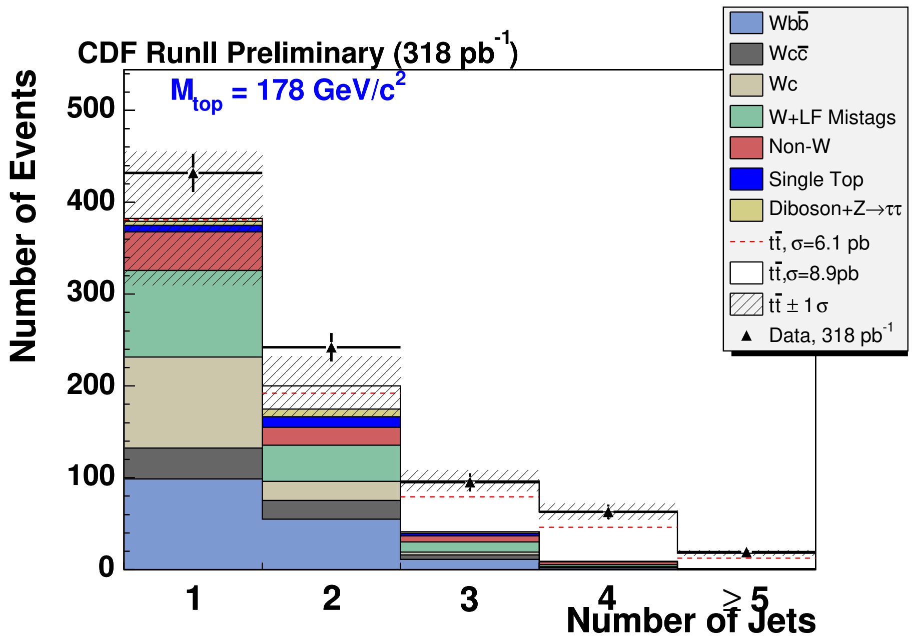

Figure 1: Number of jets for *unoptimized* ≥ 1 tags. $t\bar{t}$ cross section is shown at the *unoptimized* measured value of 8.9 pb in the solid white histogram.

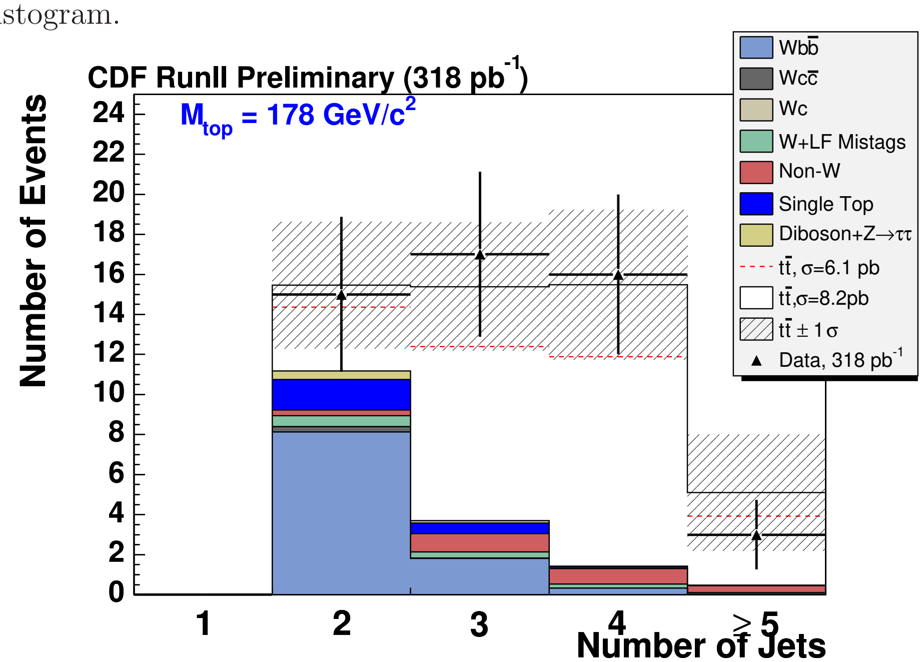

Figure 2: Number of jets for *unoptimized* ≥ 2 tags. $t\bar{t}$ cross section is shown at the *unoptimized* measured value of 8.2 pb in the solid white histogram.

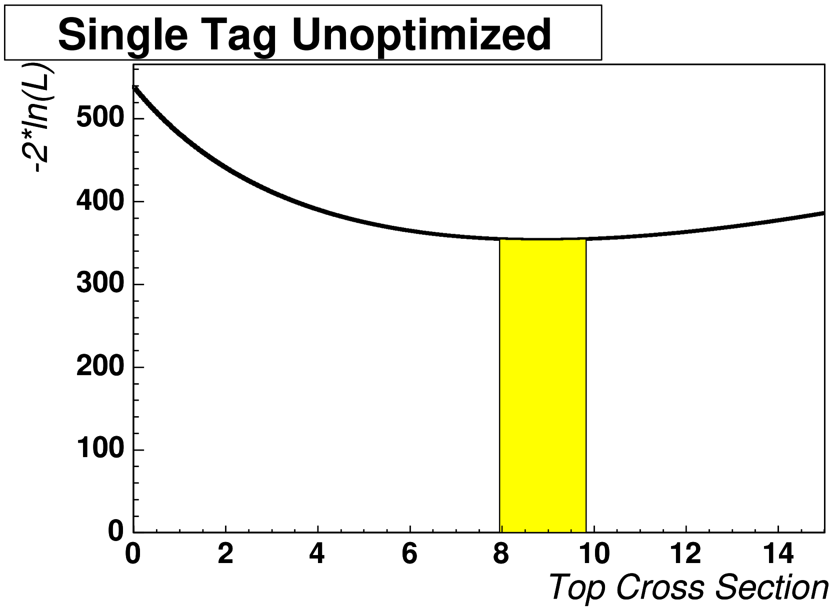

Figure 3: Likelihood curve for *unoptimized* ≥ 1 measurement with statistical error band.

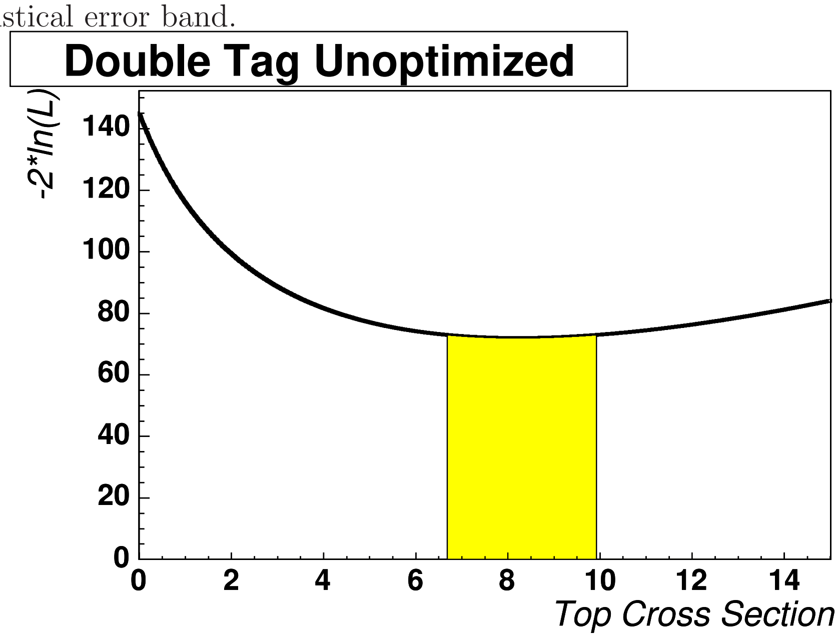

Figure 4: Likelihood curve for *unoptimized* ≥ 2 measurement with statistical error band.

2 Optimization

To optimize the cross section, we wish to minimize the cross section error. To do so, we examine the cross section formula:

$$\sigma = \frac{N - B}{\epsilon \times L} \tag{18}$$

where N is the number observed, B is the background, ϵ is the event efficiency, and L is the integrated luminosity. The error on the cross section is therefore

$$\begin{aligned} \Delta\sigma^2 &= \left(\frac{\sqrt{N}}{N-B}\right)^2 + \left(\frac{\Delta B}{N-B}\right)^2 \\ &+ \left(\frac{\Delta\epsilon}{\epsilon}\right)^2 + \left(\frac{\Delta L}{L}\right)^2 \end{aligned} \tag{19}$$

Improvements in the errors on the luminosity, the luminosity error, and the efficiency error are beyond the scope of this note, and can be considered fixed for the current discussion. Improvements in the efficiency error have been studied extensively in the `5.3.3_nt` analysis (see Ref [4] for the b-tagging scale factor, [5] for the jet energy scale, and [6] for the pretag efficiency). In the present discussion, we examine the effect of changing N and B only.

To examine this, we write $N = S + B$, where S is the expected number of $t\bar{t}$ events and B is the background. Then we rewrite Equation 19 in terms of S and S/B (without the efficiency and luminosity terms):

$$\begin{aligned} \Delta\sigma^2 &= \left(\frac{\sqrt{N}}{N-B}\right)^2 + \left(\frac{\Delta B}{N-B}\right)^2 + \ldots && (20) \\ &= \left(\frac{\sqrt{S+B}}{S}\right)^2 + \left(\frac{\Delta B}{S}\right)^2 + \ldots && (21) \\ &= \left(\frac{\sqrt{S+B}}{S}\right)^2 + \left(\frac{\Delta B}{B}\right)^2 \left(\frac{B}{S}\right)^2 + \ldots && (22) \\ &= \left(\frac{1}{\sqrt{S}}\right)^2 \left(\sqrt{1+\frac{B}{S}}\right)^2 + \left(\frac{\Delta B}{B}\right)^2 \left(\frac{B}{S}\right)^2 + \ldots && (23) \end{aligned}$$

So we see the statistical term $(1/\sqrt{S})$ and the background error in Equation 23, modified by S/B. To improve the measurement, we can either increase S, increase S/B, or decrease $\Delta B/B$.

Increasing S has already been done for the `5.3.3_nt` release. The b-tagging efficiency has increased by 20% per-jet (see Ref [7]) over the `4.11.2` tagger, and of course the luminosity increased by a factor of 2. The remaining improvements are to reduce the error on the background or improve the signal to background ratio.

In order to examine the effects of this, we examine a toy model where we can increase S/B while reducing S by some amount. For illustration, we assume that if S/B is improved by 0.5, then S is decreased by 5%. Figure 5 shows the overall cross section relative error (including statistical error, error on the b-tag scale factor, the pretag efficiency, and the luminosity) versus the relative background error, for different configurations of S/B and S. The black curve is the nominal S/B, and the star on that line is the background error of the *unoptimized* analysis presented in [1].

We see that decreasing the background error by a factor of 2 has an equivalent impact as improving S/B from 1.5 to 2.5, and keeping the same relative background error, for instance.

We now explore ways to improve both S/B (Section 2.1) and $\Delta B/B$ (Section 4).

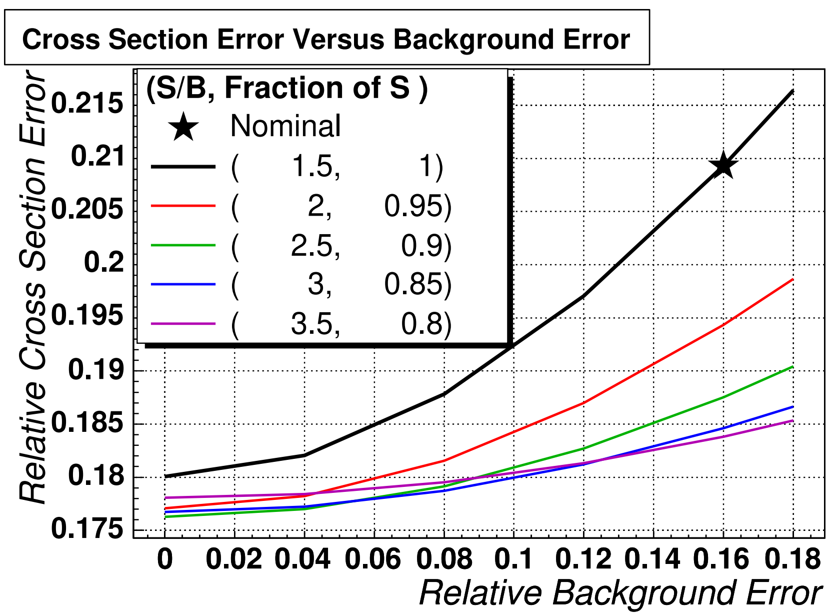

Figure 5: Cross section error as a function of the background error, for various ratios of S/B. Here, a simple model is used in that 5% of the signal is removed for every factor of 0.5 in S/B.

2.1 Improvement of S/B with Analysis Cuts

In order to find the optimal cuts for the analysis, we chose to maximize the statistical significance $\frac{S}{\sqrt{S+B}}$ (which minimizes the statistical error on the cross section). This is because simply optimizing S/B is clearly wrong because eventually we will run out of statistical power. We will assume that the background errors will remain the same throught this part of the optimization.

Several variables were examined to optimize $\frac{S}{\sqrt{S+B}}$ that were thought to have discrimination. These include

- H_T
- $\not\!\!E_T$
- M_T^W
- Jet E_T of the leading jets
- Jet η of the leading jets
- Number of good tracks in the leading jets.

The shapes of our various backgrounds in the following section is taken from the following estimates:

- **W+HF**: Taken from the $W + BB + 1p$, $W + CC + 1p$ and $W + C + 2p$ samples, using no MLM matching.
- **Mistags**: Taken from the prediction of the mistag matrix.
- **QCD**: Taken from the pretags in Region C ($\not\!\!E_T > 20\ GeV$, $iso > 0.2$).
- **EW + Single Top**: Taken from the MC, requiring ≥ 1 tag.
- **Top**: Taken from the MC, requiring ≥ 1 tag.

To examine our optimization, we take the extreme values of the theoretical range of predicted cross sections, 5 pb and 9 pb (see [8]), and show that the optimization does not depend on the cross section. Figures 6-11 show the optimization of $S/\sqrt{S+B}$ for various event variables. The top plots in this group show the optimization for $\sigma = 5$ pb, and the bottom plots show the optimization for $\sigma = 9$ pb. The red curve in each plot shows $S/\sqrt{S+B}$, with values delineated on the right hand axis. The contributions from $t\bar{t}$ are shown, as well as the contributions to several background species.

The variable with the most discrimination is the scalar sum of the transverse energies in the event, H_T. The average of the optimal points is $H_T > 200\ GeV$, which is the same value found in [9].

We have also examined the E_T and η of the leading three jets in the event. We only show plots for $\sigma = 5$ pb because the results are the same for 9 pb. So the $S/\sqrt{S+B}$ should be compared to Figure 6 with $\sigma = 5$ pb.

Figures 12-13 show E_T on the top and η on the bottom for the leading jet. Figures 14-15 show the same for the second leading jet, and 16-17 show the same for the third leading jet.

There is an optimal point if we cut on the jet E_T. However, the $S/\sqrt{S+B}$ is not as large as by cutting on H_T. Thus, we use H_T as our optimizing variable, and $H_T > 200\ GeV$ as the optimal point.

There is one other aspect of the analysis we can improve upon. If we examine the transverse mass of the W boson in Figure 10, we see that the Non-W shape is different from the others. We examine this in the following section.

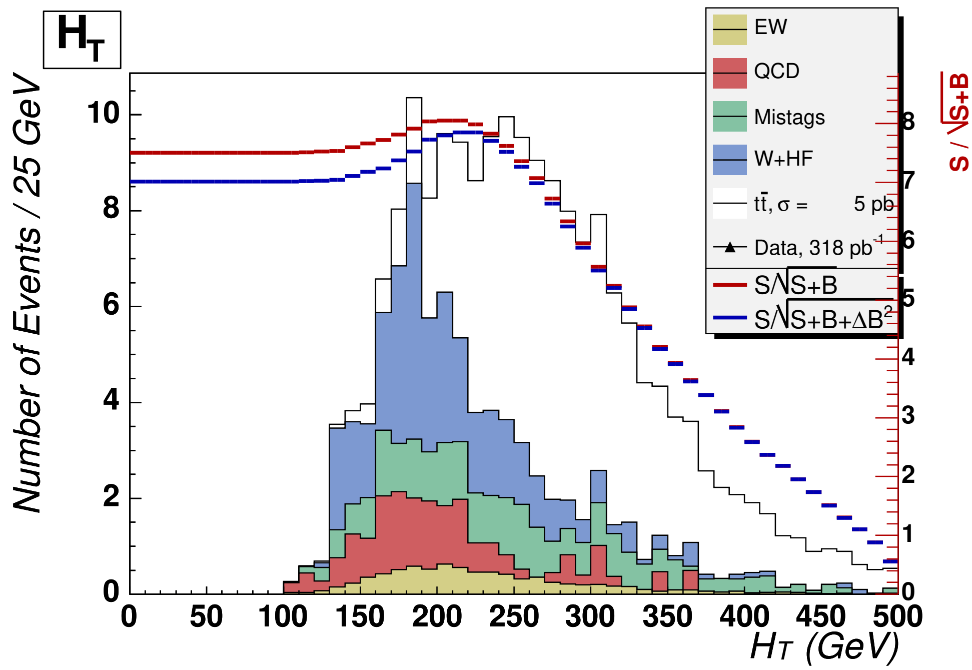

Figure 6: H_T distribution for various background contributions and the $t\bar{t}$ signal, shown at the lower limit of the theoretical calculation for the predicted cross section, 5 pb. The optimization curve of $S/\sqrt{S+B}$ is shown in red, and the axis of $S/\sqrt{S+B}$ is shown on the right.

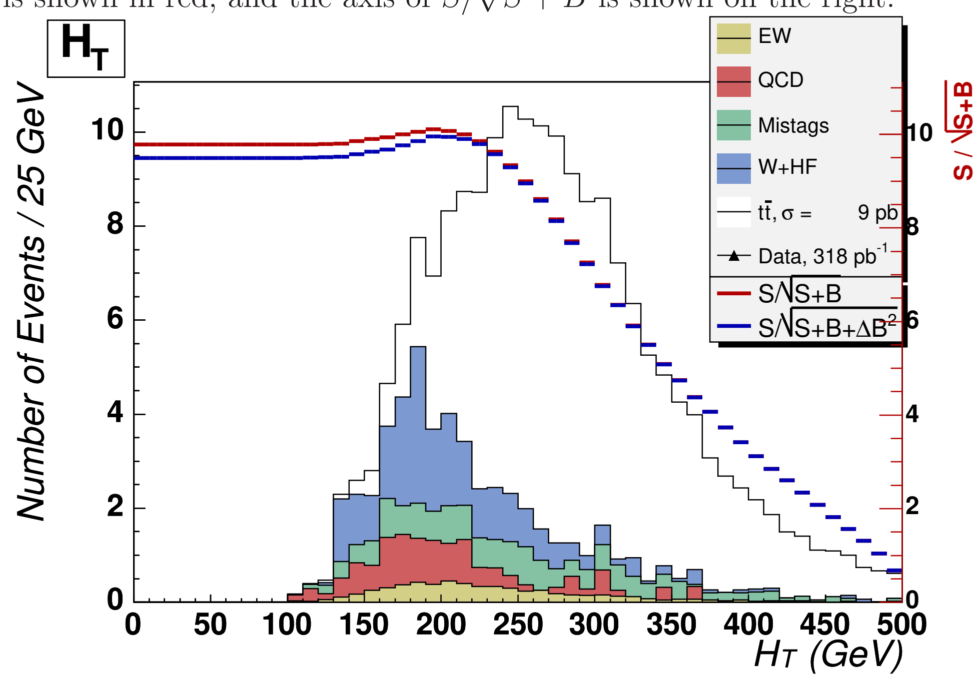

Figure 7: H_T distribution for various background contributions and the $t\bar{t}$ signal, shown at the upper limit of the theoretical calculation for the predicted cross section, 9 pb. The optimization curve of $S/\sqrt{S+B}$ is shown in red, and the axis of $S/\sqrt{S+B}$ is shown on the right.

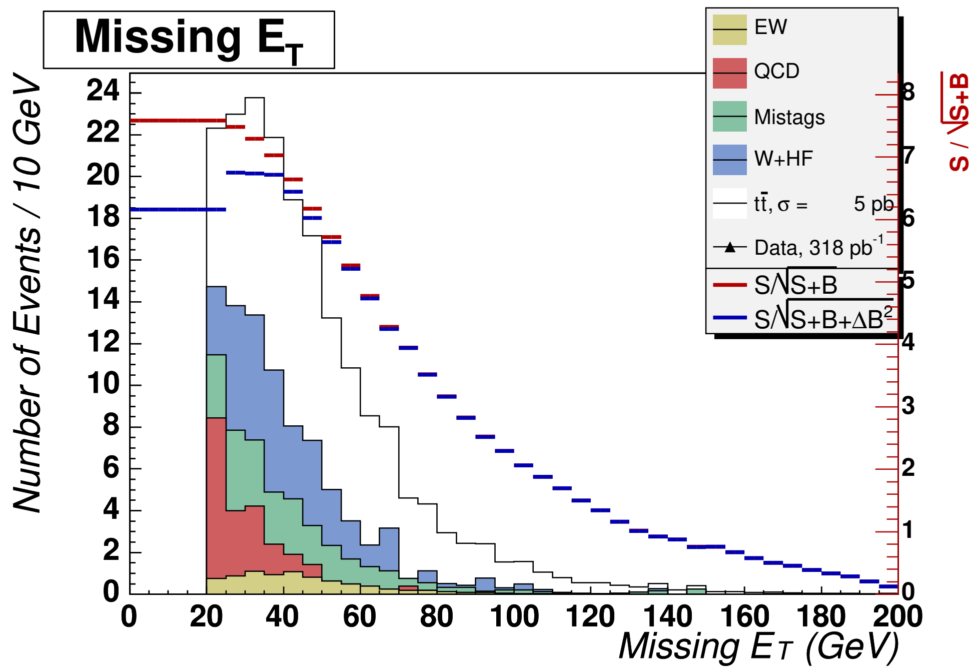

Figure 8: $\not\!\!E_T$ distribution for various background contributions and the $t\bar{t}$ signal, shown at the lower limit of the theoretical calculation for the predicted cross section, 5 pb. The optimization curve of $S/\sqrt{S+B}$ is shown in red, and the axis of $S/\sqrt{S+B}$ is shown on the right.

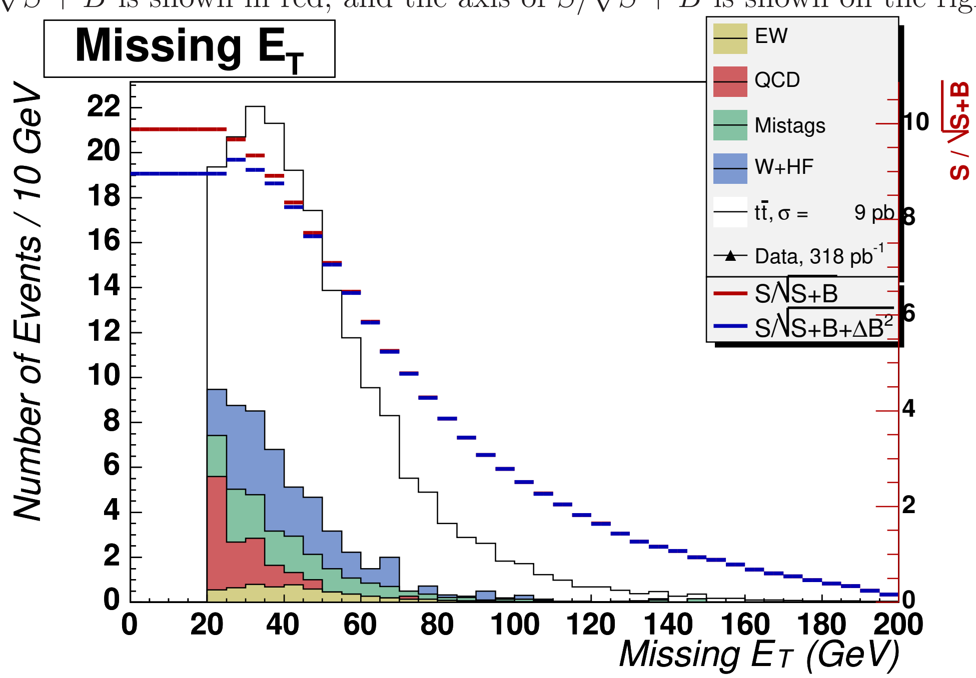

Figure 9: $\not\!\!E_T$ distribution for various background contributions and the $t\bar{t}$ signal, shown at the upper limit of the theoretical calculation for the predicted cross section, 9 pb. The optimization curve of $S/\sqrt{S+B}$ is shown in red, and the axis of $S/\sqrt{S+B}$ is shown on the right.

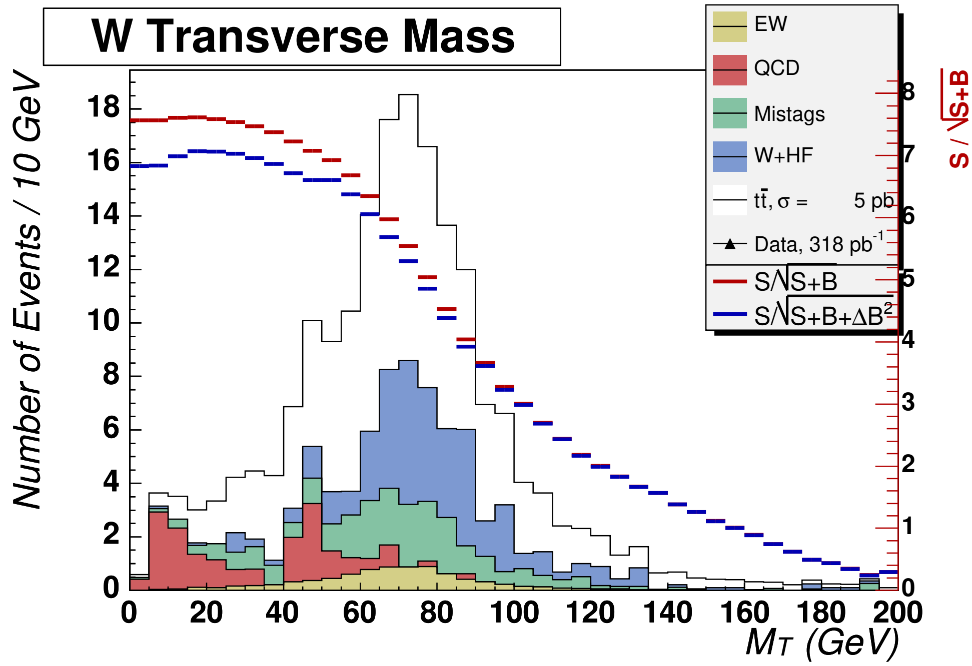

Figure 10: M_T^W distribution for various background contributions and the $t\bar{t}$ signal, shown at the lower limit of the theoretical calculation for the predicted cross section, 5 pb. The optimization curve of $S/\sqrt{S+B}$ is shown in red, and the axis of $S/\sqrt{S+B}$ is shown on the right.

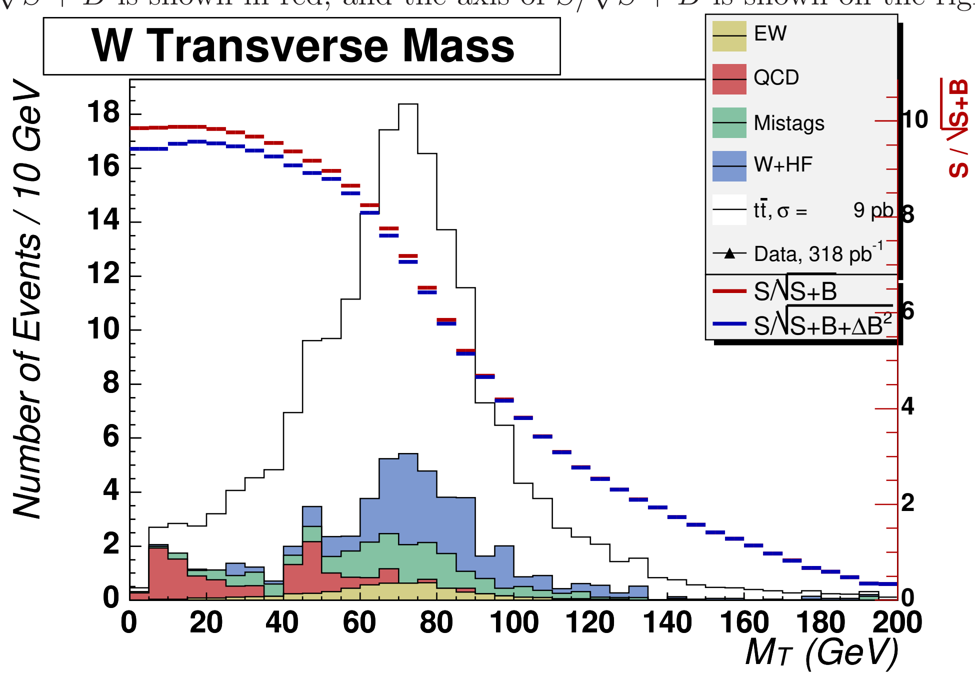

Figure 11: M_T^W distribution for various background contributions and the $t\bar{t}$ signal, shown at the upper limit of the theoretical calculation for the predicted cross section, 9 pb. The optimization curve of $S/\sqrt{S+B}$ is shown in red, and the axis of $S/\sqrt{S+B}$ is shown on the right.

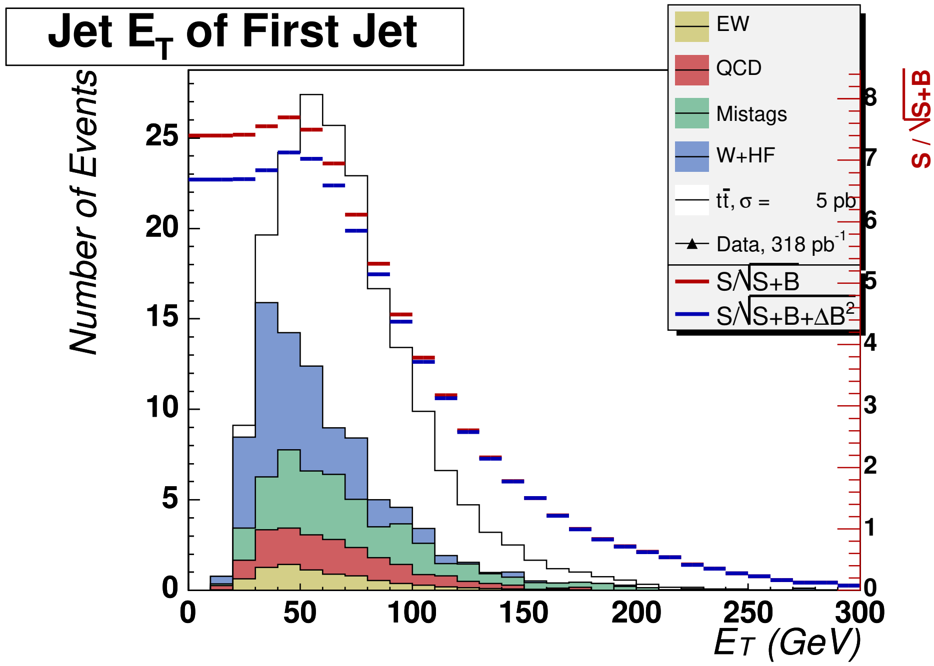

Figure 12: Leading jet E_T distribution for various background contributions and the $t\bar{t}$ signal, shown at the lower limit of the theoretical calculation for the predicted cross section, 5 pb. The optimization curve of $S/\sqrt{S+B}$ is shown in red, and the axis of $S/\sqrt{S+B}$ is shown on the right.

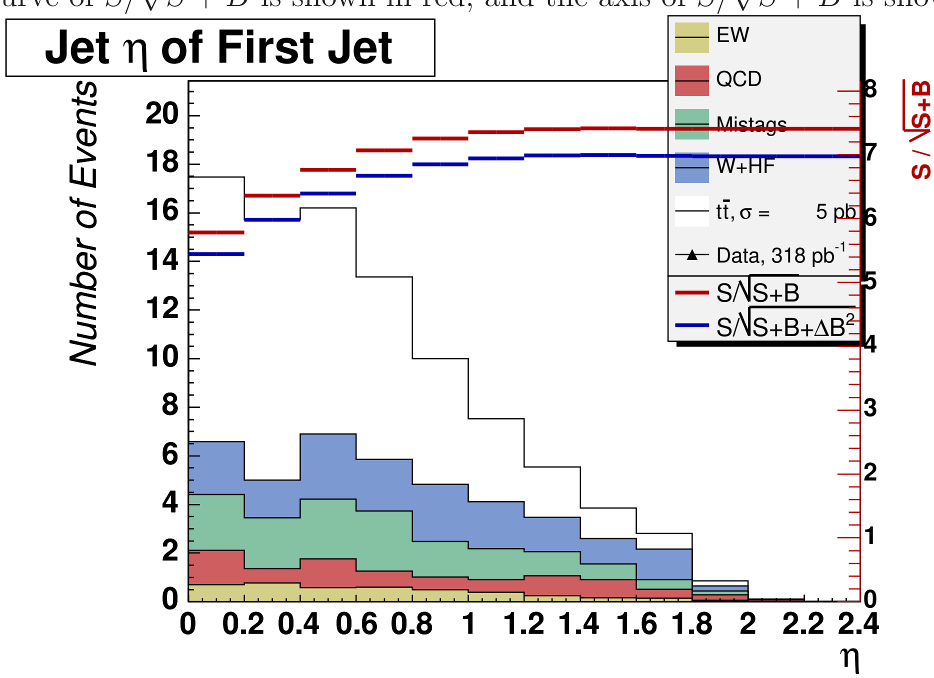

Figure 13: Leading jet η distribution for various background contributions and the $t\bar{t}$ signal, shown at the lower limit of the theoretical calculation for the predicted cross section, 5 pb. The optimization curve of $S/\sqrt{S+B}$ is shown in red, and the axis of $S/\sqrt{S+B}$ is shown on the right.

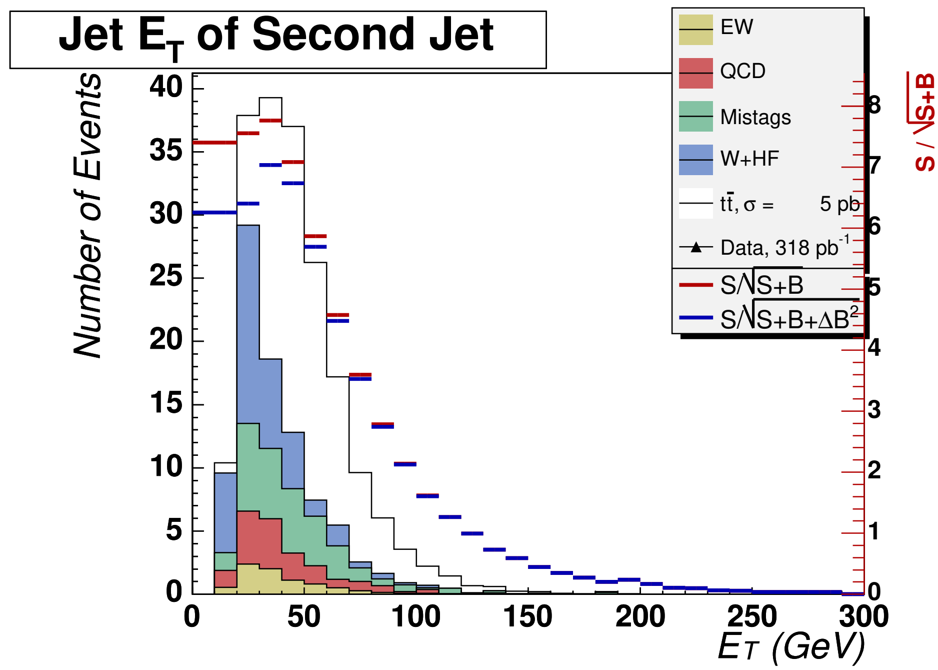

Figure 14: Second leading jet E_T distribution for various background contributions and the $t\bar{t}$ signal, shown at the lower limit of the theoretical calculation for the predicted cross section, 5 pb. The optimization curve of $S/\sqrt{S+B}$ is shown in red, and the axis of $S/\sqrt{S+B}$ is shown on the right.

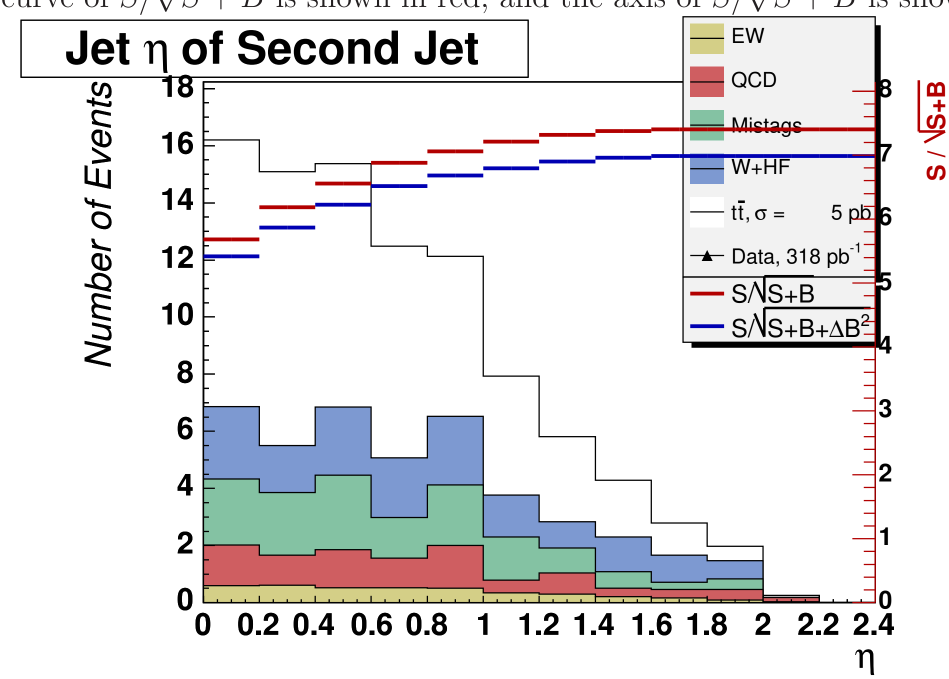

Figure 15: Second leading jet η distribution for various background contributions and the $t\bar{t}$ signal, shown at the lower limit of the theoretical calculation for the predicted cross section, 5 pb. The optimization curve of $S/\sqrt{S+B}$ is shown in red, and the axis of $S/\sqrt{S+B}$ is shown on the right.

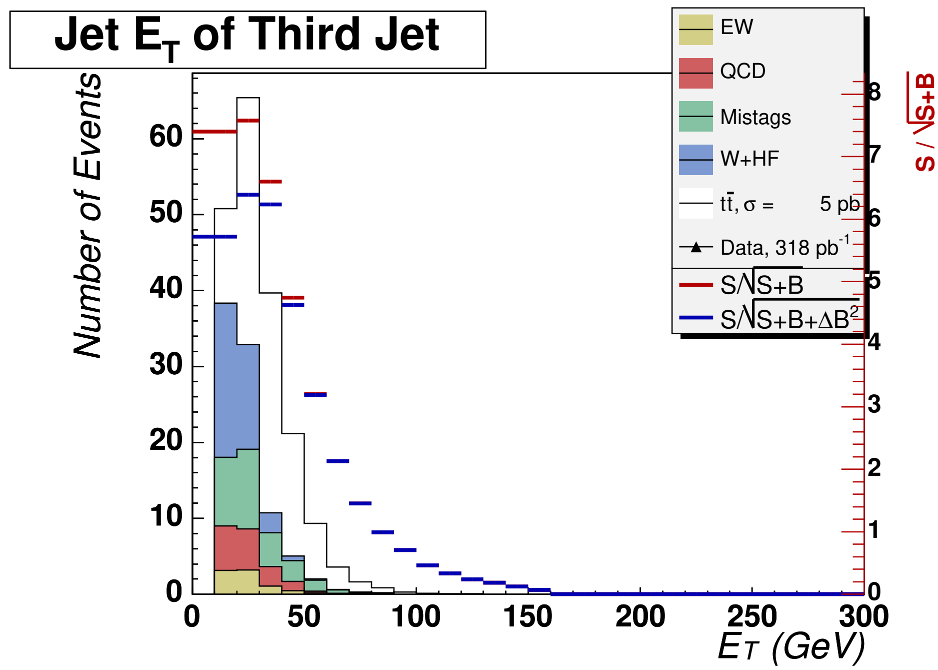

Figure 16: Third leading jet E_T distribution for various background contributions and the $t\bar{t}$ signal, shown at the lower limit of the theoretical calculation for the predicted cross section, 5 pb. The optimization curve of $S/\sqrt{S+B}$ is shown in red, and the axis of $S/\sqrt{S+B}$ is shown on the right.

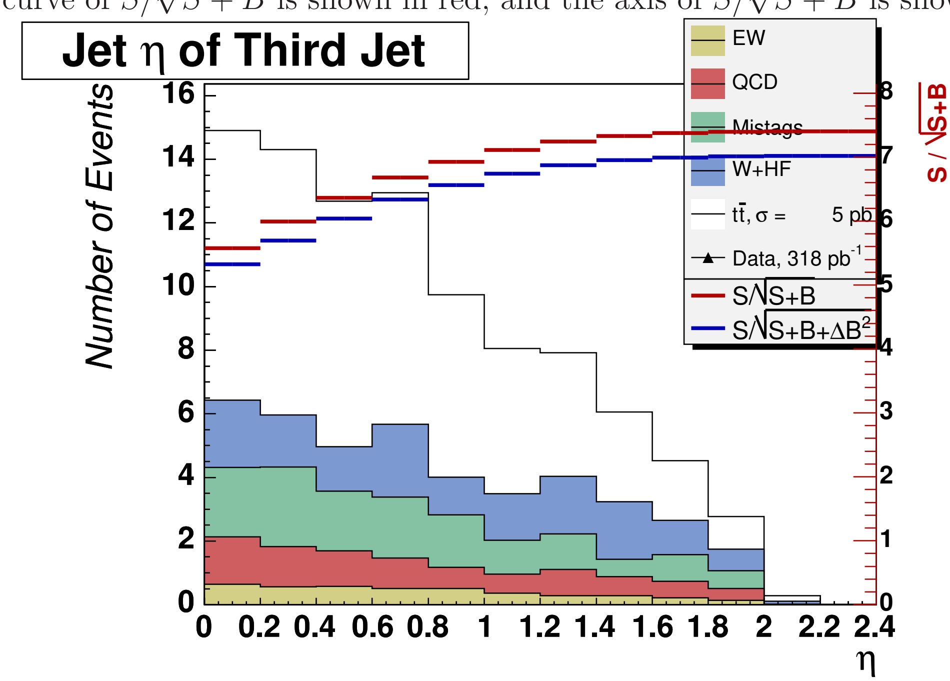

Figure 17: Third leading jet η distribution for various background contributions and the $t\bar{t}$ signal, shown at the lower limit of the theoretical calculation for the predicted cross section, 5 pb. The optimization curve of $S/\sqrt{S+B}$ is shown in red, and the axis of $S/\sqrt{S+B}$ is shown on the right.

2.2 Non-W Background Reduction

Examining the transverse mass of the W boson in Figure 10, we see that the Non-W shape is different from the others. This is expected because the Non-W background is basically QCD dijets (including $b\bar{b}$ production) and mismeasured jets. One would expect a $b\bar{b}$ event to have a low M_T^W because it contains a highly virtual W-boson, for instance.

The Non-W background is problematic because there is no good way to estimate it. There are two possibilities to deal with this background. One is to estimate it better, and the other is to eliminate it. The M_T^W distribution shows good discrimination, so we can attempt to remove it.

Examining Figures 10 and 11, it is clear that the analysis can benefit from cutting on transverse mass. The optimal point is 20 GeV/c^2.

One must also worry that the H_T and M_T^W cuts are not cutting away the same events. Figures 18 and 19 show H_T versus M_T^W for $t\bar{t}$ and the Non-W background, respectively. We can see that these two variables are not very correlated, and so we expect to gain by cutting on $M_T^W > 20\,GeV$ on top of the $H_T > 200\,GeV$ cut.

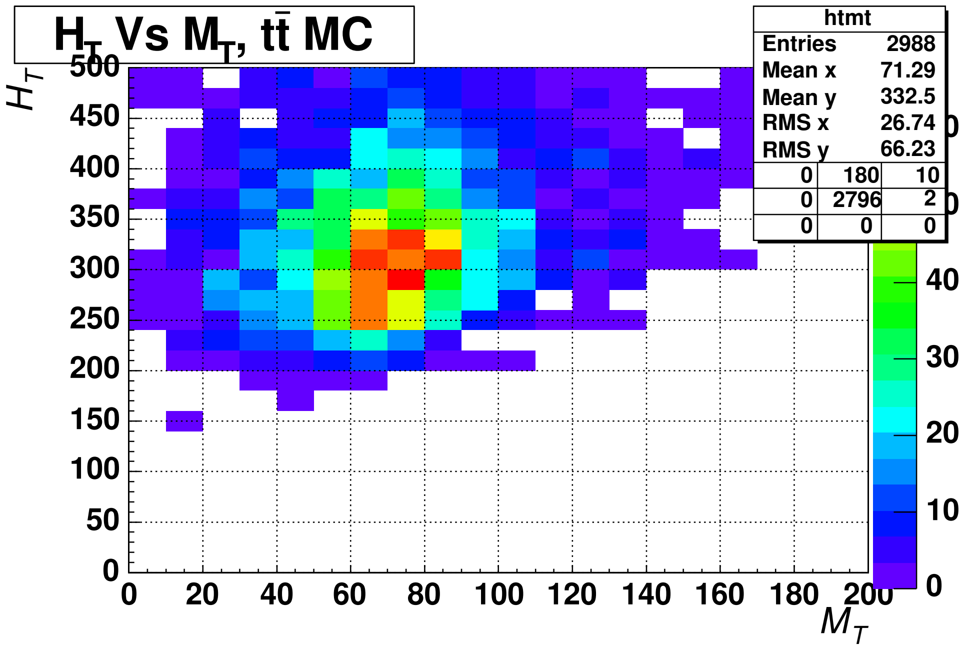

Figure 18: H_T versus M_T^W for $t\bar{t}$ Monte Carlo.

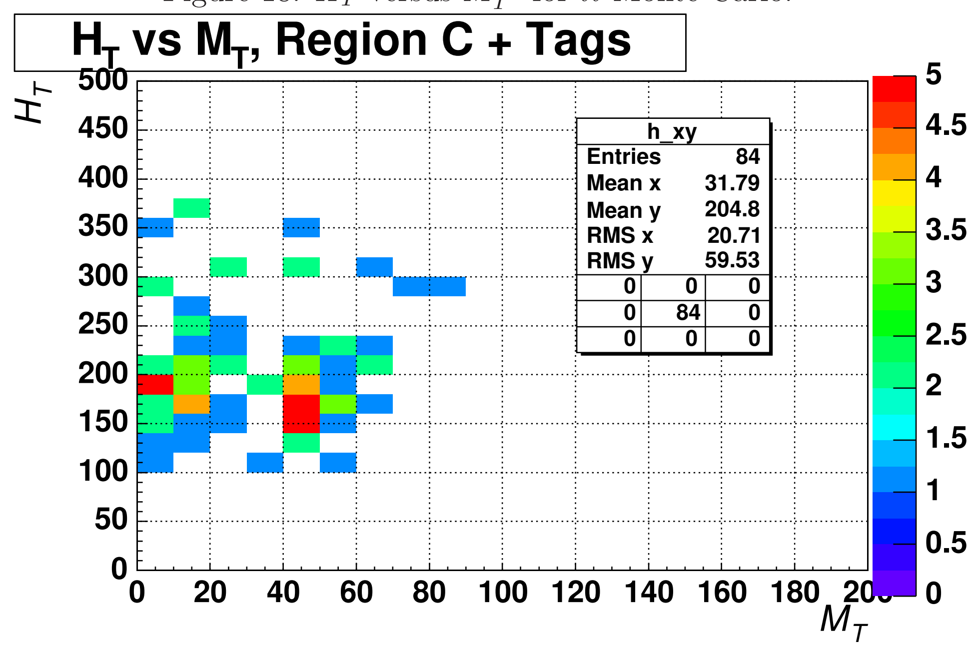

Figure 19: H_T versus M_T^W for the Non-W background, represented by the Region C positive tags.

3 Optimized Analysis

3.1 Signal Estimate

3.1.1 Pretag Acceptance × Efficiency

The H_T and M_T^W cuts will of course reduce the efficiency to have a top event in our sample. Table 9 compares the number of events before and after the cuts, and we see that there is an 8% decrease in the $t\bar{t}$ signal due to these cuts.

Tables 28-30 show the breakdown of event counts after successive cuts in the `ttopel` $t\bar{t}$ Monte Carlo.

Table 9 shows the pretag efficiency times acceptance for both the optimized an unoptimzed analyses.

$t\bar{t}$ Pretag Acceptance × Efficiency in ≥ 3 jets (ϵ_{pretag}) (%)		
	$H_T > 0$ GeV, $M_T^W > 0$ GeV/c^2	$H_T > 200$ GeV, $M_T^W > 20$ GeV/c^2
CEM Total	1106645	
CEM Pretags	51786	46353
CEM Acc	4.68 ± 0.02	4.21 ± 0.02
CEM Acc*SF	4.27 ± 0.31	3.84 ± 0.29
CMUP Total	1106645	
CMUP Pretags	32975	29126
CMUP Acc	2.98 ± 0.02	2.68 ± 0.02
CMUP Acc * SF	2.25 ± 0.15	2.02 ± 0.15
CMX Total	1106645	
CMX Pretags	11116	10077
CMX Acc	1.00 ± 0.01	0.90 ± 0.01
CMX Acc * SF	0.91 ± 0.06	0.82 ± 0.06
$t\bar{t}$ Luminosity Weighted Denominator in ≥ 3 jets ($\epsilon_{pretag} \int \mathcal{L}dt$) (%)		
Total	23.6 ± 2.1 pb^{-1}	21.2 ± 2.0 pb^{-1}

Table 9: Comparison of pretagging tagging rates before and after the $H_T > 200$ GeV and $M_T^W > 20$ GeV cuts. The H_T cut is only applied for ≥ 3 jets, but the M_T^W cut is applied everywhere. Also shown is the luminosity weighted denominator.

3.1.2 $t\bar{t}$ Event Tagging Efficiency

If we cut on the H_T of the event, we expect to introduce a shift in the tagging efficiency because we are effectively cutting harder on the jet E_T (in conjunction with the other transverse energies), and so the average tag rate will increase. The heavy flavor fractions will also change due to the H_T cut, because events with heavy flavor can be affected differently than events with no heavy flavor, and so the ratio between them can change. We examine the effect on the $t\bar{t}$ event tagging rate in Table 10. The event tagging efficiency did increase slightly as expected.

$t\bar{t}$ Event Tagging Efficiency in Data (%)						
		1 jet	2 jets	3 jets	4 jets	$\geq$ 5 jets
$H_T > 0$ GeV and $M_T^W > 0$ GeV	$\epsilon_{\geq 1} * \Phi_E^1$	33.5 ± 2.3	50.9 ± 2.9	57.2 ± 3.1	62.3 ± 3.2	63.1 ± 3.2
					60.1 ± 3.1	
	$\epsilon_{\geq 2} * \Phi_E^2$	-	9.4 ± 1.3	13.1 ± 1.8	17.7 ± 2.4	18.9 ± 2.5
					15.7 ± 2.1	
$H_T > 200$ GeV and $M_T^W > 20$ GeV	$\epsilon_{\geq 1} * \Phi_E^1$	33.4 ± 2.3	50.9 ± 2.9	58.3 ± 3.1	62.8 ± 3.2	63.2 ± 3.2
					60.9 ± 3.2	
	$\epsilon_{\geq 2} * \Phi_E^2$	-	9.4 ± 1.3	13.9 ± 1.9	18.0 ± 2.4	19.0 ± 2.5
					16.4 ± 2.2	

Table 10: Comparison of the event tagging rates before and after the $H_T > 200$ GeV and $M_T^W > 20$ GeV cuts. The H_T cut is only applied for ≥ 3 jets, but the M_T^W cut is applied everywhere.

3.2 Background Estimate

3.2.1 W+HF

The W+HF background will be affected by applying the H_T cut. Since there is a real W in this background, the effect of the M_T^W cut will be minimal. Thus, the only effect that needs to be examined is the effect due to the H_T cut. Since the H_T cut is the same as in Ref [9], we can use the same heavy flavor fractions. We reproduce them in Table 11.

Since the event efficiency can change in the same way as the $t\bar{t}$, we also examine the effects of the H_T cut on the tagging efficiencies. Table 12 shows the efficiencies before and after the optimization cuts.

W + HF Fractions (%)						
Jet Multiplicity	1 jet	2 jets	3 jets		$\geq$ 4 jets	
			$H_T > 0$	$H_T > 200$	$H_T > 0$	$H_T > 200$
$W + b\bar{b}, 1B$	1.0 ± 0.3	1.4 ± 0.4	2.0 ± 0.5	2.4 ± 0.6	2.2 ± 0.6	2.2 ± 0.6
$W + b\bar{b}, 2B$	-	1.4 ± 0.4	2.0 ± 0.5	2.3 ± 0.6	2.6 ± 0.7	2.6 ± 0.7
$W + c\bar{c}, 1C$	1.6 ± 0.4	2.4 ± 0.6	3.4 ± 0.9	3.8 ± 1.0	3.6 ± 1.0	3.5 ± 1.0
$W + c\bar{c}, 2C$	-	1.8 ± 0.5	2.7 ± 0.7	2.9 ± 0.8	3.7 ± 1.0	3.7 ± 1.0
$W + c, 1C$	4.3 ± 0.9	6.0 ± 1.3	6.3 ± 1.3	6.0 ± 1.3	6.1 ± 1.3	5.9 ± 1.3

Table 11: Heavy flavor fractions taken from Ref [10] before and after optimization cuts. These are measured using template fits derived from ALPGEN $W + Q\overline{Q} + Np$ samples applied to the lepton+jets data.

W+Heavy Flavor Tagging Efficiencies (%)				
	1 jet	2 jets	3 jets	4 jets / $\geq$ 5 jets
$H_T > 0$ GeV, $M_T^W > 0$ GeV				
WBB, 1B, 1 Tag	35.04 $\pm$ 2.35	37.93 $\pm$ 2.38	39.38 $\pm$ 4.08	42.76 $\pm$ 3.46
WBB, 2B, 1 Tag	0.00 $\pm$ 0.00	57.86 $\pm$ 3.52	59.01 $\pm$ 4.28	60.50 $\pm$ 3.92
WBB, 2B, 2 Tag	0.00 $\pm$ 0.00	14.10 $\pm$ 1.93	16.06 $\pm$ 2.42	17.45 $\pm$ 2.83
WCC, 1C, 1 Tag	7.44 $\pm$ 1.04	8.78 $\pm$ 1.37	12.57 $\pm$ 2.33	10.53 $\pm$ 4.26
WCC, 2C, 1 Tag	0.00 $\pm$ 0.00	15.48 $\pm$ 2.40	16.59 $\pm$ 3.48	23.32 $\pm$ 5.14
WCC, 2C, 2 Tag	0.00 $\pm$ 0.00	0.36 $\pm$ 0.19	0.18 $\pm$ 0.12	0.00 $\pm$ 0.00
WC, 1C, 1 Tag	8.19 $\pm$ 1.10	8.84 $\pm$ 1.23	9.53 $\pm$ 1.56	13.16 $\pm$ 2.56
$H_T > 200$ GeV, $M_T^W > 20$ GeV				
WBB, 1B, 1 Tag	34.94 $\pm$ 2.35	38.07 $\pm$ 2.34	45.77 $\pm$ 4.50	43.58 $\pm$ 3.65
WBB, 2B, 1 Tag	0.00 $\pm$ 0.00	57.90 $\pm$ 3.51	62.78 $\pm$ 4.82	62.23 $\pm$ 4.06
WBB, 2B, 2 Tag	0.00 $\pm$ 0.00	14.12 $\pm$ 1.93	18.17 $\pm$ 2.80	18.24 $\pm$ 3.02
WCC, 1C, 1 Tag	7.40 $\pm$ 1.03	8.91 $\pm$ 1.38	13.63 $\pm$ 2.79	15.22 $\pm$ 5.99
WCC, 2C, 1 Tag	0.00 $\pm$ 0.00	15.44 $\pm$ 2.39	18.71 $\pm$ 4.65	26.30 $\pm$ 6.33
WCC, 2C, 2 Tag	0.00 $\pm$ 0.00	0.33 $\pm$ 0.18	0.15 $\pm$ 0.15	0.00 $\pm$ 0.00
WC, 1C, 1 Tag	8.19 $\pm$ 1.10	8.86 $\pm$ 1.23	10.94 $\pm$ 2.10	14.37 $\pm$ 2.95

Table 12: Efficiencies of W+HF samples before and after optimization cuts, derived from exclusive matching of ALPGEN + HERWIG Monte Carlo samples. The scale factor has been applied.

3.2.2 Non-W Background

The estimation of the Non-W background is effected by both the H_T and M_T^W cuts. They also have special consideration in this case. We only apply the H_T cut for events with $\not{E}_T > 20\ GeV$ because the lower $\not{E}_T$ regions will generally fail the H_T cut by construction. We do apply the M_T^W cut for $\not{E}_T < 20$ GeV, however. This changes the result by 30%, and so we take 30% as an additional systematic uncertainty on this method. It is important to apply the M_T^W cut for $\not{E}_T < 20$. The class of events that is being removed for high $\not{E}_T$ (i.e. those with $M_T^W < 20$) should not be used to scale the Region C tags to Region D. That is, we should remove the same class of events (i.e. those with $M_T^W < 20$) for all regions symmetrically.

Table 13 shows the Non-W background estimates for single and double tags after the optimization cuts.

3.3 Systematic Uncertainties

Table 14 describes the errors on the various backgrounds and the $t\bar{t}$ signal, and how they are estimated.

Non-W					
	1 jet	2 jets	3 jets	4 jets	$\geq$ 5 jets
Electrons					
F_{Non-W} (%)	9.21 ± 2.31	12.06 ± 3.08	7.44 ± 2.34		
N_+^B/N_+^A (%)	39.60 ± 1.93	34.14 ± 3.79	42.24 ± 8.64		
$N_+^{tagmethod}$	45.43 ± 15.75	17.27 ± 6.56	3.83 ± 2.13	0.71 ± 0.80	0.56 ± 0.65
R_+^B (%)	1.63 ± 0.33	3.29 ± 0.74	7.64 ± 2.17	13.75 ± 6.96	3.39 ± 11.42
$N_+^{pretagmethod}$	26.16 ± 8.47	11.04 ± 3.75	1.12 ± 0.48	0.97 ± 0.59	0.05 ± 0.15
R_{++}^B (%)	0.00 ± 0.00	0.04 ± 0.04	1.04 ± 0.60	5.43 ± 4.14	5.99 ± 6.49
$N_{++}^{pretagmethod}$	0.00 ± 0.00	0.14 ± 0.13	0.15 ± 0.10	0.38 ± 0.32	0.08 ± 0.09
Pretag	1607.56 ± 403.69	335.18 ± 85.63	14.66 ± 4.61	7.07 ± 2.22	1.34 ± 0.42
$\geq$ 1+ Tag	30.49 ± 7.41	12.58 ± 3.23	1.25 ± 0.47	0.88 ± 0.46	0.07 ± 0.15
$\geq$ 2+ Tag	0.00 ± 0.00	0.14 ± 0.13	0.15 ± 0.10	0.38 ± 0.32	0.07 ± 0.09
Muons					
F_{Non-W} (%)	3.20 ± 0.81	3.78 ± 1.00	2.80 ± 1.10		
N_+^B/N_+^A (%)	12.68 ± 1.29	12.59 ± 2.73	22.93 ± 9.71		
$N_+^{tagmethod}$	6.31 ± 2.36	3.38 ± 1.51	0.05 ± 0.33	-0.08 ± 0.24	0.10 ± 0.24
R_+^B (%)	1.75 ± 0.39	4.60 ± 1.34	9.92 ± 5.09	44.27 ± 45.90	42.95 ± 95.94
$N_+^{pretagmethod}$	7.19 ± 2.42	3.30 ± 1.30	0.35 ± 0.23	0.58 ± 0.65	0.19 ± 0.44
R_{++}^B (%)	0.00 ± 0.00	0.23 ± 0.17	4.40 ± 2.98	19.45 ± 18.00	172.44 ± 230.49
$N_{++}^{pretagmethod}$	0.00 ± 0.00	0.17 ± 0.13	0.16 ± 0.12	0.26 ± 0.26	0.77 ± 1.08
Pretag	410.61 ± 103.74	71.71 ± 18.95	3.55 ± 1.40	1.31 ± 0.52	0.45 ± 0.18
$\geq$ 1+ Tag	6.74 ± 1.66	3.33 ± 0.98	0.25 ± 0.17	0.00 ± 0.22	0.12 ± 0.21
$\geq$ 2+ Tag	0.00 ± 0.00	0.17 ± 0.13	0.16 ± 0.12	0.00 ± 0.26	0.12 ± 1.08

Table 13: Non-W background estimation for single and double tags, for $H_T > 200$ GeV and $M_T^W > 20$ GeV. Note that the optimization cuts are only applied for $\not\!\!E_T > 20$ GeV because the loss of the 20 GeV causes most of the events to fail the H_T cut. $t\bar{t}$ is removed from the sideband regions in this table, after iterating to the measured cross section of 8.7.

Background Level Uncertainties			
	≥ 1	≥ 2	Estimated From
EW + Single Top	11%	16%	Lepton ID + modeling (7.4%), b-tag SF (6.6%), JES(4.3%), lum (6.0%)
W+HF	26%	28%	Matching (15%), ISR/FSR (10%), m_Q (6%) JES (5.0%), PDF (5%), Q^2 scale (4%), b-tag SF (6.6%)
Mistags	23%	23%	Mistag matrix (8%), light-flavor asymmetry (22%)
Non-W Tag Method	39%	n/a	Vary sidebands (25%), apply M_T^W for $\not\!\!E_T < 20$ (30%)
Non-W Pretag Method	44%	60%	F_{Non-W} (25%), R_B (20%) apply M_T^W for $\not\!\!E_T < 20$ (30%), small stats (double tags:50%)

Table 14: Background systematics summary.

	$H_T > 0,\ M_T > 0$		$H_T > 200,\ M_T > 20$	
Systematic	≥ 1 Tags	≥ 2 Tags	≥ 1 Tags	≥ 2 Tags
Lepton ID (CEM)	1.6			
Lepton ID (CMUP)	1.5			
Lepton ID (CMX)	1.5			
ISR/FSR	2.0			
PDF	2.0			
PYTHIA vs HERWIG	1.0			
Lepton Isolation	5.0			
JES	2.9		4.3	
b-tagging SF	6.6			
Backgrounds	17.6	71.1	19.6	68.9
Luminosity	6.0			

Table 15: Error of each component used to compute $\sigma_{t\bar{t}}$. All numbers are quoted in percentage.

3.4 Optimized Results

The luminosity weighted pretag efficiency in ≥ 3 jets using $H_T > 200$ GeV and $M_T^W > 20$ GeV/c^2 is

$$\epsilon_{pretag}^{t\bar{t}} \int \mathcal{L}dt = 21.2 \pm 2.0\ pb^{-1} \tag{24}$$

The tag rate in ≥ 3 jets is

$$\epsilon_{\geq 1\ tag}^{t\bar{t}} = 60.93 \pm 3.15\% \tag{25}$$

$$\epsilon_{\geq 2\ tag}^{t\bar{t}} = 16.37 \pm 2.21\% \tag{26}$$

To obtain the cross section, we start the analysis assuming $\sigma = 6.1$ pb. We then iterate until the results are stable to $< 1\%$. The number of observed events is 138 for the single tags and 33 for the double tags. After iteration, the number of background events is

$$N_{bkg}^{\geq 1\ tag} = 25.41 \pm 4.94 \tag{27}$$

$$N_{bkg}^{\geq 2\ tag} = 2.89 \pm 1.94 \tag{28}$$

This gives cross sections of

$$\sigma_{\geq 1} = 8.7 \pm 0.9(stat) \pm 1.0(sys)\ pb \tag{29}$$

$$\sigma_{\geq 2} = 8.7 \pm 1.7(stat) \pm 1.6(sys)\ pb \tag{30}$$

The results of the Method 2 background calculation are shown in Table 18, along with the prediction from $t\bar{t}$. The $t\bar{t}$ contribution is shown at the measured cross sections.

	$H_T > 0,\ M_T > 0$		$H_T > 200,\ M_T > 20$		Fit
Systematic	≥ 1 Tags	≥ 2 Tags	≥ 1 Tags	≥ 2 Tags	Combined
Lepton ID (CEM)	1.6				
Lepton ID (CMUP)	1.5				
Lepton ID (CMX)	1.5				
ISR/FSR	2.0				
PDF	2.0				
PYTHIA vs HERWIG	1.0				
Lepton Isolation	5.0				
JES	2.9		4.3		5.0
Total Pretag	6.7		7.4		7.8
b-tagging	5.2	13.5	5.2	13.5	5.0
$W + HF$	6.2	2.6	3.8	1.5	
$W + LF$	2.2	0.5	1.4	0.4	
EW and Single top	0.9	0.8	0.6	0.5	
Non-W	2.7	12.0	1.2	5.7	
Total Backgrounds	7.3	13.1	4.4	5.4	5.0
Shape Systematics	-				3.6
Luminosity	6.0				
Total Sys(w/Correlations)	12.4	20.0	11.4	17.2	15.5

Table 16: Effect of each component on $\sigma_{t\bar{t}}$ systematics. All numbers are quoted in percentage. The table includes unoptimized results from Ref [1], the optimized results from the analysis described here, and the results from a cross-check measurement of a fit to the N_{jet} spectrum to be discussed in Section 4.

The asymmetric errors of these cross sections are

$$\sigma_{\geq 1} = 8.7^{+0.9}_{-0.9}(stat)^{+1.2}_{-0.9}(sys)\ pb \tag{31}$$

$$\sigma_{\geq 2} = 8.7^{+1.8}_{-1.6}(stat)^{+1.9}_{-1.3}(sys)\ pb \tag{32}$$

Figures 23 and 24 show the likelihood curves with statistical error bands.

3.5 *A priori* Expectation

The *a priori* expectation of the variance of the $t\bar{t}$ cross sections can be determined by taking the expected background inputs for $\sigma = 6.1$ pb, and varying them within their Gaussian uncertainties. The final number of events per bin is then fluctuated in a Poisson distribution. We can then obtain the expected cross sections, and examine the ratio of $\sigma_{\geq 2}$ to $\sigma_{\geq 1}$.

Figure 20 shows the results of 10000 pseudoexperiments of the $t\bar{t}$ cross sections for ≥ 1 and ≥ 2 tags, assuming $\sigma = 6.1$ pb. It also shows the ratio $\sigma_{\geq 2}/\sigma_{\geq 1}$ to see what the possible spread is between the two measurements.

We see that the mean values of the expected experiments are at 6.1 pb, which is the input value. We also see that the average ratio is 1.0. Given this distribution, there is a probability of 6% that the cross section is 6.1, but we measure 8.7.

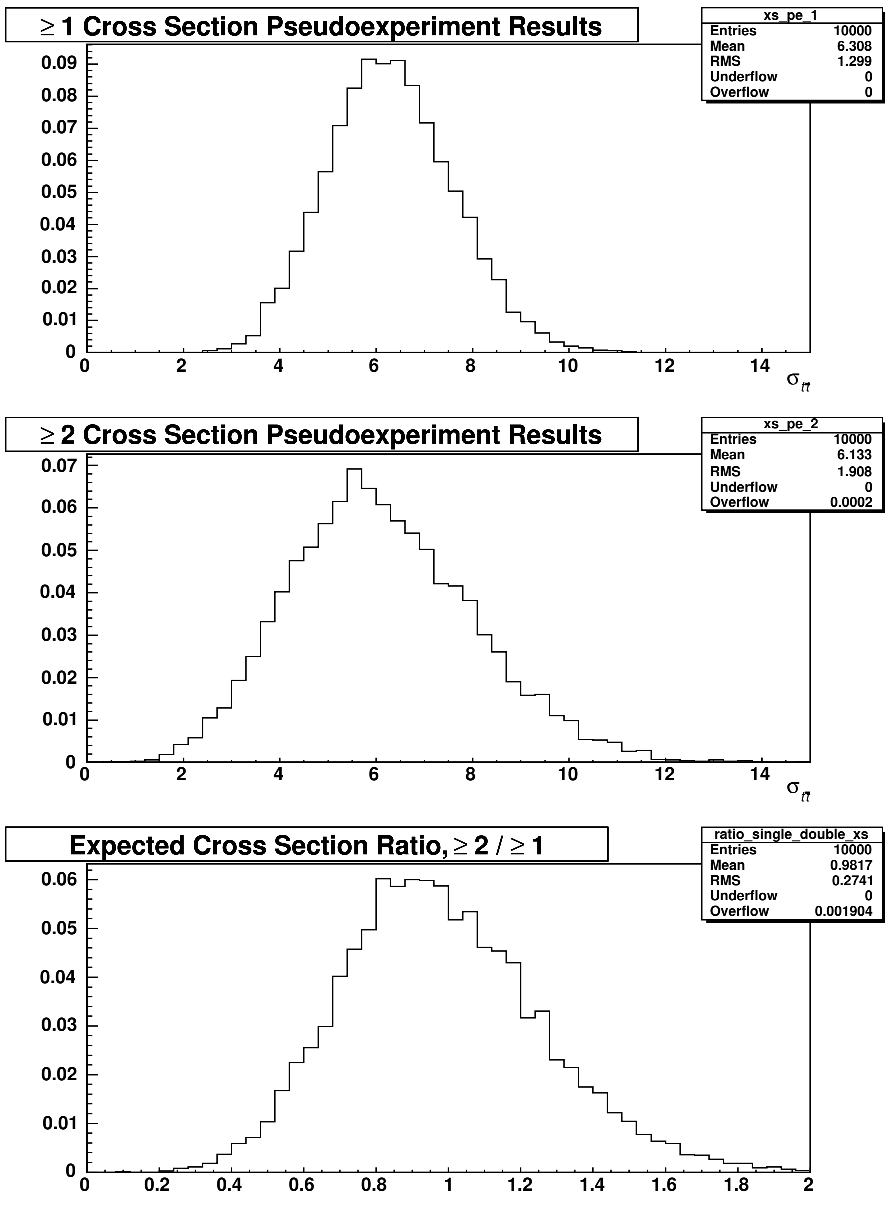

Figure 20: *A priori* expectation for the distribution of cross sections for the ≥ 1 and ≥ 2 analyses, plus their ratio (2/1).

3.6 Top Mass Dependence

Since we have quoted our cross section at a specific top mass (178 GeV/c^2), it is necessary to give the dependence on the assumed top mass input. In order to do this, we use HERWIG $t\bar{t}$ samples with top mass assumptions of 170,172.5,178,182.5, and 185. We then re-calculate our results using those assumed top masses. We then use a linear fit to interpolate to a given top mass. The way this is done is to calculate the effect on the overall event efficiency (pretag + tag) and assume that is a function of the input top mass, using the formula

$$\sigma(m) = \sigma(m_0)\frac{\epsilon(m_0)}{\alpha \times (m - m_0) + \epsilon(m_0)} \tag{33}$$

Table 19 shows the results of our efficiency calculations. Due to the differences between PYTHIA and HERWIG, we only use α from the HERWIG prediction and use ϵ from PYTHIA. Figure 26 shows the dependence of the final cross section versus the input top mass.

Our fit results are $\alpha_{\geq 1} = 0.000298 \pm 0.000061/GeV/c^2$, and $\alpha_{\geq 2} = 0.000091 \pm 0.000025/GeV/c^2$. This gives

$$\sigma_{\geq 1} = 8.9 \pm 0.9(stat) \pm 1.0(sys)\ pb \tag{34}$$

and

$$\sigma_{\geq 2} = 8.9 \pm 1.6(stat) \pm 1.5(sys)\ pb \tag{35}$$

assuming $m_{top} = 175\ GeV/c^2$.

Figure 27 shows the result versus input top mass, along with the theoretical prediction taken from [8].

3.7 Comparison with Gen4 Results

The major differences between this result and the Gen4 result outlined in [11] are as follows.

The Monte Carlo changed substantially, so the data-to-MC ratios for lepton ID have changed, as well as that for the b-tagging scale factor, and also the jet energy corrections.

Moreover, there are now two methods for evaluating the b-tagging scale factor, the electron and muon methods. The other major difference is in the Non-W background estimate and the usage of the $M_T^W > 20\ GeV/c^2$ cut, which reduces the background level and increases the systematic uncertainty.

The systematic for the light-flavor asymmetry is also increased in Gen5 relative to Gen4. The reason for this is that we feel there is a sample dependence of this correction that is not covered by the systematic in Gen4. We double the systematic to be conservative.

Table 17 shows the differences between Gen4 and Gen5 for the major parts of the analysis.

Quantity	Gen4	Gen5
CEM		
Lepton ID Scale Factor	0.931 $\pm$ 0.015	0.959 $\pm$ 0.015
Pre-tag Efficiency	4.1 $\pm$ 0.4%	3.8 $\pm$ 0.3%
CMUP		
Lepton ID Scale Factor	0.787 $\pm$ 0.016	0.784 $\pm$ 0.020
Pre-tag Efficiency	2.1 $\pm$ 0.2%	2.0 $\pm$ 0.2%
CMX		
Lepton ID Scale Factor	0.960 $\pm$ 0.018	0.941 $\pm$ 0.020
Pre-tag Efficiency	1.0 $\pm$ 0.8%	0.8 $\pm$ 0.1%
Common Systematics		
ISR/FSR	3.0%	2.0%
PDF	1.5%	2.0%
PYTHIA vs HERWIG	1.4%	1.0%
Lepton Isolation	5.0%	5.0%
Jet Energy Scale	4.9%	4.3%
B-Tagging Quantities		
$\geq$ 1 Tag Eff	53.4 $\pm$ 3.2%	60.9 $\pm$ 3.2%
$\geq$ 2 Tag Eff	11.0 $\pm$ 1.6%	16.4 $\pm$ 2.2%
Scale Factor	0.82 $\pm$ 0.06	0.909 $\pm$ 0.060
Mistag Matrix Sys	12%	22%
Background Level Systematics ($\geq$ 1 Tag)		
W+Heavy Flavor	26%	26%
Mistags	12%	22%
Non-W	14%	39%
Monte Carlo Bkgs	18%	12%
Effect on $\sigma_{t\bar{t}}$ ($\geq$ 1 Tag)		
W+Heavy Flavor	4.8%	3.8%
Mistags	2.6%	1.4%
Non-W	2.6%	1.2%
Monte Carlo Bkgs	3.2%	0.6%
Total Systematic Uncertainty on $\sigma_{t\bar{t}}$		
$\geq$ 1 Tag	13.7%	11.4%
$\geq$ 2 Tag	19.2%	17.2%

Table 17: Comparison of Gen4 and Gen5 results.

Summary					
Jet Multiplicity	1 jet	2 jets	3 jets	4 jets	$\geq$ 5 jets
Pretags					
Data	30283	4676	324	142	34
$t\bar{t}$ (8.7 pb)	8.80 ± 0.83	47.13 ± 4.45	79.67 ± 7.51	79.48 ± 7.49	25.16 ± 2.39
$\geq$ 1 Tags					
EW	4.38 ± 0.69	8.28 ± 1.25	1.13 ± 0.20	0.28 ± 0.06	0.09 ± 0.03
Single Top	6.75 ± 1.70	11.31 ± 2.41	1.59 ± 0.34	0.34 ± 0.08	0.05 ± 0.01
Non-W	37.23 ± 8.96	15.91 ± 4.01	1.51 ± 0.54	0.88 ± 0.54	0.19 ± 0.26
W + LF Mistags	93.08 ± 19.09	38.23 ± 7.68	5.80 ± 1.21	1.86 ± 0.37	0.28 ± 0.06
$W + c$	98.90 ± 26.31	20.78 ± 5.90	1.28 ± 0.41	0.39 ± 0.18	0.03 ± 0.02
$W + c\bar{c}$	33.25 ± 10.02	19.92 ± 6.49	2.22 ± 0.81	0.72 ± 0.36	0.02 ± 0.02
$W + b\bar{b}$	98.13 ± 31.97	54.39 ± 17.49	5.32 ± 1.75	1.28 ± 0.61	0.15 ± 0.12
$t\bar{t}$ (8.7 pb)	2.94 ± 0.35	23.99 ± 2.64	46.47 ± 5.04	49.88 ± 5.34	15.89 ± 1.72
Bkg	371.71 ± 71.52	168.81 ± 31.33	18.84 ± 3.30	5.75 ± 1.34	0.82 ± 0.31
Bkg + $t\bar{t}$ (8.7 pb)	374.65 ± 71.52	192.80 ± 31.44	65.31 ± 6.02	55.64 ± 5.51	16.71 ± 1.74
Data	427	232	62	58	18
$\geq$ 2 Tags					
EW	-	0.41 ± 0.08	0.06 ± 0.02	0.01 ± 0.01	0.01 ± 0.01
Single Top	-	1.48 ± 0.28	0.36 ± 0.09	0.08 ± 0.02	0.02 ± 0.01
Non-W	-	0.31 ± 0.20	0.31 ± 0.18	0.38 ± 0.44	0.19 ± 1.09
W + LF Mistags	-	0.48 ± 0.11	0.10 ± 0.04	0.17 ± 0.04	0.05 ± 0.04
$W + HF$	-	8.25 ± 2.86	0.89 ± 0.32	0.24 ± 0.12	0.02 ± 0.02
$t\bar{t}$ (8.7 pb)	-	4.42 ± 0.74	11.06 ± 1.84	14.28 ± 2.35	4.78 ± 0.78
Bkg	-	10.93 ± 2.89	1.71 ± 0.38	0.88 ± 0.46	0.29 ± 1.09
Bkg + $t\bar{t}$ (8.7 pb)	-	15.35 ± 2.99	12.78 ± 1.88	15.16 ± 2.39	5.07 ± 1.35
Data	-	15	15	15	3

Table 18: Method 2 background calculation summary for 318.5 pb^{-1}. Here the $t\bar{t}$ prediction is shown for the measured cross section of 8.7 pb (single) and 8.7 pb (double).

Input Top Mass Dependence			
m_{top}	ϵ_{pre} (%)	$\epsilon_{\geq 1\ tag}$ (%)	$\epsilon_{\geq 2\ tag}$ (%)
170	8.69 ± 0.10	64.90 ± 0.49	19.10 ± 0.40
172.5	8.69 ± 0.10	65.01 ± 0.34	19.36 ± 0.28
178	8.99 ± 0.06	65.08 ± 0.18	18.77 ± 0.15
182.5	9.15 ± 0.11	65.60 ± 0.33	19.19 ± 0.27
185	9.31 ± 0.11	64.93 ± 0.33	19.55 ± 0.27

Table 19: Input top mass dependence of efficiencies. Errors are MC statistical only. No scale factors are applied.

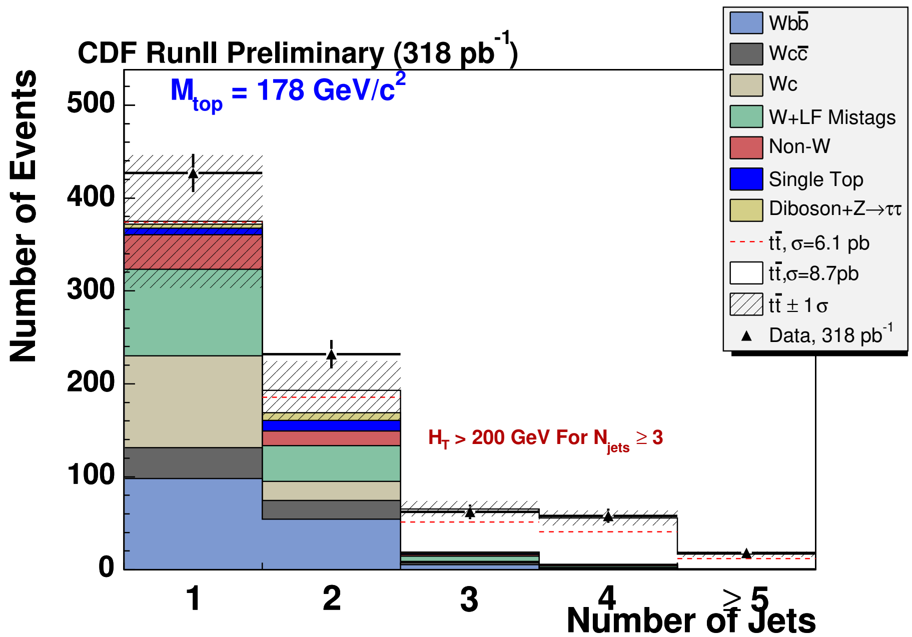

Figure 21: Number of jets for ≥ 1 tags. $t\bar{t}$ cross section is shown at the measured value of 8.7 pb in the solid white histogram.

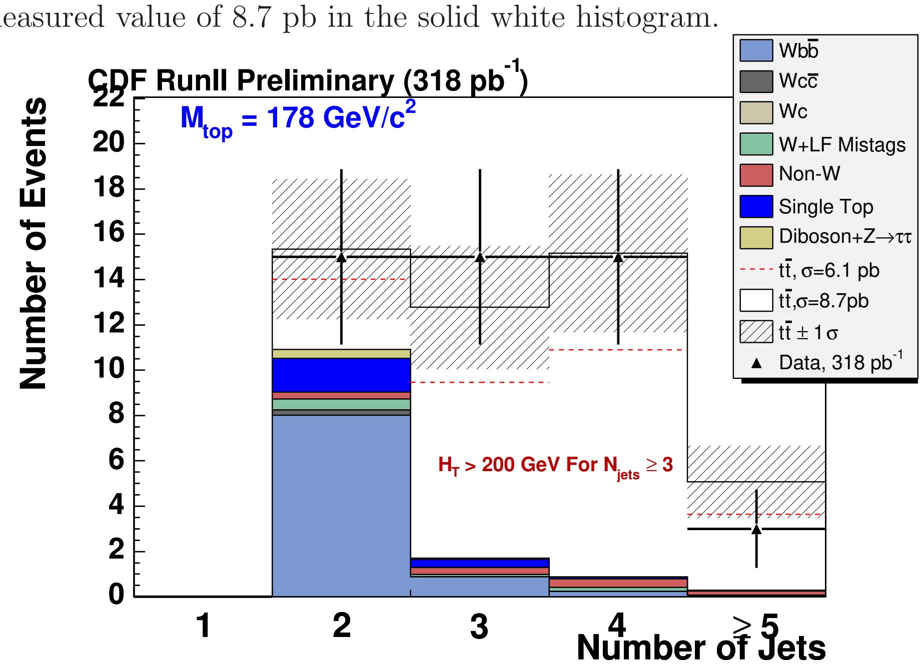

Figure 22: Number of jets for ≥ 2 tags. $t\bar{t}$ cross section is shown at the measured value of 8.7 pb in the solid white histogram.

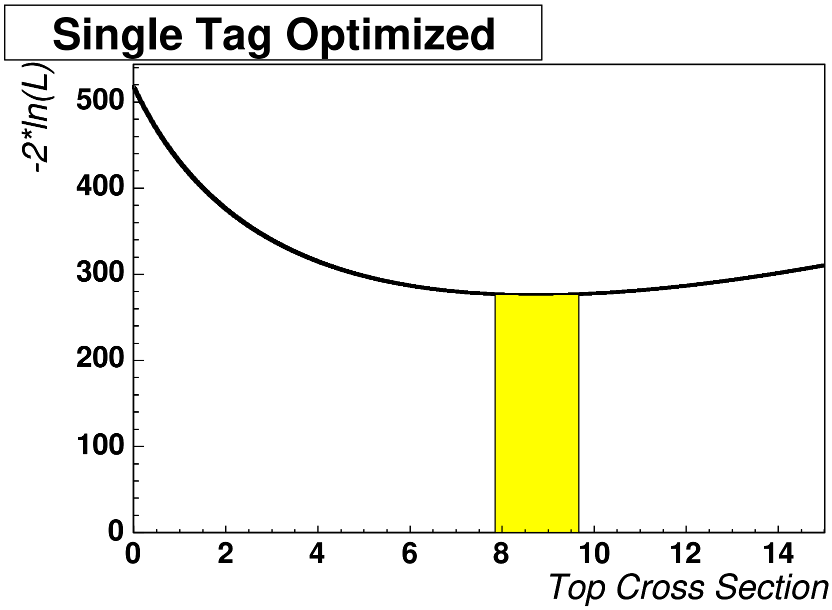

Figure 23: Likelihood curve for *optimized* ≥ 1 measurement with statistical error band.

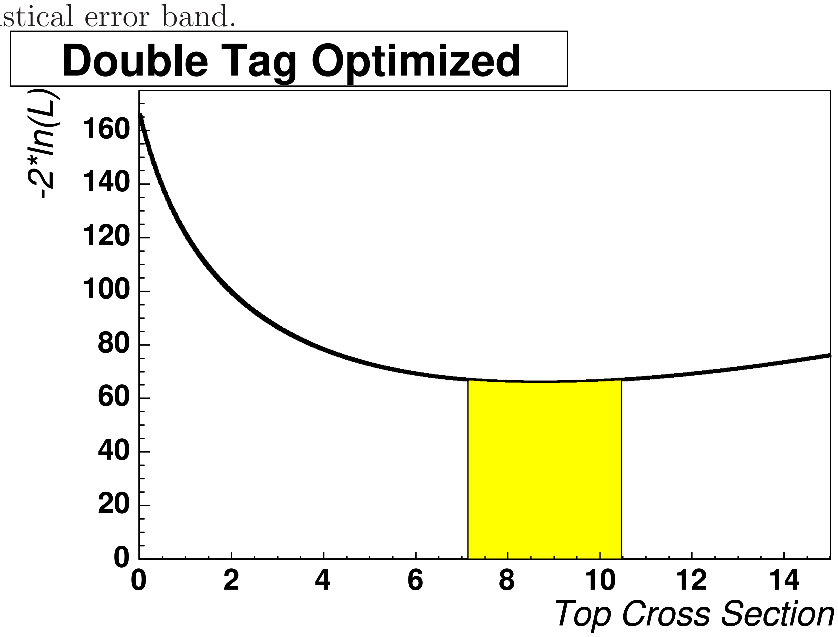

Figure 24: Likelihood curve for *optimized* ≥ 2 measurement with statistical error band.

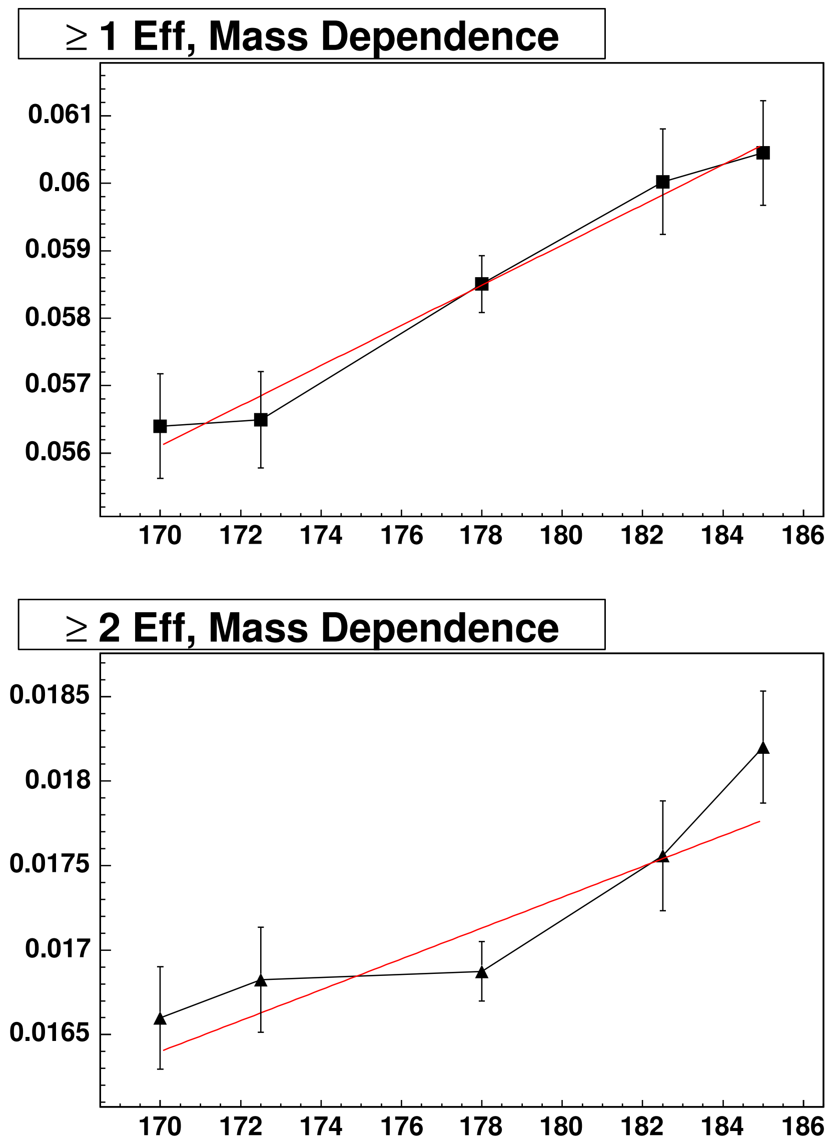

Figure 25: Top Mass dependence of efficiencies. These are the total event efficiencies before scale factors are applied. Errors are MC statistical only.

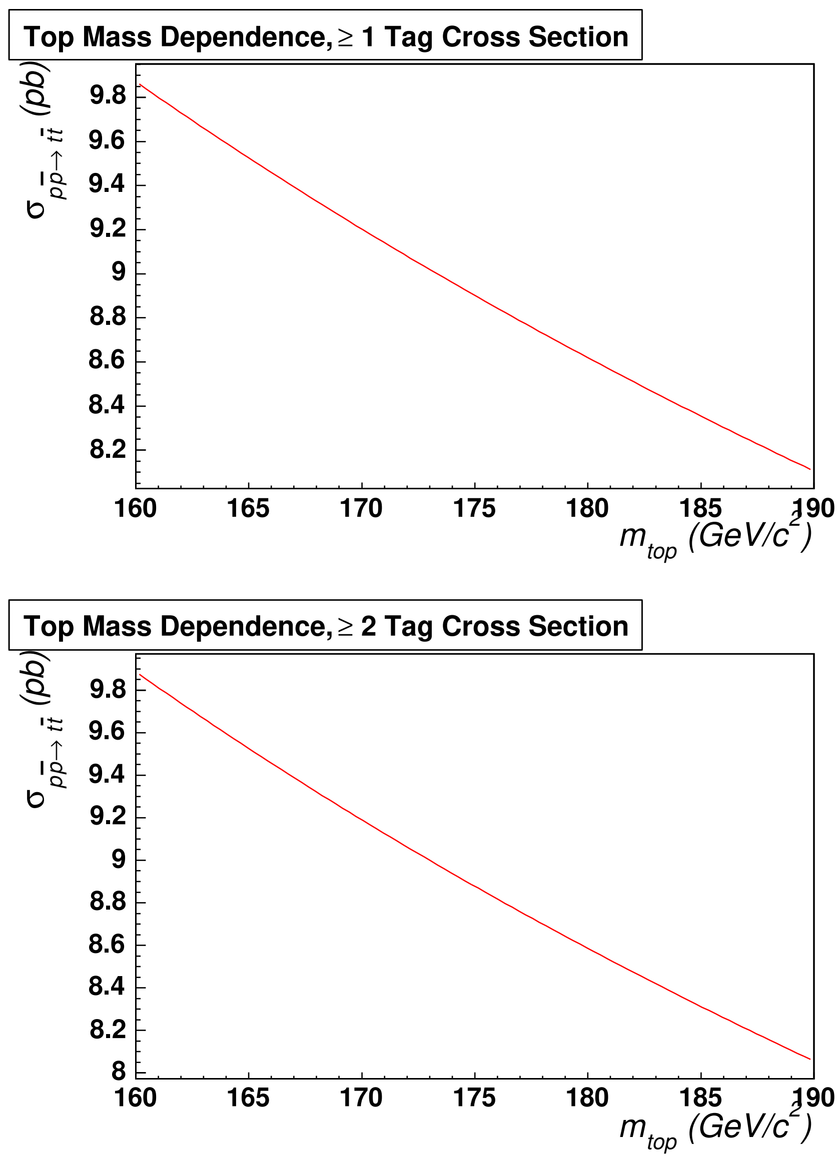

Figure 26: Cross section dependence on input top mass for ≥ 1 and ≥ 2 tag cross sections.

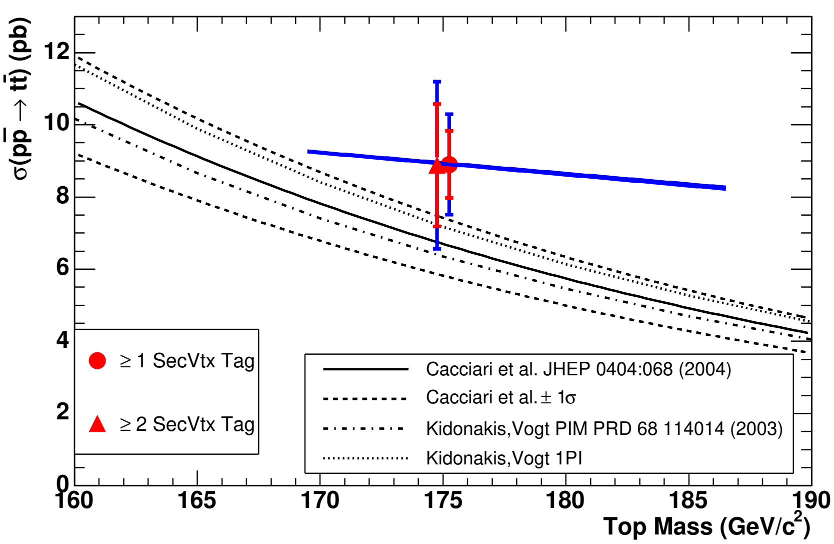

Figure 27: Cross section dependence on input top mass for ≥ 1 and ≥ 2 tag cross sections, compared to theoretical predictions.

4 Improvement of Background Uncertainties with N_{jet} Spectrum Fitting

If we examine Figure 21, we notice that there are somewhat large uncertanties in the background estimation in the 1 and 2 jet bins. The data also seems to be slightly larger than the total background prediction, although it is within the quoted uncertainty.

Examining Table 14, we see that there are large uncertainties on the W+HF and Non-W backgrounds, while the mistag and "Monte Carlo derived" backgrounds like dibosons and single top have small uncertainties. However, the Non-W background in Figure 21 is very small compared to the W+HF backgrounds, and so the W+HF backgrounds contribute much more to the overall background uncertainty level.

Because of the observation that the uncertainty in the W+HF estimate is driving the overall background estimate in the 1- and 2-jet bins, combined with the size of the sample with > 300 pb^{-1}, it is feasible to fit for the W+HF background level using a likelihood fit to the N_{jet} spectrum.

If we then assume that the *shape* of the N_{jet} spectrum is well-modelled in the Monte Carlo, but that it's overall *level* is not very well determined, we can assume the various background species will have an overall *fit factor* that will multiply the entire N_{jet} spectrum together. We can then use the information we obtain from a fit in the 1- and 2-jet bins to constrain the W+HF backgrounds in the $\geq$ 3-jet bins, and hence reducing our background uncertainty further, as can be seen in Equation 23.

4.1 Likelihood

In order to use all the information available, we will fit the N_{jet} spectrum bin-by-bin, for $= 1$ and ≥ 2 tags simultaneously. We also must take into account all the correlations between the various different backgrounds (for example, the correlation between the Non-W estimate and the mistag estimate due to the correction of $(1 - F_{Non-W})$ in the mistag matrix prediction).

We will also input the various background contributions and their errors (as shown in Table 14) and allow them all to fluctuate. We expect that only the heavy flavor fit factor will differ substantially from unity.

Before we tackle the complete likelihood with all backgrounds allowed to float independently, we first examine a likelihood with only the heavy flavor allowed to float, and all other backgrounds constrained to their values from Table 18.

4.1.1 Simple Example: Only Fit W+HF

The number of events expected in a given jet bin is given by the equation

$$N_{exp}^{jet}(\sigma_{t\bar{t}}, F_{HF}) = \sigma_{t\bar{t}}\mathrm{SF}\varepsilon_{MC}\int \mathcal{L}dt + N_{HF}^{pred}F_{HF} + \sum N_{other} \tag{36}$$

where

- $\sigma_{\mathrm{t\bar{t}}}$ is the $\mathrm{t\bar{t}}$ cross section
- F_{HF} is the *fit factor* by which the W+HF backgrounds (as shown in Table 18) should be multiplied
- ϵ_{MC} is the event efficiency in the Monte Carlo
- SF is the b-tagging scale factor
- $\int \mathcal{L}dt$ is the luminosity
- N_{HF}^{pred} is the W+HF prediction from method 2
- $\sum N_{other}$ is the sum of the other Method 2 backgrounds (constrained for the moment to the values shown in Table 18).

We then maximize the Poisson likelihood for single-tag data,

$$-2\ln\mathcal{L}(\sigma_{t\bar{t}}, F_{HF}) = 2N^i_{exp}(\sigma_{t\bar{t}}, F_{HF}) + 2\ln\Gamma(N^i_{obs} + 1) - 2N^i_{obs}\ln N^i_{exp}(\sigma_{t\bar{t}}, F_{HF}). \quad (37)$$

We can then constrain the heavy flavor fit fraction to what is externally measured from Method 2 (see [10]) by including a Gaussian constraint on F_{HF}:

$$-2\ln\mathcal{L}(\sigma_{t\bar{t}}, F_{HF}) = 2N^i_{exp}(\sigma_{t\bar{t}}, F_{HF}) + 2\ln\Gamma(N^i_{obs}+1) - 2N^i_{obs}\ln N^i_{exp}(\sigma_{t\bar{t}}, F_{HF}) + \left(\frac{F_{HF}-1}{\sigma_{HF}}\right)^2. \quad (38)$$

It is now clear how to extend the likelihood to include all backgrounds and their uncertanties.

4.1.2 Full Likelihood

In the full likelihood expression, we fit each jet bin seperately, and we also fit the $= 1$ and ≥ 2 tags simultaneously. We float the single and double mistags and Non-W backgrounds seperately because of the correlations in these backgrounds with other backgrounds. We also include the b-tagging scale factor into the likelihood, because it correlates many of the different components of the fit.

The full expression we obtain is

$$
\begin{aligned}
-2\ln\mathcal{L} &= -2\ln\mathcal{L}(\sigma_{t\bar{t}}, F_{EWK}, F_{QCD}, F_{MT}, F_{HF}, F_{MT2}, F_{QCD2}, F_{SF}) \\
&= 2\sum_{i\text{jets}}\sum_{1,2\text{tags}}[N^i_{exp}(\sigma_{t\bar{t}}, F_{EWK}, F_{QCD}, F_{MT}, F_{HF}, F_{MT2}, F_{QCD2}, F_{SF}) \\
&\quad -N^i_{obs}\ln N^i_{exp}(\sigma_{t\bar{t}}, F_{EWK}, F_{QCD}, F_{MT}, F_{HF}, F_{MT2}, F_{QCD2}, F_{SF}) \\
&\quad +\ln\Gamma(N^i_{obs}+1)] \\
&\quad +\left(\frac{F_{EWK}-1}{\sigma_{EWK}}\right)^2 + \left(\frac{F_{QCD}-1}{\sigma_{QCD}}\right)^2 + \left(\frac{F_{MT}-1}{\sigma_{MT}}\right)^2 \\
&\quad +\left(\frac{F_{HF}-1}{\sigma_{HF}}\right)^2 + \left(\frac{F_{MT2}-1}{\sigma_{MT2}}\right)^2 + \left(\frac{F_{QCD2}-1}{\sigma_{QCD2}}\right)^2 \\
&\quad +\left(\frac{F_{SF}-1}{\sigma_{SF}}\right)^2
\end{aligned}
\tag{39}
$$

where

$$
\begin{aligned}
N^i_{exp:1-tag} &= N^i_{exp}(\sigma_{t\bar{t}}, F_{EWK}, F_{QCD}, F_{MT}, F_{HF}, F_{MT2}, F_{QCD2}, F_{SF}) \\
=\sigma_{\mathrm{t\bar{t}}} &\times (\epsilon^{\mathrm{t\bar{t}}}_{pretag})(\epsilon^{\mathrm{t\bar{t}}}_{1-tag})(SF)\int\mathcal{L}dt \\
+F_{EWK} &\times \sum_{bkg=EW,s.top}\sigma^{bkg}(\epsilon^{bkg}_{pretag})(\epsilon^{bkg}_{1-tag})(SF)\int\mathcal{L}dt \\
+F_{QCD} &\times N^{\geq 1}_{Non-W} \\
+F_{HF} &\times \left(\frac{N_{pretag}-N^{NonW}_{pre}-F_{EWK}N^{EW,s.top}_{pre}-F_{\mathrm{t\bar{t}}}N^{\mathrm{t\bar{t}}}_{pre}}{N_{pretag}-N^{NonW}_{pre}-N^{EW,s.top}_{pre}-N^{\mathrm{t\bar{t}}}_{pre}}\right)(SF)(f_{HF})(\epsilon_{1-tag}) \\
+F_{MT} &\times N^{pred}_{-}\times\alpha_{LF}\beta\times\left(\frac{N_{pretag}-N^{NonW}_{pre}-F_{EWK}N^{EW,s.top}_{pre}-F_{\mathrm{t\bar{t}}}N^{\mathrm{t\bar{t}}}_{pre}-F_{WHF}N^{pre}_{WHF}}{N_{pretag}-N^{NonW}_{pre}-N^{EW,s.top}_{pre}-N^{\mathrm{t\bar{t}}}_{pre}-N^{pre}_{WHF}}\right)
\end{aligned}
\tag{40}
$$

$$
\begin{aligned}
N^i_{exp:2-tag} &= N^i_{exp}(\sigma_{t\bar{t}}, F_{EWK}, F_{QCD}, F_{MT}, F_{HF}, F_{MT2}, F_{QCD2}, F_{SF}) \\
=\sigma_{\mathrm{t\bar{t}}} &\times (\epsilon^{\mathrm{t\bar{t}}}_{pretag})(\epsilon^{\mathrm{t\bar{t}}}_{2-tag})(SF)\int\mathcal{L}dt \\
+F_{EWK} &\times \sum_{bkg=EW,s.top}\sigma^{bkg}(\epsilon^{bkg}_{pretag})(\epsilon^{bkg}_{2-tag})(SF)\int\mathcal{L}dt \\
+F_{QCD2} &\times N^{\geq 1}_{Non-W} \\
+F_{HF} &\times \left(\frac{N_{pretag}-N^{NonW}_{pre}-F_{EWK}N^{EW,s.top}_{pre}-F_{\mathrm{t\bar{t}}}N^{\mathrm{t\bar{t}}}_{pre}}{N_{pretag}-N^{NonW}_{pre}-N^{EW,s.top}_{pre}-N^{\mathrm{t\bar{t}}}_{pre}}\right)(SF)(f_{HF})(\epsilon_{2-tag}) \\
+F_{MT2} &\times N^{pred}_{+:-}\times\alpha_{LF}\beta\times\left(\frac{N_{pretag}-N^{NonW}_{+}-F_{EWK}N^{EW,s.top}_{+}-F_{\mathrm{t\bar{t}}}N^{\mathrm{t\bar{t}}}_{+}-F_{WHF}N^{+}_{WHF}}{N_{pretag}-N^{NonW}_{+}-N^{EW,s.top}_{+}-N^{\mathrm{t\bar{t}}}_{+}-N^{+}_{WHF}}\right)
\end{aligned}
\tag{41}
$$

The likelihood curve is given in Figure 30. The inputs and outputs of the likelihood are given in Table 20. All the input fit factors are sitting near their input values with the same error as input, except for the W+HF fit factor, as expected. The maximum likelihood of that fit factor is 1.22 ± 0.13. Also, examining the W+HF input value of 1.00 ± 0.30 and output value of 1.22 ± 0.13, we see that the fractional error was reduced from 30% to 12%. This improvement will be propogated into the signal region to obtain a better measurement of the cross section.

The correlations between the outputs of the likelihood are given in Table 21. The cross section is correlated strongly with the b-tagging scale factor and the heavy flavor fit fraction. The cross section is not very correlated with the other backgrounds.

The fit results include the errors due to the background uncertainty, the scale factor, and the statistical error. To this we must add the pretag and luminosity errors. Combining everything, we obtain

$$\begin{aligned} \sigma_{t\bar{t}} &= 8.86^{+0.90}_{-0.86}\ (stat)^{+1.05}_{-0.92}\ (bkg + sf) \pm 0.93\ (pretag + lum + shape)\ pb \quad (42) \\ &= 8.86^{+0.90}_{-0.86}\ (stat)^{+1.40}_{-1.31}\ (sys)\ pb \quad (43) \\ &= 8.86^{+1.66}_{-1.57}\ (stat + sys)\ pb \quad (44) \end{aligned}$$

Figures 28 and 29 show the $= 1$ and ≥ 2 N_{jet} spectra including the fit results for the various components. Figures 32-39 show the results of pseudoexperiments to determine the sensitivity of the various fit factors in Table 20.

The distribution of the expected uncertainties on the $t\bar{t}$ cross section are shown in Figure 31. The measured values of 15.3% for the upper uncertainty and 13.9% for the lower uncertainties are also shown with blue arrows.

	Input	Output
F_{EWK}	1.00 ± 0.16	1.02 ± 0.16
F_{QCD}	1.00 ± 0.33	1.08 ± 0.32
F_{MT1}	1.00 ± 0.12	1.08 ± 0.23
F_{HF}	1.00 ± 0.30	1.22 ± 0.13
F_{MT2}	1.00 ± 0.30	0.99 ± 0.30
F_{QCD2}	1.00 ± 0.66	0.97 ± 0.66
F_{SF}	1.00 ± 0.06	1.00 ± 0.06

Table 20: Input values to likelihood fit factors, and values after maximization of the likelihood.

	$\sigma_{t\bar{t}}$	F_{EWK}	F_{QCD}	F_{mistag}	F_{HF}	$F_{2-mistag}$	F_{2-QCD}	F_{SF}
$\sigma_{t\bar{t}}$	1.000	-0.016	-0.006	-0.064	0.107	-0.003	-0.028	-0.513
F_{EWK}	-0.016	1.000	-0.004	-0.009	-0.063	-0.001	-0.000	-0.010
F_{QCD}	-0.006	-0.004	1.000	-0.068	-0.343	0.002	0.004	0.007
F_{mistag}	-0.064	-0.009	-0.068	1.000	-0.641	0.003	0.010	0.033
F_{HF}	0.107	-0.063	-0.343	-0.641	1.000	-0.002	0.005	-0.299
$F_{2-mistag}$	-0.003	-0.001	0.002	0.003	-0.002	1.000	-0.001	-0.008
F_{2-QCD}	-0.028	-0.000	0.004	0.010	0.005	-0.001	1.000	-0.042
F_{SF}	-0.513	-0.010	0.007	0.033	-0.299	-0.008	-0.042	1.000

Table 21: Correlation matrix for likelihood fit. It is clear that the backgrounds are not very correlated with the cross section. The only thing that is correlated is the scale factor, which is expected.

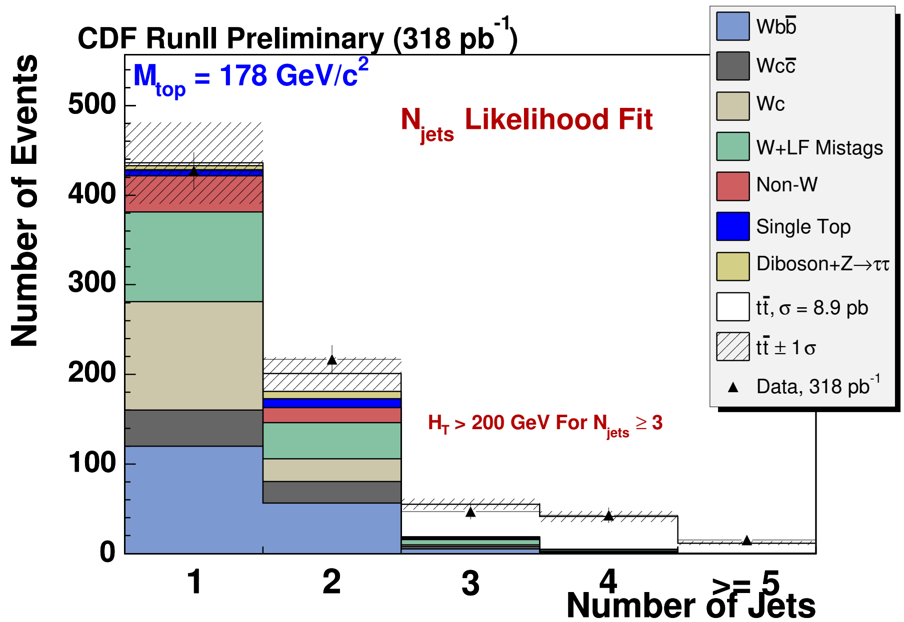

Figure 28: Fit results for *exactly 1* tag. $t\bar{t}$ cross section is shown at the measured value of 8.9 pb in the solid white histogram.

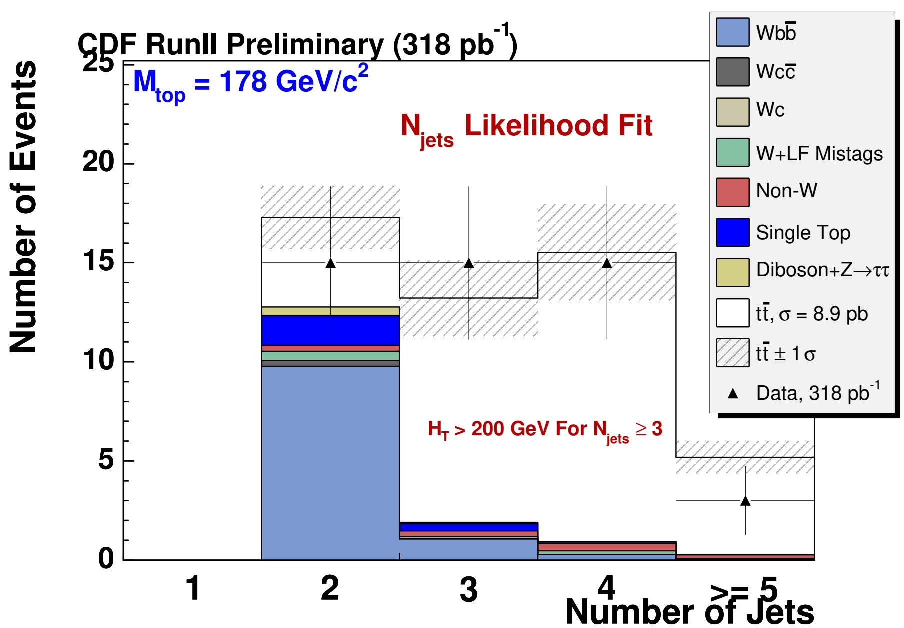

Figure 29: Fit results for $\geq$ 2 tags. $t\bar{t}$ cross section is shown at the measured value of 8.9 pb in the solid white histogram.

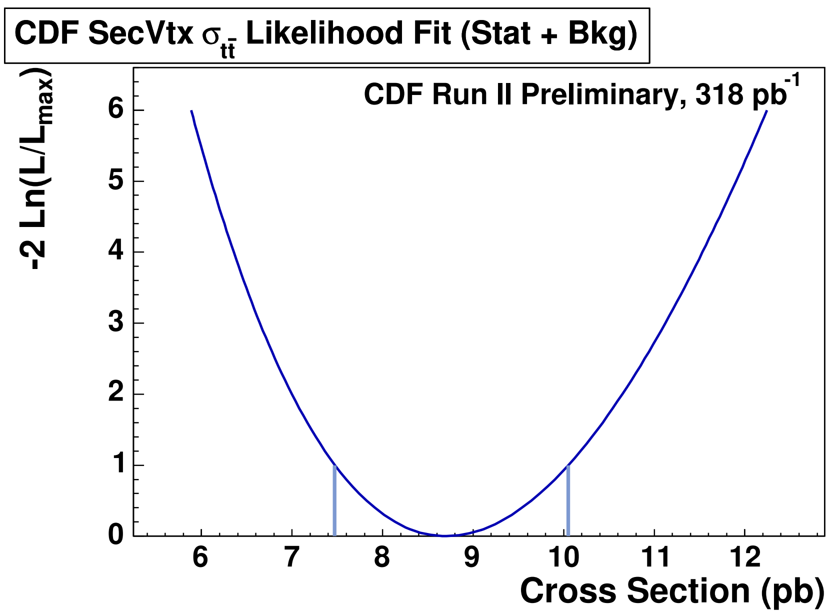

Figure 30: Likelihood curve for N_{jets} fit.

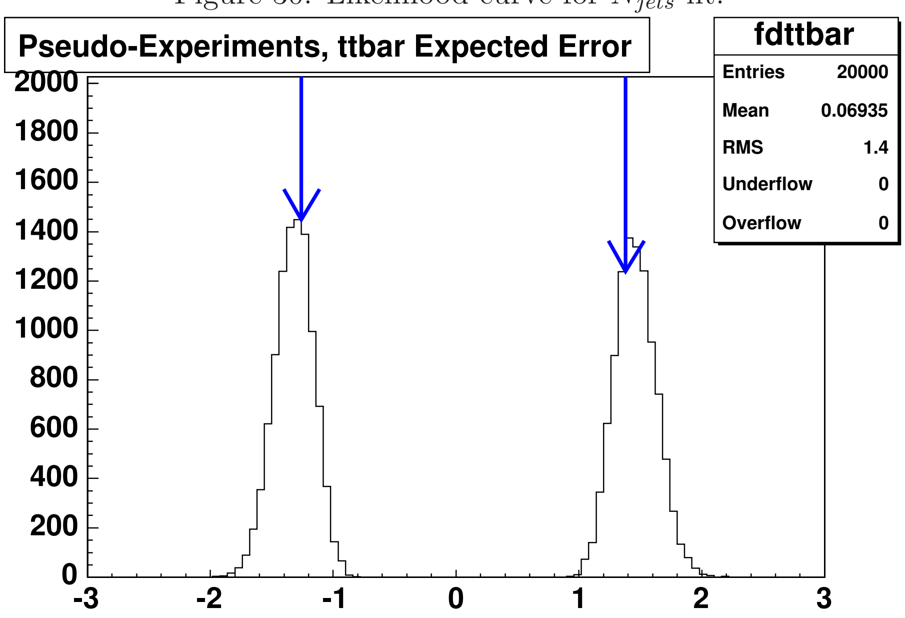

Figure 31: Examination of sensitivity of N_{jets} fit.

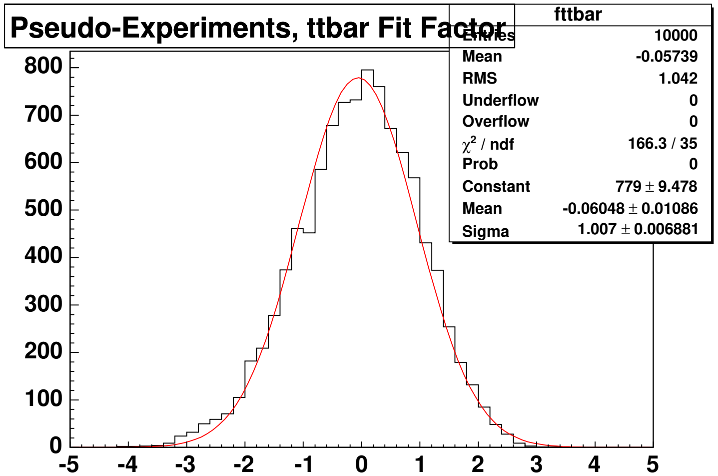

Figure 32: Sensitivity of the top cross section.

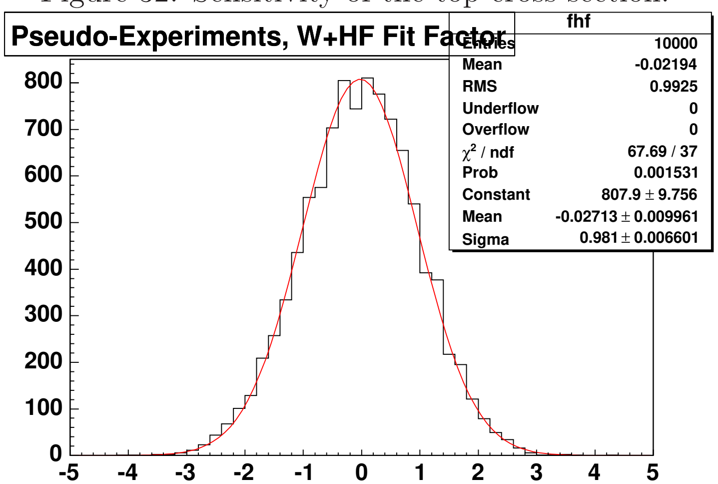

Figure 33: Sensitivity of the heavy flavor fraction.

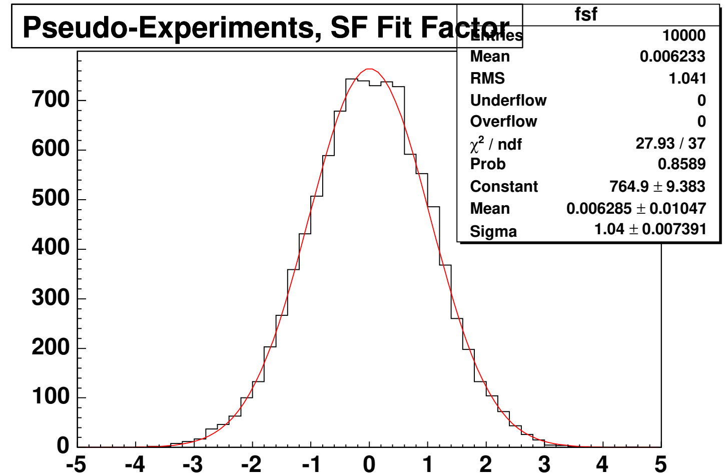

Figure 34: Sensitivity of the fit factor for the b-tagging scale factor.

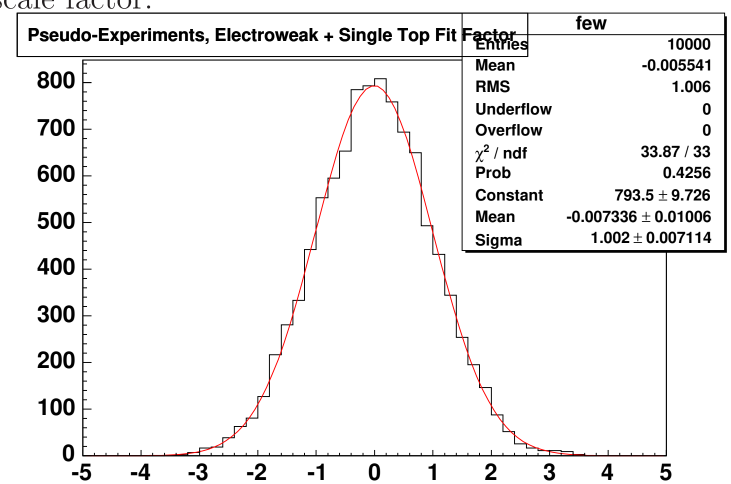

Figure 35: Sensitivity of the fit factor for the “Monte Carlo derived” backgrounds.

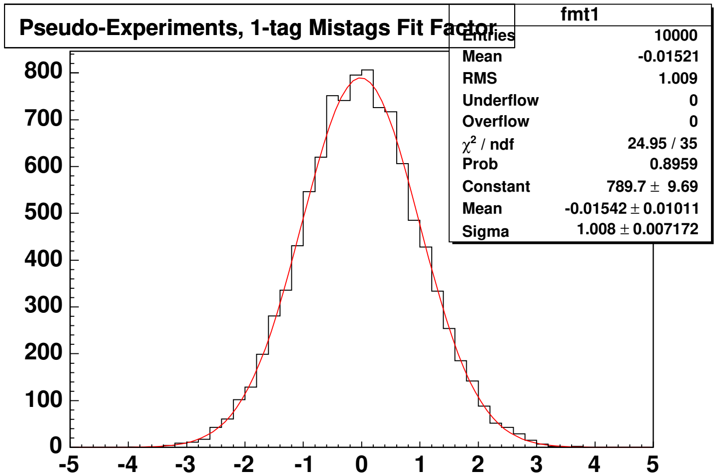

Figure 36: Sensitivity of the fit factor for the single mistag background.

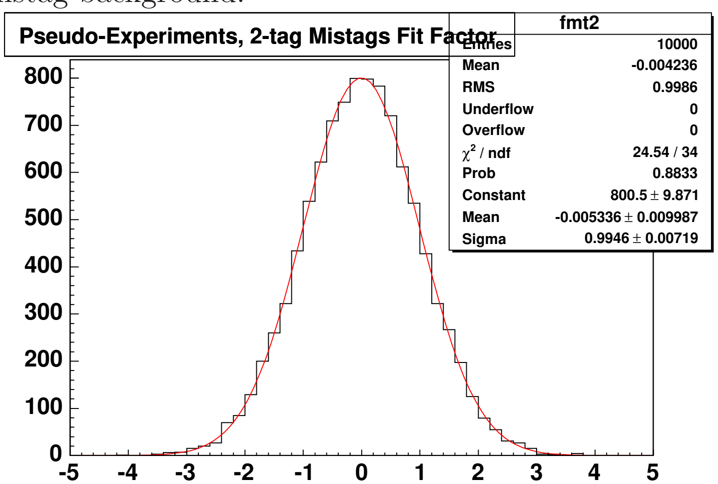

Figure 37: Sensitivity of the fit factor for the double mistag background.

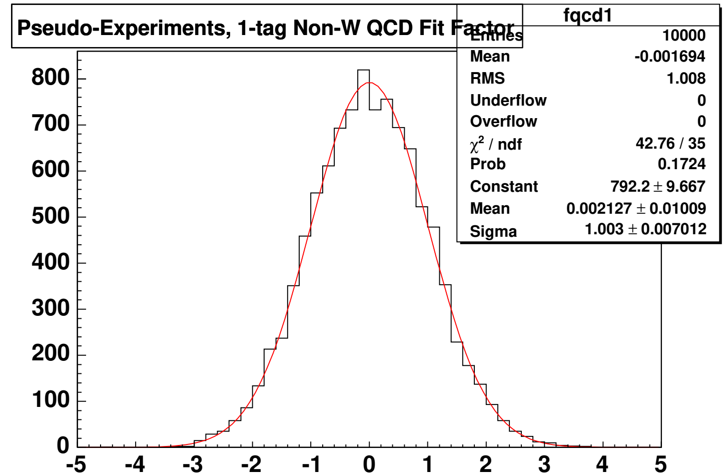

Figure 38: Sensitivity of the fit factor for the single Non-W background.

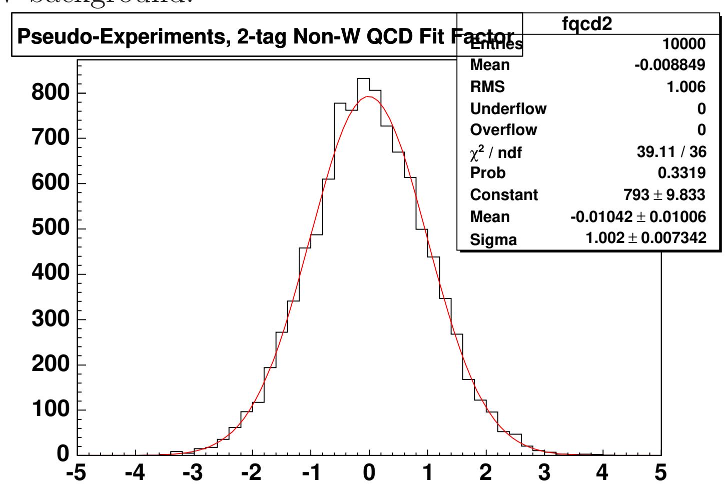

Figure 39: Sensitivity of the fit factor for the double Non-W background.

5 Conclusions

We have presented an optimized measurement of the $t\bar{t}$ production cross section with 318.5 pb^{-1} of data in the `5.3.3_nt` release. The unoptimized results are

$$\sigma_{\geq 1} = 8.9^{+1.0}_{-0.9}(stat)^{+1.2}_{-1.0}(sys)\ pb \tag{45}$$

$$\sigma_{\geq 2} = 8.2^{+1.7}_{-1.5}(stat)^{+2.0}_{-1.5}(sys)\ pb \tag{46}$$

For the optimized analysis with $H_T > 200$ GeV and $M_T^W > 20$ GeV, we obtain values of

$$\sigma_{\geq 1} = 8.7^{+0.9}_{-0.9}(stat)^{+1.2}_{-0.9}(sys)\ pb \tag{47}$$

$$\sigma_{\geq 2} = 8.7^{+1.8}_{-1.6}(stat)^{+1.9}_{-1.3}(sys)\ pb \tag{48}$$

We have also presented a measurement of the $t\bar{t}$ cross section by fitting the N_{jet} spectrum. We combine the $= 1$ and ≥ 2 tag cross sections to obtain

$$\sigma_{t\bar{t}} = 8.9^{+0.9}_{-0.9}(stat)^{+1.4}_{-1.3}(syst)\ pb. \tag{49}$$

A Electron Versus Muon Cross-Check

We have performed cross checks on the different trigger types. We perform the full analysis using only leptons from each trigger (CEM, CMUP, CMX). We then combine the CMUP and CMX results, and compare electrons versus muons.

The cross sections we obtain are

$$\sigma_{t\bar{t}}^{ele} = 8.8 \pm 1.2(stat) \pm 1.0(sys)\ pb \tag{50}$$

$$\sigma_{t\bar{t}}^{muo} = 8.7 \pm 1.4(stat) \pm 1.0(sys)\ pb \tag{51}$$

CEM Summary					
Jet Multiplicity	1 jet	2 jets	3 jets	4 jets	$\geq$ 5 jets
$\geq$ 1 Tags					
EW	2.50 ± 0.40	4.79 ± 0.73	0.65 ± 0.12	0.15 ± 0.03	0.06 ± 0.02
Single Top	4.01 ± 1.40	6.73 ± 1.92	0.95 ± 0.27	0.20 ± 0.06	0.04 ± 0.01
Non-W	37.23 ± 8.96	15.91 ± 4.01	1.51 ± 0.54	0.88 ± 0.54	0.19 ± 0.26
W + LF Mistags	93.08 ± 19.09	38.23 ± 7.68	5.80 ± 1.21	1.86 ± 0.37	0.28 ± 0.06
$W + c$	98.90 ± 26.31	20.78 ± 5.90	1.28 ± 0.41	0.39 ± 0.18	0.03 ± 0.02
$W + c\bar{c}$	33.25 ± 10.02	19.92 ± 6.49	2.22 ± 0.81	0.72 ± 0.36	0.02 ± 0.02
$W + b\bar{b}$	98.13 ± 31.97	54.39 ± 17.49	5.32 ± 1.75	1.28 ± 0.61	0.15 ± 0.12
$t\bar{t}$ (8.7 pb)	2.94 ± 0.35	23.99 ± 2.64	46.47 ± 5.04	49.88 ± 5.34	15.89 ± 1.72
Bkg	219.92 ± 41.56	101.28 ± 18.76	11.94 ± 2.09	4.55 ± 1.00	0.28 ± 0.17
Bkg + $t\bar{t}$ (8.7 pb)	221.66 ± 41.56	115.05 ± 18.82	38.54 ± 3.58	33.52 ± 3.28	9.53 ± 1.02
Data	427	232	62	58	18
$\geq$ 2 Tags					
EW	0	0.23 ± 0.05	0.04 ± 0.01	0.01 ± 0.00	0.01 ± 0.01
Single Top	0	0.88 ± 0.19	0.22 ± 0.06	0.04 ± 0.02	0.01 ± 0.00
Non-W	0	0.31 ± 0.20	0.31 ± 0.18	0.38 ± 0.44	0.19 ± 1.09
W + LF Mistags	0	0.48 ± 0.11	0.10 ± 0.04	0.17 ± 0.04	0.05 ± 0.04
$W + c$	0	0	0	0	0
$W + c\bar{c}$	0	0.24 ± 0.10	0.01 ± 0.00	0	0
$W + b\bar{b}$	0	8.01 ± 2.76	0.88 ± 0.32	0.24 ± 0.12	0.02 ± 0.02
$t\bar{t}$ (8.7 pb)	0	4.42 ± 0.74	11.06 ± 1.84	14.28 ± 2.35	4.78 ± 0.78
Bkg	0	6.28 ± 1.71	1.08 ± 0.24	0.68 ± 0.33	0.03 ± 0.09
Bkg + $t\bar{t}$ (8.7 pb)	0	8.82 ± 1.77	7.41 ± 1.08	8.97 ± 1.41	2.82 ± 0.47
Data	0	15	15	15	3

Table 22: Summary table for CEM electrons only.

CMUP Summary					
Jet Multiplicity	1 jet	2 jets	3 jets	4 jets	$\geq$ 5 jets
$\geq$ 1 Tags					
EW	1.29 $\pm$ 0.21	2.39 $\pm$ 0.37	0.33 $\pm$ 0.06	0.09 $\pm$ 0.02	0.03 $\pm$ 0.01
Single Top	1.92 $\pm$ 0.67	3.30 $\pm$ 0.95	0.46 $\pm$ 0.13	0.10 $\pm$ 0.04	0.01 $\pm$ 0.00
Non-W	37.23 $\pm$ 8.96	15.91 $\pm$ 4.01	1.51 $\pm$ 0.54	0.88 $\pm$ 0.54	0.19 $\pm$ 0.26
W + LF Mistags	93.08 $\pm$ 19.09	38.23 $\pm$ 7.68	5.80 $\pm$ 1.21	1.86 $\pm$ 0.37	0.28 $\pm$ 0.06
$W + c$	98.90 $\pm$ 26.31	20.78 $\pm$ 5.90	1.28 $\pm$ 0.41	0.39 $\pm$ 0.18	0.03 $\pm$ 0.02
$W + \mathrm{c\bar{c}}$	33.25 $\pm$ 10.02	19.92 $\pm$ 6.49	2.22 $\pm$ 0.81	0.72 $\pm$ 0.36	0.02 $\pm$ 0.02
$W + \mathrm{b\bar{b}}$	98.13 $\pm$ 31.97	54.39 $\pm$ 17.49	5.32 $\pm$ 1.75	1.28 $\pm$ 0.61	0.15 $\pm$ 0.12
$\mathrm{t\bar{t}}$ (8.7 pb)	2.94 $\pm$ 0.35	23.99 $\pm$ 2.64	46.47 $\pm$ 5.04	49.88 $\pm$ 5.34	15.89 $\pm$ 1.72
Bkg	100.27 $\pm$ 19.78	44.25 $\pm$ 8.21	4.56 $\pm$ 0.85	0.87 $\pm$ 0.33	0.31 $\pm$ 0.21
Bkg + $\mathrm{t\bar{t}}$ (8.7 pb)	101.16 $\pm$ 19.78	51.61 $\pm$ 8.25	18.86 $\pm$ 1.78	15.95 $\pm$ 1.67	5.03 $\pm$ 0.57
Data	427	232	62	58	18
$\geq$ 2 Tags					
EW	0	0.12 $\pm$ 0.03	0.02 $\pm$ 0.01	0	0
Single Top	0	0.43 $\pm$ 0.09	0.10 $\pm$ 0.03	0.02 $\pm$ 0.01	0
Non-W	0	0.31 $\pm$ 0.20	0.31 $\pm$ 0.18	0.38 $\pm$ 0.44	0.19 $\pm$ 1.09
W + LF Mistags	0	0.48 $\pm$ 0.11	0.10 $\pm$ 0.04	0.17 $\pm$ 0.04	0.05 $\pm$ 0.04
$W + c$	0	0	0	0	0
$W + \mathrm{c\bar{c}}$	0	0.24 $\pm$ 0.10	0.01 $\pm$ 0.00	0	0
$W + \mathrm{b\bar{b}}$	0	8.01 $\pm$ 2.76	0.88 $\pm$ 0.32	0.24 $\pm$ 0.12	0.02 $\pm$ 0.02
$\mathrm{t\bar{t}}$ (8.7 pb)	0	4.42 $\pm$ 0.74	11.06 $\pm$ 1.84	14.28 $\pm$ 2.35	4.78 $\pm$ 0.78
Bkg	0	3.03 $\pm$ 0.77	0.44 $\pm$ 0.15	0.18 $\pm$ 0.26	0.18 $\pm$ 1.08
Bkg + $\mathrm{t\bar{t}}$ (8.7 pb)	0	4.39 $\pm$ 0.80	3.85 $\pm$ 0.59	4.50 $\pm$ 0.76	1.60 $\pm$ 1.11
Data	0	15	15	15	3

Table 23: Summary table for CMUP muons only.

CMX Summary					
Jet Multiplicity	1 jet	2 jets	3 jets	4 jets	$\geq$ 5 jets
$\geq$ 1 Tags					
EW	0.59 $\pm$ 0.10	1.11 $\pm$ 0.17	0.15 $\pm$ 0.03	0.04 $\pm$ 0.01	0
Single Top	0.81 $\pm$ 0.29	1.28 $\pm$ 0.37	0.18 $\pm$ 0.05	0.04 $\pm$ 0.01	0
Non-W	37.23 $\pm$ 8.96	15.91 $\pm$ 4.01	1.51 $\pm$ 0.54	0.88 $\pm$ 0.54	0.19 $\pm$ 0.26
W + LF Mistags	93.08 $\pm$ 19.09	38.23 $\pm$ 7.68	5.80 $\pm$ 1.21	1.86 $\pm$ 0.37	0.28 $\pm$ 0.06
$W + c$	98.90 $\pm$ 26.31	20.78 $\pm$ 5.90	1.28 $\pm$ 0.41	0.39 $\pm$ 0.18	0.03 $\pm$ 0.02
$W + c\bar{c}$	33.25 $\pm$ 10.02	19.92 $\pm$ 6.49	2.22 $\pm$ 0.81	0.72 $\pm$ 0.36	0.02 $\pm$ 0.02
$W + b\bar{b}$	98.13 $\pm$ 31.97	54.39 $\pm$ 17.49	5.32 $\pm$ 1.75	1.28 $\pm$ 0.61	0.15 $\pm$ 0.12
$t\bar{t}$ (8.7 pb)	2.94 $\pm$ 0.35	23.99 $\pm$ 2.64	46.47 $\pm$ 5.04	49.88 $\pm$ 5.34	15.89 $\pm$ 1.72
Bkg	51.52 $\pm$ 10.58	23.29 $\pm$ 4.57	2.35 $\pm$ 0.42	0.34 $\pm$ 0.09	0.23 $\pm$ 0.04
Bkg + $t\bar{t}$ (8.7 pb)	51.83 $\pm$ 10.58	26.15 $\pm$ 4.58	7.92 $\pm$ 0.75	6.17 $\pm$ 0.65	2.14 $\pm$ 0.21
Data	427	232	62	58	18
$\geq$ 2 Tags					
EW	0	0.06 $\pm$ 0.01	0.01 $\pm$ 0.00	0	0
Single Top	0	0.17 $\pm$ 0.04	0.04 $\pm$ 0.01	0.01 $\pm$ 0.00	0
Non-W	0	0.31 $\pm$ 0.20	0.31 $\pm$ 0.18	0.38 $\pm$ 0.44	0.19 $\pm$ 1.09
W + LF Mistags	0	0.48 $\pm$ 0.11	0.10 $\pm$ 0.04	0.17 $\pm$ 0.04	0.05 $\pm$ 0.04
$W + c$	0	0	0	0	0
$W + c\bar{c}$	0	0.24 $\pm$ 0.10	0.01 $\pm$ 0.00	0	0
$W + b\bar{b}$	0	8.01 $\pm$ 2.76	0.88 $\pm$ 0.32	0.24 $\pm$ 0.12	0.02 $\pm$ 0.02
$t\bar{t}$ (8.7 pb)	0	4.42 $\pm$ 0.74	11.06 $\pm$ 1.84	14.28 $\pm$ 2.35	4.78 $\pm$ 0.78
Bkg	0	1.61 $\pm$ 0.43	0.19 $\pm$ 0.04	0.02 $\pm$ 0.01	0.08 $\pm$ 0.02
Bkg + $t\bar{t}$ (8.7 pb)	0	2.14 $\pm$ 0.44	1.52 $\pm$ 0.23	1.69 $\pm$ 0.28	0.65 $\pm$ 0.10
Data	0	15	15	15	3

Table 24: Summary table for CMX muons only.

B 162 pb^{-1} Cross-Check

We have performed a cross-check of the analysis using only the initial 162 pb^{-1}. We find a cross section of

$$\sigma_{t\bar{t}}^{162\ pb^{-1}} = \sigma_{\geq 1} = 8.7 \pm 1.3(stat) \pm 1.0(sys) \tag{52}$$

Good Run List 4.0 Summary					
Jet Multiplicity	1 jet	2 jets	3 jets	4 jets	$\geq$ 5 jets
Pretags					
Data	14681	2286	153	70	13
$t\bar{t}$ (8.7 pb)	4.46 ± 0.42	23.86 ± 2.25	40.33 ± 3.80	40.24 ± 3.79	12.74 ± 1.21
$\geq$ 1 Tags					
EW	2.22 ± 0.35	4.19 ± 0.63	0.57 ± 0.10	0.14 ± 0.03	0.05 ± 0.01
Single Top	3.41 ± 0.86	5.73 ± 1.22	0.81 ± 0.17	0.17 ± 0.04	0.03 ± 0.01
Non-W	17.37 ± 4.30	6.66 ± 1.84	0.76 ± 0.33	0.61 ± 0.41	-0.12 ± 0.06
W + LF Mistags	44.27 ± 9.36	18.77 ± 3.78	2.86 ± 0.58	0.97 ± 0.20	-0.06 ± 0.01
$W + c$	48.07 ± 12.75	10.16 ± 2.88	0.59 ± 0.19	0.18 ± 0.09	-0.00 ± 0.01
$W + c\bar{c}$	16.16 ± 4.86	9.74 ± 3.17	1.02 ± 0.38	0.34 ± 0.18	-0.00 ± 0.01
$W + b\bar{b}$	47.70 ± 15.50	26.60 ± 8.55	2.44 ± 0.81	0.61 ± 0.31	-0.02 ± 0.04
$t\bar{t}$ (8.7 pb)	1.49 ± 0.17	12.14 ± 1.34	23.52 ± 2.55	25.25 ± 2.71	8.04 ± 0.87
Bkg	179.21 ± 34.70	81.85 ± 15.30	9.03 ± 1.56	3.04 ± 0.75	-0.13 ± 0.08
Bkg + $t\bar{t}$ (8.7 pb)	180.70 ± 34.70	93.99 ± 15.36	32.55 ± 2.99	28.29 ± 2.81	7.92 ± 0.87
Data	201	98	27	34	8
$\geq$ 2 Tags					
EW	0	0.21 ± 0.04	0.03 ± 0.01	0.01 ± 0.00	0.01 ± 0.00
Single Top	0	0.75 ± 0.14	0.18 ± 0.04	0.04 ± 0.01	0.01 ± 0.00
Non-W	0	0.31 ± 0.19	0.11 ± 0.08	0.41 ± 0.49	-0.12 ± 0.64
W + LF Mistags	0	0.15 ± 0.03	-0.01 ± 0.03	0.25 ± 0.06	0.01 ± 0.01
$W + c$	0	0	0	0	0
$W + c\bar{c}$	0	0.12 ± 0.05	0	0	0
$W + b\bar{b}$	0	3.92 ± 1.35	0.40 ± 0.15	0.11 ± 0.06	-0.00 ± 0.01
$t\bar{t}$ (8.7 pb)	0	2.24 ± 0.37	5.60 ± 0.93	7.23 ± 1.19	2.42 ± 0.40
Bkg	0	5.45 ± 1.42	0.72 ± 0.18	0.81 ± 0.50	-0.10 ± 0.64
Bkg + $t\bar{t}$ (8.7 pb)	0	7.69 ± 1.47	6.32 ± 0.95	8.04 ± 1.29	2.32 ± 0.76
Data	0	8	7	10	2

Table 25: Summary for 162 pb^{-1} cross check.

C Cross Check Using Muon χ^2 Probability Cut

We have performed a cross check cutting on the muon COT χ^2 probability $> 1 \times 10^{-8}$. This removes Non-W backgrounds that have been observed in the dilepton group.

Because most of our sample is $\mathrm{t\bar{t}}$ for the optimized case, the results are the same as the default. We obtain

$$\sigma_{\geq 1} = 8.70 \pm 0.91(stat) \pm 1.00(sys) \tag{53}$$

$$\sigma_{\geq 2} = 8.82 \pm 1.67(stat) \pm 1.55(sys) \tag{54}$$

which is consistent with our results.

For the unoptimized analysis, we obtain

$$\sigma_{\geq 1} = 8.61 \pm 0.93(stat) \pm 1.08(sys) \tag{55}$$

$$\sigma_{\geq 2} = 8.34 \pm 1.63(stat) \pm 1.67(sys) \tag{56}$$

The single tag results are not consistent with the analysis we have performed for the unoptimized case. This is because the $\mathrm{t\bar{t}}$ fraction is the smallest in this case, and the cross section is more sensitive to the background levels. However, because the unoptimized result is a cross check measurement, we do not feel obligated to use the muon χ^2 probability cut in our analysis at this time.

Summary					
Jet Multiplicity	1 jet	2 jets	3 jets	4 jets	$\geq$ 5 jets
Pretags					
Data	29182	4483	304	136	32
$t\bar{t}$ (8.7 pb)	8.75 $\pm$ 0.82	46.87 $\pm$ 4.43	79.23 $\pm$ 7.48	79.05 $\pm$ 7.46	25.03 $\pm$ 2.38
$\geq$ 1 Tags					
EW	4.36 $\pm$ 0.69	8.24 $\pm$ 1.24	1.12 $\pm$ 0.20	0.28 $\pm$ 0.06	0.09 $\pm$ 0.03
Single Top	6.71 $\pm$ 1.69	11.25 $\pm$ 2.40	1.58 $\pm$ 0.34	0.34 $\pm$ 0.08	0.05 $\pm$ 0.01
Non-W	35.88 $\pm$ 8.65	15.58 $\pm$ 3.94	1.39 $\pm$ 0.56	0.90 $\pm$ 0.54	0.20 $\pm$ 0.27
W + LF Mistags	90.08 $\pm$ 18.51	36.54 $\pm$ 7.34	5.31 $\pm$ 1.11	1.63 $\pm$ 0.33	0.19 $\pm$ 0.04
$W + c$	95.38 $\pm$ 25.35	19.84 $\pm$ 5.65	1.16 $\pm$ 0.38	0.35 $\pm$ 0.17	0.02 $\pm$ 0.02
$W + c\bar{c}$	32.06 $\pm$ 9.65	19.03 $\pm$ 6.21	2.02 $\pm$ 0.75	0.64 $\pm$ 0.34	0.01 $\pm$ 0.01
$W + b\bar{b}$	94.64 $\pm$ 30.80	51.94 $\pm$ 16.75	4.83 $\pm$ 1.62	1.14 $\pm$ 0.57	0.11 $\pm$ 0.10
$t\bar{t}$ (8.7 pb)	2.93 $\pm$ 0.34	23.85 $\pm$ 2.63	46.21 $\pm$ 5.02	49.61 $\pm$ 5.32	15.81 $\pm$ 1.71
Bkg	359.12 $\pm$ 68.95	162.41 $\pm$ 30.02	17.42 $\pm$ 3.06	5.27 $\pm$ 1.26	0.67 $\pm$ 0.31
Bkg + $t\bar{t}$ (8.7 pb)	362.04 $\pm$ 68.95	186.26 $\pm$ 30.13	63.63 $\pm$ 5.88	54.88 $\pm$ 5.47	16.48 $\pm$ 1.74
Data	411	222	62	56	17
$\geq$ 2 Tags					
EW	0	0.41 $\pm$ 0.08	0.06 $\pm$ 0.02	0.01 $\pm$ 0.01	0.01 $\pm$ 0.01
Single Top	0	1.47 $\pm$ 0.28	0.36 $\pm$ 0.09	0.08 $\pm$ 0.02	0.02 $\pm$ 0.01
Non-W	0	0.30 $\pm$ 0.19	0.29 $\pm$ 0.17	0.39 $\pm$ 0.43	0.20 $\pm$ 1.05
W + LF Mistags	0	0.45 $\pm$ 0.10	0.11 $\pm$ 0.04	0.08 $\pm$ 0.02	0.00 $\pm$ 0.03
$W + c$	0	0	0	0	0
$W + c\bar{c}$	0	0.23 $\pm$ 0.10	0.01 $\pm$ 0.00	0	0
$W + b\bar{b}$	0	7.65 $\pm$ 2.64	0.79 $\pm$ 0.29	0.21 $\pm$ 0.11	0.02 $\pm$ 0.02
$t\bar{t}$ (8.8 pb)	0	4.45 $\pm$ 0.75	11.13 $\pm$ 1.86	14.36 $\pm$ 2.36	4.81 $\pm$ 0.79
Bkg	0	10.50 $\pm$ 2.77	1.62 $\pm$ 0.36	0.77 $\pm$ 0.45	0.24 $\pm$ 1.05
Bkg + $t\bar{t}$ (8.8 pb)	0	14.95 $\pm$ 2.87	12.75 $\pm$ 1.89	15.13 $\pm$ 2.40	5.06 $\pm$ 1.32
Data	0	15	15	15	3

Table 26: Results of muon track χ^2 cut cross-check for the optimized analysis.

Summary					
Jet Multiplicity	1 jet	2 jets	3 jets	4 jets	$\geq$ 5 jets
Pretags					
Data	29511	4592	736	173	34
$t\bar{t}$ (8.6 pb)	8.84 ± 0.78	47.61 ± 4.24	92.88 ± 8.25	83.00 ± 7.38	25.60 ± 2.29
$\geq$ 1 Tags					
EW	4.44 ± 0.68	8.43 ± 1.24	2.09 ± 0.33	0.38 ± 0.08	0.10 ± 0.03
Single Top	6.83 ± 1.70	11.48 ± 2.41	2.48 ± 0.53	0.41 ± 0.09	0.06 ± 0.01
Non-W	41.16 ± 9.80	19.10 ± 4.71	6.62 ± 1.90	3.07 ± 1.05	0.64 ± 0.41
W + LF Mistags	90.97 ± 18.68	37.37 ± 7.51	10.48 ± 2.13	2.18 ± 0.44	0.18 ± 0.04
$W + c$	95.63 ± 25.63	20.10 ± 5.77	3.07 ± 0.93	0.49 ± 0.22	0.02 ± 0.02
$W + c\bar{c}$	32.31 ± 9.80	19.21 ± 6.31	4.64 ± 1.63	0.79 ± 0.39	0.02 ± 0.02
$W + b\bar{b}$	95.16 ± 31.19	52.63 ± 17.09	10.41 ± 3.28	1.64 ± 0.77	0.10 ± 0.11
$t\bar{t}$ (8.6 pb)	2.96 ± 0.33	24.21 ± 2.55	53.12 ± 5.52	51.68 ± 5.29	16.14 ± 1.67
Bkg	366.49 ± 69.92	168.34 ± 30.71	39.80 ± 6.56	8.96 ± 1.79	1.11 ± 0.43
Bkg + $t\bar{t}$ (8.6 pb)	369.46 ± 69.92	192.55 ± 30.81	92.92 ± 8.57	60.65 ± 5.59	17.25 ± 1.72
Data	416	232	92	61	18
$\geq$ 2 Tags					
EW	0	0.42 ± 0.09	0.14 ± 0.04	0.02 ± 0.01	0.01 ± 0.01
Single Top	0	1.51 ± 0.28	0.53 ± 0.13	0.09 ± 0.03	0.02 ± 0.01
Non-W	0	0.28 ± 0.16	0.88 ± 0.48	0.77 ± 0.49	0.36 ± 2.34
W + LF Mistags	0	0.52 ± 0.12	0.26 ± 0.06	0.11 ± 0.04	0.04 ± 0.04
$W + c$	0	0	0	0	0
$W + c\bar{c}$	0	0.25 ± 0.10	0.03 ± 0.01	0	0
$W + b\bar{b}$	0	7.75 ± 2.70	1.71 ± 0.58	0.31 ± 0.15	0.02 ± 0.02
$t\bar{t}$ (8.3 pb)	0	4.31 ± 0.71	11.76 ± 1.92	14.15 ± 2.28	4.66 ± 0.75
Bkg	0	10.74 ± 2.83	3.54 ± 0.78	1.29 ± 0.51	0.45 ± 2.34
Bkg + $t\bar{t}$ (8.3 pb)	0	15.05 ± 2.92	15.30 ± 2.08	15.45 ± 2.34	5.11 ± 2.46
Data	0	15	17	16	3

Table 27: Results of muon track χ^2 cut cross-check for the unoptimized analysis.

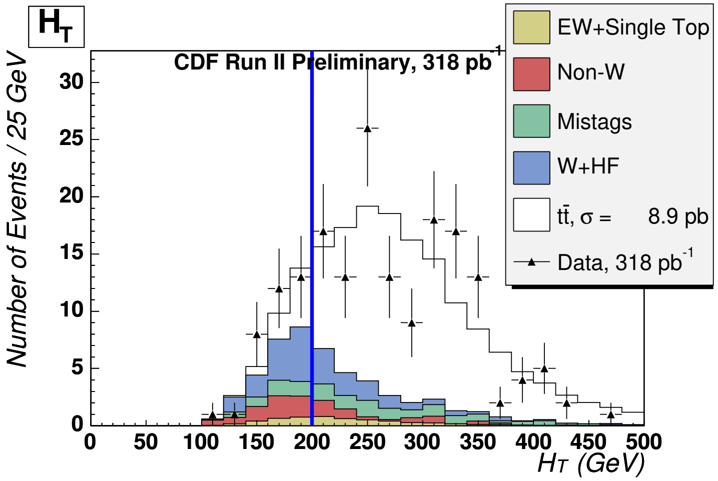

Figure 40: Comparison of H_T between the data and the various background contributions and the expectation from $t\bar{t}$, taken from the *unoptimized* measured cross section of 8.9 pb.

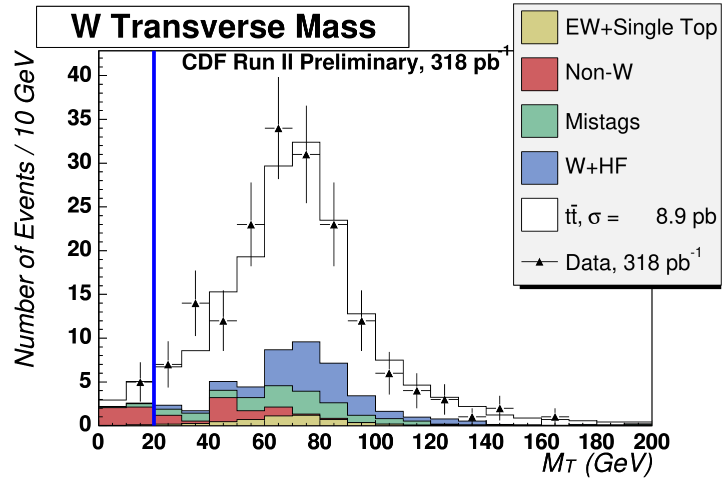

Figure 42: Comparison of M_T^W between the data and the various background contributions and the expectation from $t\bar{t}$, taken from the *unoptimized* measured cross section of 8.9 pb.

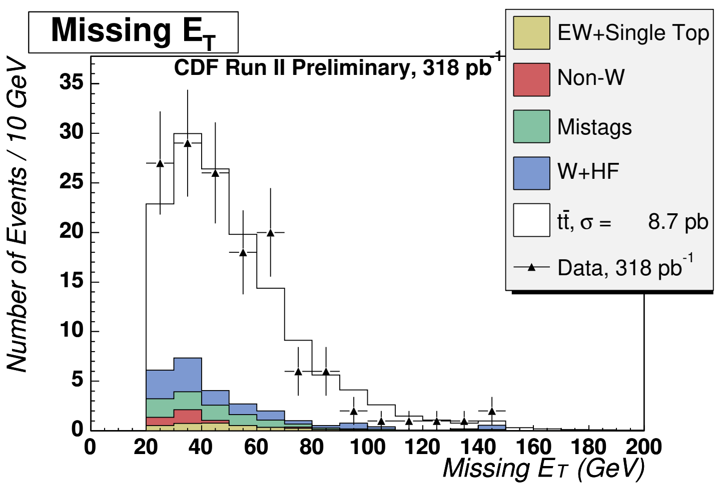

Figure 41: Comparison of $\not{E}_T$ between the data and the various background contributions and the expectation from $t\bar{t}$, taken from the *optimized* measured cross section of 8.8 pb.

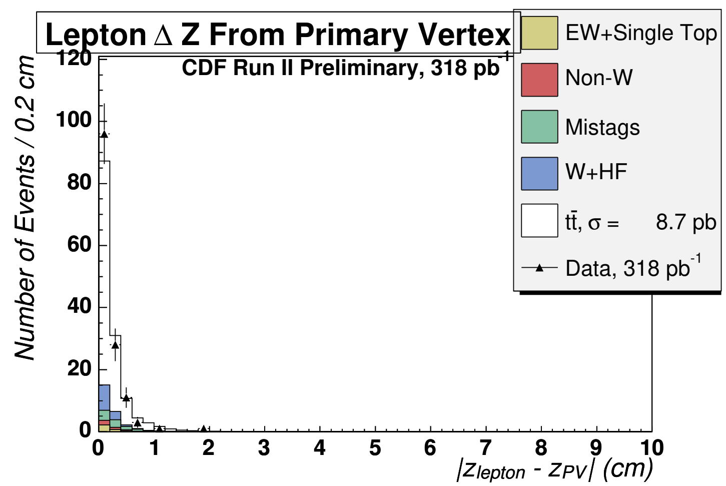

Figure 43: Comparison of $z_{lep} - z_{vtx}$ between the data and the various background contributions and the expectation from $t\bar{t}$, taken from the *optimized* measured cross section of 8.8 pb.

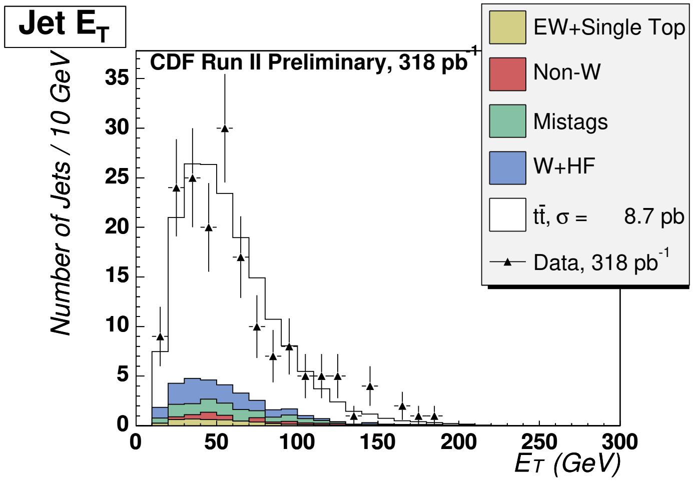

Figure 44: Comparison of jet E_T between the data and the various background contributions and the expectation from $t\bar{t}$, taken from the *optimized* measured cross section of 8.8 pb.

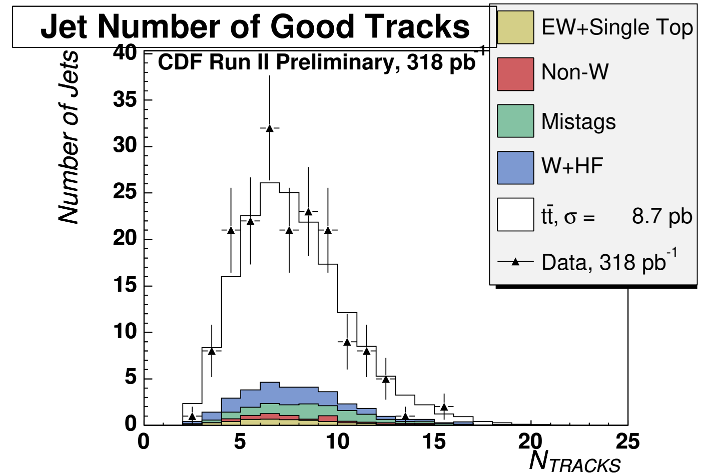

Figure 46: Comparison of jet N_{good} between the data and the various background contributions and the expectation from $t\bar{t}$, taken from the *optimized* measured cross section of 8.8 pb.

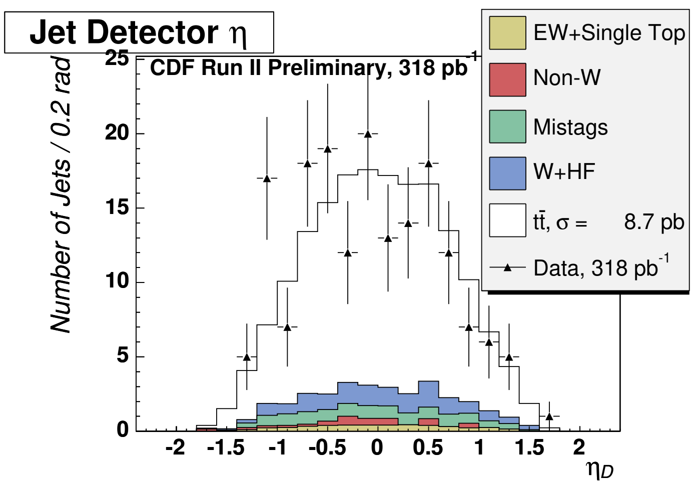

Figure 45: Comparison of jet η between the data and the various background contributions and the expectation from $t\bar{t}$, taken from the *optimized* measured cross section of 8.8 pb.

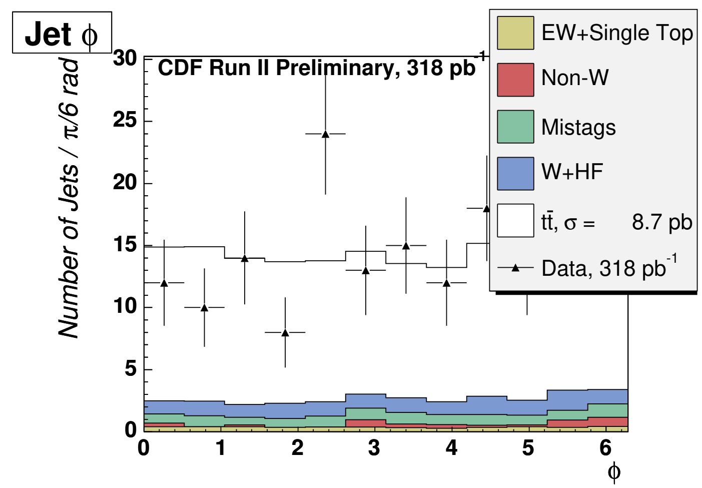

Figure 47: Comparison of jet ϕ between the data and the various background contributions and the expectation from $t\bar{t}$, taken from the *optimized* measured cross section of 8.8 pb.

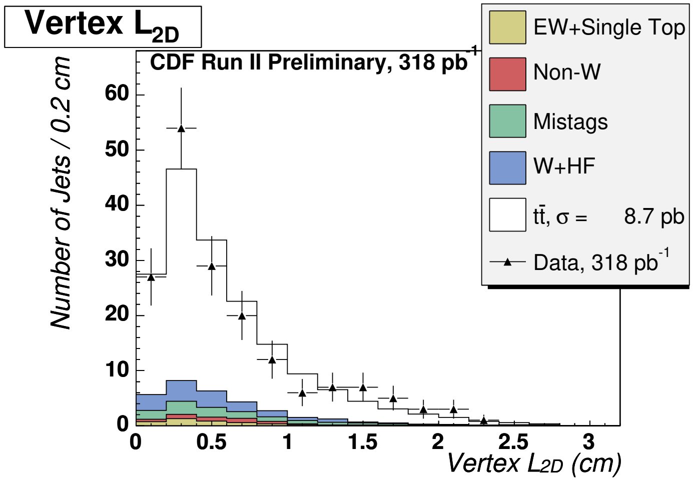

Figure 48: Comparison of vertex L_{2D} between the data and the various background contributions and the expectation from $t\bar{t}$, taken from the *optimized* measured cross section of 8.8 pb.

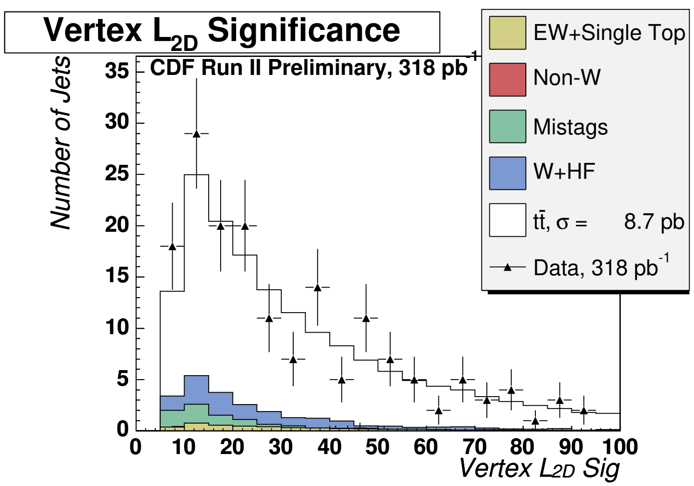

Figure 49: Comparison of vertex L_{2D} significance between the data and the various background contributions and the expectation from $t\bar{t}$, taken from the *optimized* measured cross section of 8.8 pb.

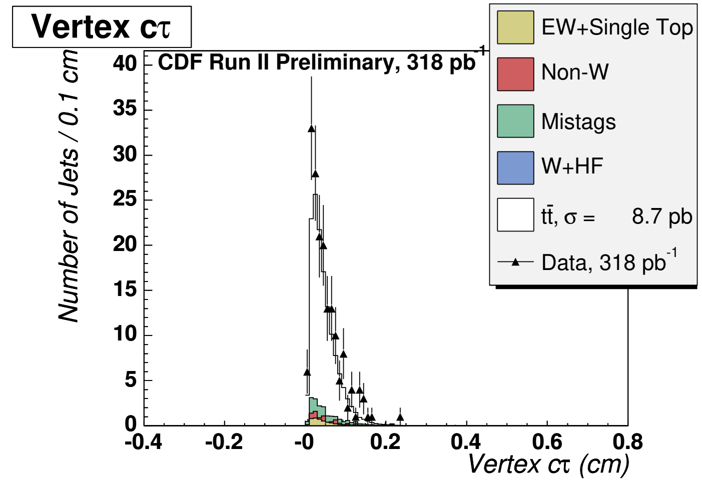

Figure 50: Comparison of vertex pseudo-$c\tau$ between the data and the various background contributions and the expectation from $t\bar{t}$, taken from the *optimized* measured cross section of 8.8 pb.

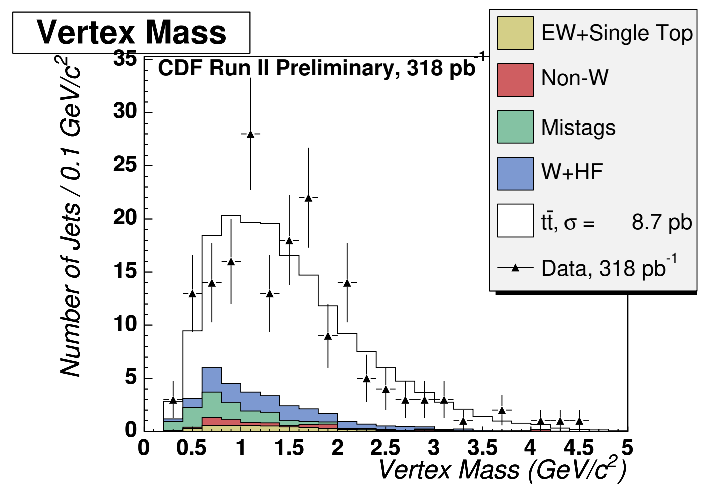

Figure 51: Comparison of vertex mass between the data and the various background contributions and the expectation from $t\bar{t}$, taken from the *optimized* measured cross section of 8.8 pb.

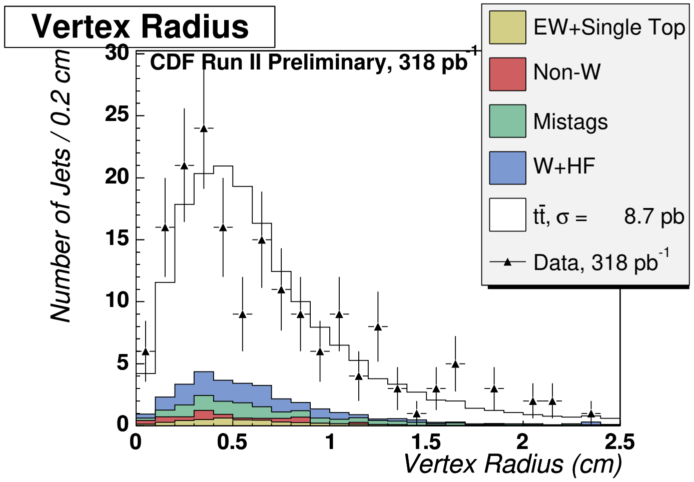

Figure 52: Comparison of vertex radius between the data and the various background contributions and the expectation from $t\bar{t}$, taken from the *optimized* measured cross section of 8.8 pb.

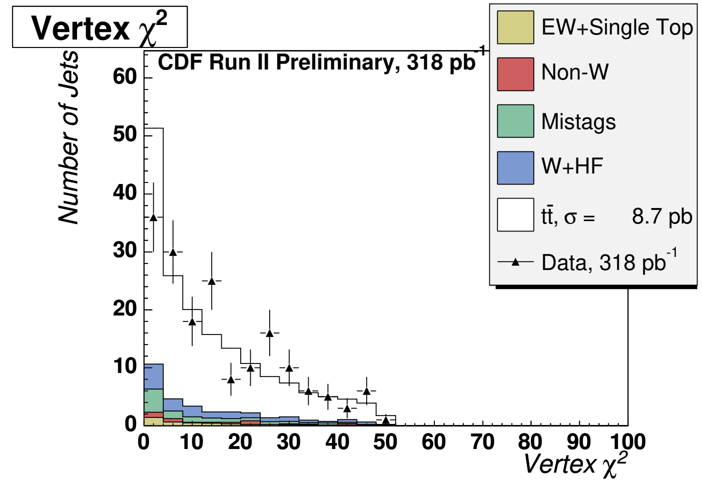

Figure 54: Comparison of vertex χ^2 between the data and the various background contributions and the expectation from $t\bar{t}$, taken from the *optimized* measured cross section of 8.8 pb.

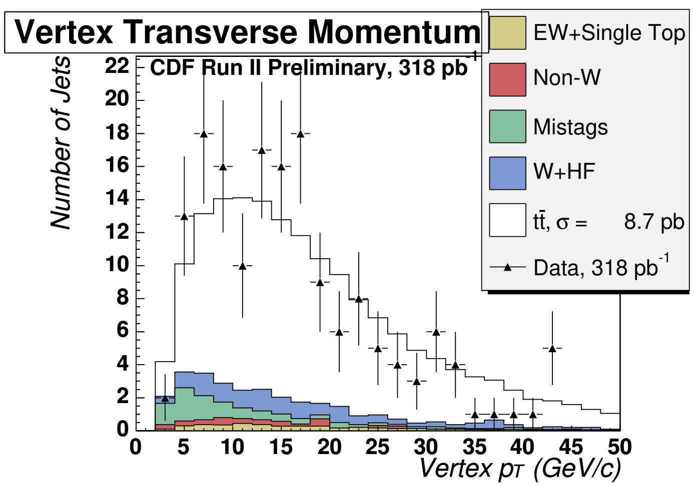

Figure 53: Comparison of vertex transverse momentum between the data and the various background contributions and the expectation from $t\bar{t}$, taken from the *optimized* measured cross section of 8.8 pb.

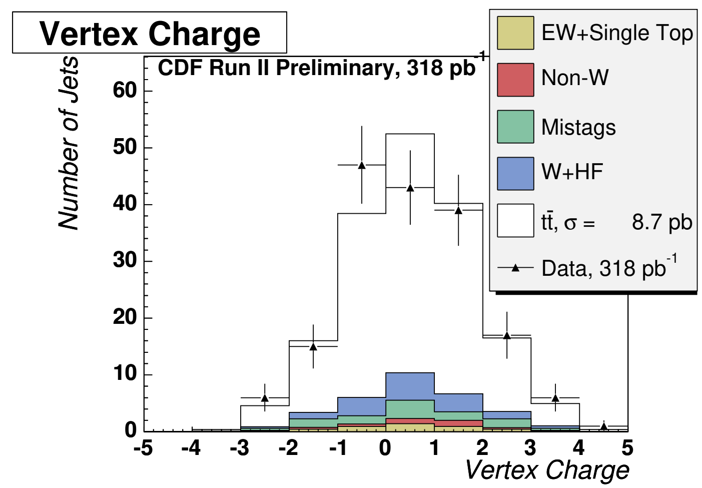

Figure 55: Comparison of vertex charge between the data and the various background contributions and the expectation from $t\bar{t}$, taken from the *optimized* measured cross section of 8.8 pb.

Channel	0-jet	1-jet	2-jet	3-jet	4-jet	≥5-jet	Total
			CEM				
Stage 0 INITIAL	888	16286	90293	218306	327888	496382	1150043
Stage 1 OBSV	868	15789	87418	210316	315204	477050	1106645
Stage 2 TRIGGER	868	15789	87418	210316	315204	477050	1106645
Stage 3 ≥1TLEP	267	4694	20939	32232	29308	12254	99694
Stage 4 MET	248	4316	19126	29009	26134	10254	89087
Stage 5 ISO	248	4251	18401	26508	22516	6896	78820
Stage 6 !DILEP	138	2515	13107	24939	22117	6799	69615
Stage 7 !Z	127	2294	12198	23706	21479	6605	66409
Stage 8 !CONV	127	2294	12198	23706	21479	6605	66409
Stage 9 !DIFFZ	127	2294	12198	23706	21476	6604	66405
Stage 10 KIN VETOS	0	2249	11882	19809	20162	6382	60484
Stage 11 SI GOOD	0	2249	11882	19809	20162	6382	60484
Stage 12 TAGGABLE	0	1815	10950	18854	19402	6181	57202
Stage 13 ≥1+BTAG	0	824	6453	12383	13371	4267	37298
Stage 14 ≥2+BTAG	0	0	1309	3309	4158	1392	10168
Stage 15 ≥1-BTAG	0	18	209	436	427	198	1288
Stage 16 ≥1+-BTAG	0	0	67	198	225	123	613
Stage 17 ≥2-BTAG	0	0	1	4	4	4	13
Stage 18 LTAGGABLE	0	1855	11084	18978	19524	6218	57659
Stage 19 ≥1+LTAG	0	961	7418	13981	15040	4800	42200
Stage 20 ≥2+LTAG	0	0	1869	4664	5887	1976	14396
Stage 21 ≥1-LTAG	0	40	427	976	1044	463	2950
Stage 22 ≥1+-LTAG	0	0	161	541	664	321	1687
Stage 23 ≥2-LTAG	0	0	5	22	26	21	74
			CMUP				
Stage 0 INITIAL	888	16286	90293	218306	327888	496382	1150043
Stage 1 OBSV	868	15789	87418	210316	315204	477050	1106645
Stage 2 TRIGGER	868	15789	87418	210316	315204	477050	1106645
Stage 3 ≥1TLEP	188	3160	14047	21180	18780	6781	64136
Stage 4 MET	172	2922	12762	18958	16494	5946	57254
Stage 5 ISO	166	2770	11811	16780	14015	4247	49789
Stage 6 !DILEP	88	1596	8243	15789	13746	4195	43657
Stage 7 !Z	82	1485	7810	15332	13516	4132	42357
Stage 8 !COSMIC	82	1485	7810	15332	13516	4132	42357
Stage 9 !DIFFZ	82	1485	7809	15331	13510	4130	42347
Stage 10 KIN VETOS	0	1439	7493	12680	12514	3928	38054
Stage 11 SI GOOD	0	1439	7493	12680	12514	3928	38054
Stage 12 TAGGABLE	0	1147	6919	12044	12070	3798	35978
Stage 13 ≥1+BTAG	0	513	4082	7822	8315	2621	23353
Stage 14 ≥2+BTAG	0	0	852	2011	2626	871	6360
Stage 15 ≥1-BTAG	0	10	121	309	299	109	848
Stage 16 ≥1+-BTAG	0	0	36	135	161	69	401
Stage 17 ≥2-BTAG	0	0	0	1	2	2	5
Stage 18 LTAGGABLE	0	1180	7001	12136	12139	3820	36276
Stage 19 ≥1+LTAG	0	608	4691	8857	9312	2973	26441
Stage 20 ≥2+LTAG	0	0	1208	2906	3717	1226	9057
Stage 21 ≥1-LTAG	0	22	250	636	683	266	1857
Stage 22 ≥1+-LTAG	0	0	88	316	423	175	1002
Stage 23 ≥2-LTAG	0	0	2	7	18	6	33
			CMX				
Stage 0 INITIAL	888	16286	90293	218306	327888	496382	1150043
Stage 1 OBSV	868	15789	87418	210316	315204	477050	1106645
Stage 2 TRIGGER	868	15789	87418	210316	315204	477050	1106645
Stage 3 ≥1TLEP	70	1079	4807	7184	6278	2346	21764
Stage 4 MET	64	981	4376	6412	5519	2046	19398
Stage 5 ISO	61	921	3974	5638	4623	1444	16661
Stage 6 !DILEP	31	493	2718	5264	4543	1426	14475
Stage 7 !Z	28	460	2590	5099	4463	1408	14048
Stage 8 !COSMIC	28	460	2590	5099	4463	1408	14048
Stage 9 !DIFFZ	28	460	2588	5098	4463	1407	14044
Stage 10 KIN VETOS	0	456	2579	4275	4273	1389	12972
Stage 11 SI GOOD	0	456	2579	4275	4273	1389	12972
Stage 12 TAGGABLE	0	374	2415	4113	4136	1342	12380
Stage 13 ≥1+BTAG	0	163	1432	2703	2925	931	8154
Stage 14 ≥2+BTAG	0	0	292	690	948	307	2237
Stage 15 ≥1-BTAG	0	8	38	107	93	39	285
Stage 16 ≥1+-BTAG	0	0	10	43	58	24	135
Stage 17 ≥2-BTAG	0	0	0	0	2	1	3
Stage 18 LTAGGABLE	0	387	2442	4145	4153	1348	12475
Stage 19 ≥1+LTAG	0	192	1647	3055	3255	1059	9208
Stage 20 ≥2+LTAG	0	0	408	1004	1336	427	3175
Stage 21 ≥1-LTAG	0	10	90	199	244	100	643
Stage 22 ≥1+-LTAG	0	0	32	91	145	71	339
Stage 23 ≥2-LTAG	0	0	0	2	5	3	10

Table 28: Event counts at each successive stage for `ttopel` top Monte Carlo, with $m_{top} = 178\ GeV/c^2$.

Channel	Total	evqqbb	mvqqbb	tvqqbb	evevbb	mvmvbb	tvtvbb	evmvbb	evtvbb	mvtvbb	qqqqbb
CEM											
Stage 0 INITIAL	1150043	168044	167958	167694	13446	13312	13587	26963	26950	27170	524919
Stage 1 OBSV	1106645	161714	161679	161329	12981	12824	13099	25931	25942	26094	505052
Stage 2 TRIGGER	1106645	161714	161679	161329	12981	12824	13099	25931	25942	26094	505052
Stage 3 $\geq$1TLEP	99694	61468	639	5437	8087	50	875	10023	10433	877	1805
Stage 4 MET	89087	55280	588	4665	7430	47	792	9248	9578	795	664
Stage 5 ISO	78820	49102	156	3793	6940	20	683	8559	8807	688	72
Stage 5 $\geq$3jets	55920	43666	125	3376	2966	1	283	1604	3699	128	72
Stage 6 !DILEP	53855	43336	97	3351	2427	0	263	721	3521	67	72
Stage 7 !Z	51790	42435	96	3297	1834	0	243	616	3146	57	66
Stage 8 !CONV	51790	42435	96	3297	1834	0	243	616	3146	57	66
Stage 9 !DIFFZ	51786	42431	96	3297	1834	0	243	616	3146	57	66
Stage 10 KIN VETOS	46353	38767	72	2594	1584	0	162	494	2589	39	52
Stage 11 SI GOOD	46353	38767	72	2594	1584	0	162	494	2589	39	52
Stage 12 TAGGABLE	44437	37245	68	2491	1487	0	150	459	2453	35	49
Stage 13 $\geq$1+BTAG	30021	25066	40	1664	1036	0	110	328	1730	25	22
Stage 14 $\geq$2+BTAG	8859	7388	14	488	289	0	32	108	527	7	6
Stage 15 $\geq$1-BTAG	1061	885	4	69	33	0	1	9	54	3	3
Stage 16 $\geq$1+-BTAG	546	457	3	36	12	0	1	4	30	1	2
Stage 17 $\geq$2-BTAG	12	11	0	1	0	0	0	0	0	0	0
Stage 18 LTAGGABLE	44720	37467	69	2504	1500	0	151	468	2475	35	51
Stage 19 $\geq$1+LTAG	33821	28247	45	1864	1157	0	122	371	1959	26	30
Stage 20 $\geq$2+LTAG	12527	10447	16	698	405	0	49	146	744	11	11
Stage 21 $\geq$1-LTAG	2483	2100	5	159	68	0	7	18	118	4	4
Stage 22 $\geq$1+-LTAG	1526	1294	3	97	33	0	7	11	77	1	3
Stage 23 $\geq$2-LTAG	69	58	2	4	2	0	0	0	2	0	1
CMUP											
Stage 0 INITIAL	1150043	168044	167958	167694	13446	13312	13587	26963	26950	27170	524919
Stage 1 OBSV	1106645	161714	161679	161329	12981	12824	13099	25931	25942	26094	505052
Stage 2 TRIGGER	1106645	161714	161679	161329	12981	12824	13099	25931	25942	26094	505052
Stage 3 $\geq$1TLEP	64136	313	39640	3339	16	5556	574	6419	526	6791	962
Stage 4 MET	57254	272	35095	2917	13	5145	515	5836	481	6196	784
Stage 5 ISO	49789	10	30724	2341	0	4854	451	5313	419	5671	6
Stage 5 $\geq$3jets	35042	7	27260	2096	0	921	194	2097	160	2301	6
Stage 6 !DILEP	33730	6	27051	2087	0	491	183	1609	119	2178	6
Stage 7 !Z	32980	6	26746	2075	0	432	175	1423	105	2012	6
Stage 8 !COSMIC	32980	6	26746	2075	0	432	175	1423	105	2012	6
Stage 9 !DIFFZ	32971	6	26737	2075	0	432	175	1423	105	2012	6
Stage 10 KIN VETOS	29122	5	24232	1481	0	334	113	1230	68	1655	4
Stage 11 SI GOOD	29122	5	24232	1481	0	334	113	1230	68	1655	4
Stage 12 TAGGABLE	27912	5	23301	1406	0	316	102	1151	65	1562	4
Stage 13 $\geq$1+BTAG	18758	3	15594	942	0	227	71	795	45	1077	4
Stage 14 $\geq$2+BTAG	5508	0	4586	271	0	66	22	226	11	325	1
Stage 15 $\geq$1-BTAG	717	0	606	30	0	4	3	31	1	42	0
Stage 16 $\geq$1+-BTAG	365	0	309	14	0	3	1	17	1	20	0
Stage 17 $\geq$2-BTAG	5	0	5	0	0	0	0	0	0	0	0
Stage 18 LTAGGABLE	28095	5	23447	1413	0	319	106	1163	66	1572	4
Stage 19 $\geq$1+LTAG	21142	3	17587	1067	0	250	74	894	50	1213	4
Stage 20 $\geq$2+LTAG	7849	0	6570	377	0	90	29	318	17	446	2
Stage 21 $\geq$1-LTAG	1585	0	1350	84	0	12	6	57	2	74	0
Stage 22 $\geq$1+-LTAG	914	0	778	48	0	5	1	35	2	45	0
Stage 23 $\geq$2-LTAG	31	0	31	0	0	0	0	0	0	0	0
CMX											
Stage 0 INITIAL	1150043	168044	167958	167694	13446	13312	13587	26963	26950	27170	524919
Stage 1 OBSV	1106645	161714	161679	161329	12981	12824	13099	25931	25942	26094	505052
Stage 2 TRIGGER	1106645	161714	161679	161329	12981	12824	13099	25931	25942	26094	505052
Stage 3 $\geq$1TLEP	21764	146	13221	1133	12	1981	143	2146	183	2331	468
Stage 4 MET	19398	128	11725	963	10	1831	126	1964	160	2125	366
Stage 5 ISO	16661	1	10273	739	0	1691	105	1771	141	1938	2
Stage 5 $\geq$3jets	11705	0	9122	654	0	321	52	711	52	791	2
Stage 6 !DILEP	11233	0	9068	651	0	143	48	534	34	753	2
Stage 7 !Z	10970	0	8974	644	0	124	46	457	32	691	2
Stage 8 !COSMIC	10970	0	8974	644	0	124	46	457	32	691	2
Stage 9 !DIFFZ	10968	0	8972	644	0	124	46	457	32	691	2
Stage 10 KIN VETOS	9937	0	8242	579	0	104	29	408	27	546	2
Stage 11 SI GOOD	9937	0	8242	579	0	104	29	408	27	546	2
Stage 12 TAGGABLE	9591	0	7968	554	0	100	28	390	24	525	2
Stage 13 $\geq$1+BTAG	6559	0	5434	370	0	78	22	271	15	367	2
Stage 14 $\geq$2+BTAG	1945	0	1636	88	0	24	7	79	3	107	1
Stage 15 $\geq$1-BTAG	239	0	199	11	0	3	2	9	1	14	0
Stage 16 $\geq$1+-BTAG	125	0	108	7	0	2	1	3	0	4	0
Stage 17 $\geq$2-BTAG	3	0	3	0	0	0	0	0	0	0	0
Stage 18 LTAGGABLE	9646	0	8008	556	0	102	28	393	24	533	2
Stage 19 $\geq$1+LTAG	7369	0	6104	429	0	81	24	301	18	410	2
Stage 20 $\geq$2+LTAG	2767	0	2317	139	0	35	10	101	4	160	1
Stage 21 $\geq$1-LTAG	543	0	467	25	0	5	2	14	2	28	0
Stage 22 $\geq$1+-LTAG	307	0	267	17	0	3	1	6	1	12	0
Stage 23 $\geq$2-LTAG	10	0	10	0	0	0	0	0	0	0	0

Table 29: Event counts at each successive stage for `ttopel` top Monte Carlo, with $m_{top} = 178\ GeV/c^2$, for the ≥ 3 jet bin for each decay type.

Channel	Total	evqqbb	mvqqbb	tvqqbb	evevbb	mvmvbb	tvtvbb	evmvbb	evtvbb	mvtvbb	qqqqbb
CEM											
Stage 0 INITIAL	1150043	168044	167958	167694	13446	13312	13587	26963	26950	27170	524919
Stage 1 OBSV	1106645	161714	161679	161329	12981	12824	13099	25931	25942	26094	505052
Stage 2 TRIGGER	1106645	161714	161679	161329	12981	12824	13099	25931	25942	26094	505052
Stage 3 $\geq$1TLEP	99694	61468	639	5437	8087	50	875	10023	10433	877	1805
Stage 4 MET	89087	55280	588	4665	7430	47	792	9248	9578	795	664
Stage 5 ISO	78820	49102	156	3793	6940	20	683	8559	8807	688	72
Stage 5 $\geq$4jets	29412	25645	63	1965	610	1	65	234	748	20	61
Stage 6 !DILEP	28916	25462	54	1954	491	0	61	110	713	10	61
Stage 7 !Z	28084	24911	54	1921	376	0	55	90	615	7	55
Stage 8 !CONV	28084	24911	54	1921	376	0	55	90	615	7	55
Stage 9 !DIFFZ	28080	24907	54	1921	376	0	55	90	615	7	55
Stage 10 KIN VETOS	26544	23795	41	1615	352	0	48	82	559	5	47
Stage 11 SI GOOD	26544	23795	41	1615	352	0	48	82	559	5	47
Stage 12 TAGGABLE	25583	22952	38	1551	334	0	47	74	538	5	44
Stage 13 $\geq$1+BTAG	17638	15831	22	1070	238	0	35	47	369	4	22
Stage 14 $\geq$2+BTAG	5550	5008	9	321	66	0	9	14	117	0	6
Stage 15 $\geq$1-BTAG	625	553	2	43	7	0	1	2	13	1	3
Stage 16 $\geq$1+-BTAG	348	311	2	23	3	0	1	0	5	1	2
Stage 17 $\geq$2-BTAG	8	8	0	0	0	0	0	0	0	0	0
Stage 18 LTAGGABLE	25742	23088	38	1563	337	0	47	76	542	5	46
Stage 19 $\geq$1+LTAG	19840	17829	26	1172	261	0	38	60	422	4	28
Stage 20 $\geq$2+LTAG	7863	7081	9	466	98	0	16	21	160	1	11
Stage 21 $\geq$1-LTAG	1507	1341	2	107	17	0	1	6	28	1	4
Stage 22 $\geq$1+-LTAG	985	884	2	65	9	0	1	4	16	1	3
Stage 23 $\geq$2-LTAG	47	40	1	2	1	0	0	0	2	0	1
CMUP											
Stage 0 INITIAL	1150043	168044	167958	167694	13446	13312	13587	26963	26950	27170	524919
Stage 1 OBSV	1106645	161714	161679	161329	12981	12824	13099	25931	25942	26094	505052
Stage 2 TRIGGER	1106645	161714	161679	161329	12981	12824	13099	25931	25942	26094	505052
Stage 3 $\geq$1TLEP	64136	313	39640	3339	16	5556	574	6419	526	6791	962
Stage 4 MET	57254	272	35095	2917	13	5145	515	5836	481	6196	784
Stage 5 ISO	49789	10	30724	2341	0	4854	451	5313	419	5671	6
Stage 5 $\geq$4jets	18262	5	15965	1186	0	178	38	410	25	449	6
Stage 6 !DILEP	17941	5	15840	1181	0	95	36	335	18	425	6
Stage 7 !Z	17648	5	15650	1176	0	87	33	290	17	384	6
Stage 8 !COSMIC	17648	5	15650	1176	0	87	33	290	17	384	6
Stage 9 !DIFFZ	17640	5	15642	1176	0	87	33	290	17	384	6
Stage 10 KIN VETOS	16442	4	14815	891	0	76	26	265	14	347	4
Stage 11 SI GOOD	16442	4	14815	891	0	76	26	265	14	347	4
Stage 12 TAGGABLE	15868	4	14318	854	0	75	25	247	14	327	4
Stage 13 $\geq$1+BTAG	10936	2	9868	586	0	59	19	165	12	221	4
Stage 14 $\geq$2+BTAG	3497	0	3156	194	0	15	5	52	5	69	1
Stage 15 $\geq$1-BTAG	408	0	364	22	0	0	1	9	0	12	0
Stage 16 $\geq$1+-BTAG	230	0	204	11	0	0	1	7	0	7	0
Stage 17 $\geq$2-BTAG	4	0	4	0	0	0	0	0	0	0	0
Stage 18 LTAGGABLE	15959	4	14402	856	0	75	26	250	14	328	4
Stage 19 $\geq$1+LTAG	12285	2	11092	658	0	65	21	184	12	247	4
Stage 20 $\geq$2+LTAG	4943	0	4479	258	0	22	8	72	8	94	2
Stage 21 $\geq$1-LTAG	949	0	861	53	0	1	2	14	0	18	0
Stage 22 $\geq$1+-LTAG	598	0	541	32	0	0	1	10	0	14	0
Stage 23 $\geq$2-LTAG	24	0	24	0	0	0	0	0	0	0	0
CMX											
Stage 0 INITIAL	1150043	168044	167958	167694	13446	13312	13587	26963	26950	27170	524919
Stage 1 OBSV	1106645	161714	161679	161329	12981	12824	13099	25931	25942	26094	505052
Stage 2 TRIGGER	1106645	161714	161679	161329	12981	12824	13099	25931	25942	26094	505052
Stage 3 $\geq$1TLEP	21764	146	13221	1133	12	1981	143	2146	183	2331	468
Stage 4 MET	19398	128	11725	963	10	1831	126	1964	160	2125	366
Stage 5 ISO	16661	1	10273	739	0	1691	105	1771	141	1938	2
Stage 5 $\geq$4jets	6067	0	5311	377	0	50	10	145	9	163	2
Stage 6 !DILEP	5969	0	5279	375	0	24	10	113	8	158	2
Stage 7 !Z	5871	0	5225	368	0	23	9	93	8	143	2
Stage 8 !COSMIC	5871	0	5225	368	0	23	9	93	8	143	2
Stage 9 !DIFFZ	5870	0	5224	368	0	23	9	93	8	143	2
Stage 10 KIN VETOS	5662	0	5060	351	0	21	8	85	8	127	2
Stage 11 SI GOOD	5662	0	5060	351	0	21	8	85	8	127	2
Stage 12 TAGGABLE	5478	0	4898	336	0	21	8	85	7	121	2
Stage 13 $\geq$1+BTAG	3856	0	3438	234	0	16	6	65	5	90	2
Stage 14 $\geq$2+BTAG	1255	0	1137	61	0	4	3	20	1	28	1
Stage 15 $\geq$1-BTAG	132	0	114	8	0	2	1	3	0	4	0
Stage 16 $\geq$1+-BTAG	82	0	71	6	0	2	1	2	0	0	0
Stage 17 $\geq$2-BTAG	3	0	3	0	0	0	0	0	0	0	0
Stage 18 LTAGGABLE	5501	0	4919	336	0	21	8	85	7	123	2
Stage 19 $\geq$1+LTAG	4314	0	3848	268	0	17	7	71	5	96	2
Stage 20 $\geq$2+LTAG	1763	0	1593	94	0	7	3	27	1	37	1
Stage 21 $\geq$1-LTAG	344	0	306	18	0	4	1	4	1	10	0
Stage 22 $\geq$1+-LTAG	216	0	188	16	0	3	1	3	1	4	0
Stage 23 $\geq$2-LTAG	8	0	8	0	0	0	0	0	0	0	0

Table 30: Event counts at each successive stage for `ttopel` top Monte Carlo, with $m_{top} = 178\ GeV/c^2$, for the ≥ 4 jet bin for each decay type.

Channel	0-jet	1-jet	2-jet	3-jet	4-jet	≥5-jet	Total
CEM							
Stage 0 INITIAL	557801	313245	230088	31576	4707	703	1138120
Stage 1 GOODRUN	557801	313245	230088	31576	4707	703	1138120
Stage 2 TRIGGER	286581	214598	184723	23046	3290	468	712706
Stage 3 ≥1TLEP	286581	210845	183236	22700	3229	455	707046
Stage 4 MET	179837	26552	7593	1868	392	87	216329
Stage 5 ISO	179837	18696	3159	549	130	23	202394
Stage 6 !DILEP	179701	18569	3101	527	128	22	202048
Stage 7 !Z	177993	17653	2848	469	115	20	199098
Stage 8 !CONV	177993	17653	2848	469	115	20	199098
Stage 9 !DIFFZ	177843	17648	2846	469	115	19	198940
Stage 10 KIN VETOS	177843	17648	2846	469	115	19	198940
Stage 11 SI GOOD	0	17648	2846	469	115	19	21097
Stage 12 TAGGABLE	0	11773	2481	433	112	19	14818
Stage 13 ≥1+BTAG	0	249	142	59	39	8	497
Stage 14 ≥2+BTAG	0	0	10	11	7	1	29
Stage 15 ≥1-BTAG	0	62	24	8	3	1	98
Stage 16 ≥1+-BTAG	0	0	1	2	1	1	5
Stage 17 ≥2-BTAG	0	0	0	0	0	0	0
Stage 18 LTAGGABLE	0	12161	2514	434	112	19	15240
Stage 19 ≥1+LTAG	0	447	212	78	47	12	796
Stage 20 ≥2+LTAG	0	0	20	18	12	2	52
Stage 21 ≥1-LTAG	0	140	74	22	11	2	249
Stage 22 ≥1+-LTAG	0	0	3	4	3	2	12
Stage 23 ≥2-LTAG	0	0	0	0	0	0	0
CMUP							
Stage 0 INITIAL	557801	313245	230088	31576	4707	703	1138120
Stage 1 GOODRUN	557801	313245	230088	31576	4707	703	1138120
Stage 2 TRIGGER	150614	45689	15701	3013	485	85	215587
Stage 3 ≥1TLEP	150267	45471	15520	2966	468	81	214773
Stage 4 MET	111651	21748	8174	1896	308	58	143835
Stage 5 ISO	106975	9548	1419	230	49	12	118233
Stage 6 !DILEP	103508	9115	1348	212	48	12	114243
Stage 7 !Z	99009	8630	1280	207	46	11	109183
Stage 8 !COSMIC	93507	8612	1277	207	46	11	103660
Stage 9 !DIFFZ	91131	8514	1263	202	46	11	101167
Stage 10 KIN VETOS	91131	8514	1263	202	46	11	101167
Stage 11 SI GOOD	0	8514	1263	202	46	11	10036
Stage 12 TAGGABLE	0	5573	1085	191	45	10	6904
Stage 13 ≥1+BTAG	0	110	66	25	18	7	226
Stage 14 ≥2+BTAG	0	0	5	5	6	2	18
Stage 15 ≥1-BTAG	0	27	12	2	1	0	42
Stage 16 ≥1+-BTAG	0	0	0	0	0	0	0
Stage 17 ≥2-BTAG	0	0	0	0	0	0	0
Stage 18 LTAGGABLE	0	5754	1099	192	45	10	7100
Stage 19 ≥1+LTAG	0	177	98	35	23	8	341
Stage 20 ≥2+LTAG	0	0	11	7	10	2	30
Stage 21 ≥1-LTAG	0	60	32	5	2	0	99
Stage 22 ≥1+-LTAG	0	0	1	0	0	0	1
Stage 23 ≥2-LTAG	0	0	1	1	0	0	2
CMX							
Stage 0 INITIAL	557801	313245	230088	31576	4707	703	1138120
Stage 1 GOODRUN	536748	302000	221601	30391	4540	684	1095964
Stage 2 TRIGGER	92725	28998	10548	1989	296	51	134607
Stage 3 ≥1TLEP	91042	28253	10140	1918	281	50	131684
Stage 4 MET	65140	13331	5116	1119	178	30	84914
Stage 5 ISO	61929	5107	790	117	21	6	67970
Stage 6 !DILEP	60352	4885	741	106	19	6	66109
Stage 7 !Z	58218	4659	710	104	18	6	63715
Stage 8 !COSMIC	57566	4655	710	103	18	6	63058
Stage 9 !DIFFZ	52061	4466	682	98	18	6	57331
Stage 10 KIN VETOS	52061	4466	682	98	18	6	57331
Stage 11 SI GOOD	0	4466	682	98	18	6	5270
Stage 12 TAGGABLE	0	2993	586	89	17	6	3691
Stage 13 ≥1+BTAG	0	73	34	11	6	4	128
Stage 14 ≥2+BTAG	0	0	0	1	3	0	4
Stage 15 ≥1-BTAG	0	11	7	1	0	0	19
Stage 16 ≥1+-BTAG	0	0	0	0	0	0	0
Stage 17 ≥2-BTAG	0	0	0	0	0	0	0
Stage 18 LTAGGABLE	0	3084	596	91	17	6	3794
Stage 19 ≥1+LTAG	0	106	52	14	8	4	184
Stage 20 ≥2+LTAG	0	0	0	2	4	2	8
Stage 21 ≥1-LTAG	0	33	16	3	0	0	52
Stage 22 ≥1+-LTAG	0	0	2	0	0	0	2
Stage 23 ≥2-LTAG	0	0	0	0	0	0	0

Table 31: Event counts at each successive stage for the data sample.

Corrections to Pretag data					
	1 jet	2 jets	3 jets	4 jets	$\geq$ 5 jets
Data	30283.00 $\pm$ 0.00	4676.00 $\pm$ 0.00	324.00 $\pm$ 0.00	142.00 $\pm$ 0.00	34.00 $\pm$ 0.00
Non-W	2018.18 $\pm$ 506.23	406.89 $\pm$ 103.52	18.21 $\pm$ 5.57	8.38 $\pm$ 2.57	1.79 $\pm$ 0.55
$t\bar{t}$ (8.7 pb)	8.80 $\pm$ 0.83	47.13 $\pm$ 4.45	79.67 $\pm$ 7.51	79.48 $\pm$ 7.49	25.16 $\pm$ 2.39
EW	154.17 $\pm$ 14.85	148.47 $\pm$ 14.20	13.81 $\pm$ 1.40	3.77 $\pm$ 0.36	0.76 $\pm$ 0.07
Single Top	18.44 $\pm$ 4.49	22.89 $\pm$ 5.01	2.74 $\pm$ 0.58	0.58 $\pm$ 0.13	0.09 $\pm$ 0.02
Data, Corrected	28083.42 $\pm$ 523.16	4050.62 $\pm$ 123.78	209.57 $\pm$ 14.18	49.79 $\pm$ 10.21	6.20 $\pm$ 2.96

Table 32: Corrections to pretag data for the W+HF background estimate. After an initial measurement, the $t\bar{t}$ cross section is input back into this calculation, and the process is iterated until the result is stable to 1%.

$t\bar{t}$ (8.7 pb)					
	1 jet	2 jets	3 jets	4 jets	$\geq$ 5 jets
$\epsilon_{b-jet}(\%)$	44.44 ± 0.80	44.85 ± 0.26	45.37 ± 0.19	45.07 ± 0.18	43.91 ± 0.31
$\epsilon_{c-jet}(\%)$	10.39 ± 2.46	10.37 ± 0.57	10.23 ± 0.28	9.46 ± 0.21	9.77 ± 0.36
$\epsilon_{b-jet} * SF(\%)$	40.40 ± 2.76	40.77 ± 2.70	41.24 ± 2.73	40.97 ± 2.71	39.91 ± 2.65
$\epsilon_{c-jet} * SF(\%)$	9.44 ± 2.56	9.43 ± 1.35	9.30 ± 1.25	8.60 ± 1.15	8.88 ± 1.22
$\Phi_e^{\geq 1}(\%)$	91.04 ± 6.14	92.67 ± 5.22	93.34 ± 5.00	93.81 ± 4.76	94.17 ± 4.77
$\Phi_e^{\geq 2}(\%)$	0.00 ± 0.00	83.21 ± 11.41	84.57 ± 11.59	85.22 ± 11.44	86.43 ± 11.45
$\epsilon_{\geq 1}(\%)$	36.72 ± 0.70	54.92 ± 0.32	62.49 ± 0.24	66.90 ± 0.23	67.07 ± 0.41
$\epsilon_{\geq 2}$ (%)	0.00 ± 0.00	11.28 ± 0.20	16.42 ± 0.18	21.08 ± 0.20	22.00 ± 0.36
$\epsilon_{\geq 1} * \Phi_e$ (%)	33.43 ± 2.34	50.89 ± 2.88	58.33 ± 3.13	62.76 ± 3.19	63.16 ± 3.22
$\epsilon_{\geq 2} * \Phi_e(\%)$	0.00 ± 0.00	9.39 ± 1.30	13.89 ± 1.91	17.96 ± 2.42	19.01 ± 2.54
$\epsilon_{bjet}(\%)$				45.03 ± 0.12	
$\epsilon_{cjet}(\%)$				9.76 ± 0.15	
$\epsilon_{bjet} * SF(\%)$				40.93 ± 2.70	
$\epsilon_{cjet} * SF(\%)$				8.87 ± 1.18	
$\epsilon_{\geq 1}(\%)$				65.02 ± 0.15	
$\epsilon_{\geq 2}(\%)$				19.20 ± 0.13	
$\Phi_E^1(\%)$				93.71 ± 4.84	
$\Phi_E^2(\%)$				85.25 ± 11.49	
$\epsilon_{\geq 1}(\%) * \Phi_E^1$				60.93 ± 3.15	
$\epsilon_{\geq 2}(\%) * \Phi_E^2$				16.37 ± 2.21	
CEM					
ϵ_{Pretag}	0.21 ± 0.00	1.07 ± 0.01	1.80 ± 0.01	1.83 ± 0.01	0.58 ± 0.01
$\epsilon_{Pretag} * SF$	0.19 ± 0.01	0.98 ± 0.07	1.65 ± 0.12	1.67 ± 0.12	0.53 ± 0.04
ϵ_{pretag}				4.21 ± 0.02	
$\epsilon_{pretag} * SF$				3.84 ± 0.29	
Pretag	5.19 ± 0.49	27.05 ± 2.58	45.60 ± 4.33	46.15 ± 4.39	14.65 ± 1.41
$\geq$ 1+ Tag	1.74 ± 0.20	13.77 ± 1.53	26.60 ± 2.90	28.97 ± 3.12	9.26 ± 1.01
$\geq$ 2+ Tag	0.00 ± 0.00	2.54 ± 0.43	6.33 ± 1.06	8.29 ± 1.37	2.79 ± 0.46
CMUP					
ϵ_{Pretag}	0.13 ± 0.00	0.69 ± 0.01	1.17 ± 0.01	1.15 ± 0.01	0.36 ± 0.01
$\epsilon_{Pretag} * SF$	0.10 ± 0.01	0.52 ± 0.04	0.89 ± 0.07	0.87 ± 0.07	0.27 ± 0.02
ϵ_{pretag}				2.68 ± 0.02	
$\epsilon_{pretag} * SF$				2.02 ± 0.15	
Pretag	2.66 ± 0.25	14.45 ± 1.40	24.52 ± 2.35	24.03 ± 2.30	7.48 ± 0.75
$\geq$ 1+ Tag	0.89 ± 0.11	7.36 ± 0.82	14.30 ± 1.57	15.08 ± 1.64	4.73 ± 0.53
$\geq$ 2+ Tag	0.00 ± 0.00	1.36 ± 0.23	3.41 ± 0.57	4.32 ± 0.71	1.42 ± 0.24
CMX					
ϵ_{Pretag}	0.04 ± 0.00	0.23 ± 0.00	0.40 ± 0.01	0.39 ± 0.01	0.13 ± 0.00
$\epsilon_{Pretag} * SF$	0.04 ± 0.00	0.21 ± 0.02	0.36 ± 0.03	0.35 ± 0.03	0.11 ± 0.01
ϵ_{pretag}				0.90 ± 0.01	
$\epsilon_{pretag} * SF$				0.82 ± 0.06	
Pretag	0.94 ± 0.09	5.63 ± 0.53	9.55 ± 0.93	9.30 ± 0.91	3.03 ± 0.29
$\geq$ 1+ Tag	0.32 ± 0.04	2.86 ± 0.32	5.57 ± 0.62	5.84 ± 0.65	1.91 ± 0.21
$\geq$ 2+ Tag	0.00 ± 0.00	0.53 ± 0.09	1.33 ± 0.22	1.67 ± 0.28	0.58 ± 0.09
Total					
Pretag	8.80 ± 0.83	47.13 ± 4.45	79.67 ± 7.51	79.48 ± 7.49	25.16 ± 2.39
$\geq$ 1 Tag	2.94 ± 0.35	23.99 ± 2.64	46.47 ± 5.04	49.88 ± 5.34	15.89 ± 1.72
$\geq$ 2 Tag	0.00 ± 0.00	4.42 ± 0.74	11.06 ± 1.84	14.28 ± 2.35	4.78 ± 0.78

Table 33: Summary table for $t\bar{t}$ at the measured cross section of 8.8 pb. ϵ_{q-jet} is the MC per-jet efficiency to tag a jet with flavor q, $\epsilon_{q-jet}SF$ is the efficiency times b-tag scale factor (0.909 ± 0.060), Φ_E is the "effective event scale factor", $\epsilon_{\geq 1}$ is the $\geq$ 1 event efficiency in the data, and similarly for $\geq$ 2. ϵ_{pretag} is the lepton ID efficiency in the Monte Carlo, and $\epsilon_{pretag} * SF$ is the pretag efficiency times the product of the pretag data-to-Monte Carlo scale factors.

Data					
	1 jet	2 jets	3 jets	4 jets	$\geq$ 5 jets
CEM					
Pretag	17448.00 $\pm$ 0.00	2780.00 $\pm$ 0.00	197.00 $\pm$ 0.00	95.00 $\pm$ 0.00	18.00 $\pm$ 0.00
$\geq 1+$ Tag	246.00 $\pm$ 0.00	137.00 $\pm$ 0.00	40.00 $\pm$ 0.00	34.00 $\pm$ 0.00	8.00 $\pm$ 0.00
$\geq 2+$ Tag	0.00 $\pm$ 0.00	10.00 $\pm$ 0.00	10.00 $\pm$ 0.00	6.00 $\pm$ 0.00	1.00 $\pm$ 0.00
$\geq 1-$ Tag	61.00 $\pm$ 0.00	23.00 $\pm$ 0.00	4.00 $\pm$ 0.00	3.00 $\pm$ 0.00	1.00 $\pm$ 0.00
$\geq 1+-$ Tag	0.00 $\pm$ 0.00	1.00 $\pm$ 0.00	1.00 $\pm$ 0.00	1.00 $\pm$ 0.00	1.00 $\pm$ 0.00
$\geq 2-$ Tag	0.00 $\pm$ 0.00	0.00 $\pm$ 0.00	0.00 $\pm$ 0.00	0.00 $\pm$ 0.00	0.00 $\pm$ 0.00
CMUP					
Pretag	8383.00 $\pm$ 0.00	1219.00 $\pm$ 0.00	86.00 $\pm$ 0.00	34.00 $\pm$ 0.00	10.00 $\pm$ 0.00
$\geq 1+$ Tag	108.00 $\pm$ 0.00	61.00 $\pm$ 0.00	14.00 $\pm$ 0.00	18.00 $\pm$ 0.00	6.00 $\pm$ 0.00
$\geq 2+$ Tag	0.00 $\pm$ 0.00	5.00 $\pm$ 0.00	4.00 $\pm$ 0.00	6.00 $\pm$ 0.00	2.00 $\pm$ 0.00
$\geq 1-$ Tag	25.00 $\pm$ 0.00	10.00 $\pm$ 0.00	2.00 $\pm$ 0.00	1.00 $\pm$ 0.00	0.00 $\pm$ 0.00
$\geq 1+-$ Tag	0.00 $\pm$ 0.00	0.00 $\pm$ 0.00	0.00 $\pm$ 0.00	0.00 $\pm$ 0.00	0.00 $\pm$ 0.00
$\geq 2-$ Tag	0.00 $\pm$ 0.00	0.00 $\pm$ 0.00	0.00 $\pm$ 0.00	0.00 $\pm$ 0.00	0.00 $\pm$ 0.00
CMX					
Pretag	4452.00 $\pm$ 0.00	677.00 $\pm$ 0.00	41.00 $\pm$ 0.00	13.00 $\pm$ 0.00	6.00 $\pm$ 0.00
$\geq 1+$ Tag	73.00 $\pm$ 0.00	34.00 $\pm$ 0.00	8.00 $\pm$ 0.00	6.00 $\pm$ 0.00	4.00 $\pm$ 0.00
$\geq 2+$ Tag	0.00 $\pm$ 0.00	0.00 $\pm$ 0.00	1.00 $\pm$ 0.00	3.00 $\pm$ 0.00	0.00 $\pm$ 0.00
$\geq 1-$ Tag	11.00 $\pm$ 0.00	7.00 $\pm$ 0.00	0.00 $\pm$ 0.00	0.00 $\pm$ 0.00	0.00 $\pm$ 0.00
$\geq 1+-$ Tag	0.00 $\pm$ 0.00	0.00 $\pm$ 0.00	0.00 $\pm$ 0.00	0.00 $\pm$ 0.00	0.00 $\pm$ 0.00
$\geq 2-$ Tag	0.00 $\pm$ 0.00	0.00 $\pm$ 0.00	0.00 $\pm$ 0.00	0.00 $\pm$ 0.00	0.00 $\pm$ 0.00
Total					
Pretag	30283.00 $\pm$ 0.00	4676.00 $\pm$ 0.00	324.00 $\pm$ 0.00	142.00 $\pm$ 0.00	34.00 $\pm$ 0.00
≥ 1 Tag	427.00 $\pm$ 0.00	232.00 $\pm$ 0.00	62.00 $\pm$ 0.00	58.00 $\pm$ 0.00	18.00 $\pm$ 0.00
≥ 2 Tag	0.00 $\pm$ 0.00	15.00 $\pm$ 0.00	15.00 $\pm$ 0.00	15.00 $\pm$ 0.00	3.00 $\pm$ 0.00
$\geq 1-$ Tag	97.00 $\pm$ 0.00	40.00 $\pm$ 0.00	6.00 $\pm$ 0.00	4.00 $\pm$ 0.00	1.00 $\pm$ 0.00
$\geq 1+-$ Tag	0.00 $\pm$ 0.00	1.00 $\pm$ 0.00	1.00 $\pm$ 0.00	1.00 $\pm$ 0.00	1.00 $\pm$ 0.00
$\geq 2-$ Tag	0.00 $\pm$ 0.00	0.00 $\pm$ 0.00	0.00 $\pm$ 0.00	0.00 $\pm$ 0.00	0.00 $\pm$ 0.00

Table 34: Event yields for 318.5 pb^{-1}.

WW					
	1 jet	2 jets	3 jets	4 jets	$\geq$ 5 jets
$\epsilon_{b-jet}(\%)$	41.94 ± 8.86	37.25 ± 4.79	54.00 ± 7.05	33.33 ± 11.11	30.00 ± 14.49
$\epsilon_{c-jet}(\%)$	7.74 ± 0.47	8.43 ± 0.33	9.31 ± 1.10	7.00 ± 1.80	8.33 ± 3.99
$\epsilon_{b-jet} * SF(\%)$	38.12 ± 8.44	33.86 ± 4.89	49.09 ± 7.18	30.30 ± 10.30	27.27 ± 13.29
$\epsilon_{c-jet} * SF(\%)$	7.04 ± 1.02	7.66 ± 1.06	8.46 ± 1.50	6.36 ± 1.84	7.57 ± 3.76
$\Phi_e^{\geq 1}(\%)$	90.90 ± 12.21	90.93 ± 12.12	91.13 ± 11.39	91.51 ± 10.98	92.23 ± 9.54
$\Phi_e^{\geq 2}(\%)$	0.00 ± 0.00	82.63 ± 18.57	82.65 ± 17.98	82.79 ± 17.88	83.08 ± 17.17
$\epsilon_{\geq 1}(\%)$	2.06 ± 0.11	4.41 ± 0.16	7.20 ± 0.66	5.65 ± 1.12	11.63 ± 3.46
$\epsilon_{\geq 2}$ (%)	0.00 ± 0.00	0.04 ± 0.01	0.13 ± 0.09	0.00 ± 0.00	1.16 ± 1.16
$\epsilon_{\geq 1} * \Phi_e$ (%)	1.87 ± 0.27	4.01 ± 0.55	6.56 ± 1.02	5.17 ± 1.20	10.73 ± 3.38
$\epsilon_{\geq 2} * \Phi_e(\%)$	0.00 ± 0.00	0.03 ± 0.01	0.11 ± 0.08	0.00 ± 0.00	0.96 ± 0.98
$\epsilon_{bjet}(\%)$				46.15 ± 5.64	
$\epsilon_{cjet}(\%)$				8.77 ± 0.92	
$\epsilon_{bjet} * SF(\%)$				41.95 ± 5.83	
$\epsilon_{cjet} * SF(\%)$				7.97 ± 1.34	
$\epsilon_{\geq 1}(\%)$				7.06 ± 0.57	
$\epsilon_{\geq 2}(\%)$				0.15 ± 0.09	
$\Phi_E^1(\%)$				91.33 ± 11.12	
$\Phi_E^2(\%)$				82.82 ± 17.72	
$\epsilon_{\geq 1}(\%) * \Phi_E^1$				6.45 ± 0.94	
$\epsilon_{\geq 2}(\%) * \Phi_E^2$				0.12 ± 0.08	
CEM					
ϵ_{Pretag}	1.91 ± 0.02	1.89 ± 0.02	0.17 ± 0.01	0.04 ± 0.00	0.01 ± 0.00
$\epsilon_{Pretag} * SF$	1.74 ± 0.13	1.73 ± 0.13	0.16 ± 0.01	0.04 ± 0.00	0.01 ± 0.00
ϵ_{pretag}				0.23 ± 0.01	
$\epsilon_{pretag} * SF$				0.21 ± 0.02	
Pretag	73.58 ± 7.16	72.88 ± 7.09	6.55 ± 0.70	1.66 ± 0.17	0.36 ± 0.04
$\geq$ 1+ Tag	1.38 ± 0.24	2.92 ± 0.49	0.43 ± 0.08	0.09 ± 0.02	0.04 ± 0.01
$\geq$ 2+ Tag	0.00 ± 0.00	0.02 ± 0.01	0.01 ± 0.01	0.00 ± 0.00	0.00 ± 0.00
CMUP					
ϵ_{Pretag}	1.19 ± 0.02	1.12 ± 0.02	0.11 ± 0.00	0.03 ± 0.00	0.01 ± 0.00
$\epsilon_{Pretag} * SF$	0.90 ± 0.07	0.85 ± 0.07	0.08 ± 0.01	0.02 ± 0.00	0.01 ± 0.00
ϵ_{pretag}				0.14 ± 0.01	
$\epsilon_{pretag} * SF$				0.11 ± 0.01	
Pretag	37.88 ± 3.74	35.83 ± 3.55	3.48 ± 0.40	0.92 ± 0.09	0.29 ± 0.03
$\geq$ 1+ Tag	0.71 ± 0.12	1.44 ± 0.24	0.23 ± 0.04	0.05 ± 0.01	0.03 ± 0.01
$\geq$ 2+ Tag	0.00 ± 0.00	0.01 ± 0.00	0.00 ± 0.00	0.00 ± 0.00	0.00 ± 0.00
CMX					
ϵ_{Pretag}	0.49 ± 0.01	0.45 ± 0.01	0.04 ± 0.00	0.01 ± 0.00	0.00 ± 0.00
$\epsilon_{Pretag} * SF$	0.44 ± 0.03	0.41 ± 0.03	0.04 ± 0.00	0.01 ± 0.00	0.00 ± 0.00
ϵ_{pretag}				0.06 ± 0.00	
$\epsilon_{pretag} * SF$				0.05 ± 0.01	
Pretag	17.81 ± 1.77	16.64 ± 1.66	1.44 ± 0.14	0.53 ± 0.05	0.00 ± 0.00
$\geq$ 1+ Tag	0.33 ± 0.06	0.67 ± 0.11	0.09 ± 0.02	0.03 ± 0.01	0.00 ± 0.00
$\geq$ 2+ Tag	0.00 ± 0.00	0.01 ± 0.00	0.00 ± 0.00	0.00 ± 0.00	0.00 ± 0.00
Total					
Pretag	129.26 ± 12.32	125.35 ± 11.95	11.48 ± 1.15	3.10 ± 0.30	0.65 ± 0.06
$\geq$ 1 Tag	2.42 ± 0.42	5.03 ± 0.84	0.75 ± 0.14	0.16 ± 0.04	0.07 ± 0.02
$\geq$ 2 Tag	0.00 ± 0.00	0.04 ± 0.01	0.01 ± 0.01	0.00 ± 0.00	0.01 ± 0.01

Table 35: Summary table for WW. See Table 33 for a description of the variables.

WZ					
	1 jet	2 jets	3 jets	4 jets	$\geq$ 5 jets
$\epsilon_{b-jet}(\%)$	41.05 $\pm$ 1.10	40.49 $\pm$ 0.81	39.47 $\pm$ 2.52	39.29 $\pm$ 4.61	47.83 $\pm$ 10.42
$\epsilon_{c-jet}(\%)$	7.42 $\pm$ 0.78	9.31 $\pm$ 0.57	12.62 $\pm$ 1.89	11.43 $\pm$ 3.10	12.90 $\pm$ 6.02
$\epsilon_{b-jet} * SF(\%)$	37.31 $\pm$ 2.66	36.81 $\pm$ 2.54	35.88 $\pm$ 3.29	35.71 $\pm$ 4.81	43.48 $\pm$ 9.90
$\epsilon_{c-jet} * SF(\%)$	6.74 $\pm$ 1.14	8.46 $\pm$ 1.23	11.47 $\pm$ 2.29	10.39 $\pm$ 3.13	11.73 $\pm$ 5.69
$\Phi_e^{\geq 1}(\%)$	90.90 $\pm$ 6.90	92.08 $\pm$ 6.43	92.31 $\pm$ 6.45	92.42 $\pm$ 6.47	92.42 $\pm$ 7.22
$\Phi_e^{\geq 2}(\%)$	0.00 $\pm$ 0.00	82.63 $\pm$ 11.74	82.84 $\pm$ 11.58	83.05 $\pm$ 11.78	82.80 $\pm$ 12.15
$\epsilon_{\geq 1}(\%)$	10.79 $\pm$ 0.33	16.03 $\pm$ 0.37	17.84 $\pm$ 1.23	20.15 $\pm$ 2.43	20.63 $\pm$ 5.10
$\epsilon_{\geq 2}$ $(\%)$	0.00 $\pm$ 0.00	2.00 $\pm$ 0.14	2.58 $\pm$ 0.51	2.56 $\pm$ 0.96	4.76 $\pm$ 2.68
$\epsilon_{\geq 1} * \Phi_e$ $(\%)$	9.81 $\pm$ 0.80	14.76 $\pm$ 1.09	16.47 $\pm$ 1.62	18.62 $\pm$ 2.60	19.07 $\pm$ 4.94
$\epsilon_{\geq 2} * \Phi_e(\%)$	0.00 $\pm$ 0.00	1.65 $\pm$ 0.26	2.14 $\pm$ 0.52	2.13 $\pm$ 0.85	3.94 $\pm$ 2.29
$\epsilon_{bjet}(\%)$				39.80 $\pm$ 2.17	
$\epsilon_{cjet}(\%)$				12.36 $\pm$ 1.56	
$\epsilon_{bjet} * SF(\%)$				36.18 $\pm$ 3.10	
$\epsilon_{cjet} * SF(\%)$				11.24 $\pm$ 2.05	
$\epsilon_{\geq 1}(\%)$				18.45 $\pm$ 1.07	
$\epsilon_{\geq 2}(\%)$				2.68 $\pm$ 0.45	
$\Phi_E^1(\%)$				92.35 $\pm$ 6.50	
$\Phi_E^2(\%)$				82.90 $\pm$ 11.67	
$\epsilon_{\geq 1}(\%) * \Phi_E^1$				17.04 $\pm$ 1.55	
$\epsilon_{\geq 2}(\%) * \Phi_E^2$				2.22 $\pm$ 0.49	
CEM					
ϵ_{Pretag}	0.93 $\pm$ 0.02	1.06 $\pm$ 0.02	0.11 $\pm$ 0.01	0.03 $\pm$ 0.00	0.01 $\pm$ 0.00
$\epsilon_{Pretag} * SF$	0.85 $\pm$ 0.07	0.97 $\pm$ 0.07	0.10 $\pm$ 0.01	0.03 $\pm$ 0.00	0.01 $\pm$ 0.00
ϵ_{pretag}				0.14 $\pm$ 0.01	
$\epsilon_{pretag} * SF$				0.13 $\pm$ 0.01	
Pretag	10.74 $\pm$ 1.06	12.17 $\pm$ 1.19	1.21 $\pm$ 0.14	0.33 $\pm$ 0.03	0.11 $\pm$ 0.01
$\geq$ 1+ Tag	1.05 $\pm$ 0.13	1.80 $\pm$ 0.22	0.20 $\pm$ 0.03	0.06 $\pm$ 0.01	0.02 $\pm$ 0.01
$\geq$ 2+ Tag	0.00 $\pm$ 0.00	0.20 $\pm$ 0.04	0.03 $\pm$ 0.01	0.01 $\pm$ 0.00	0.00 $\pm$ 0.00
CMUP					
ϵ_{Pretag}	0.58 $\pm$ 0.01	0.64 $\pm$ 0.01	0.06 $\pm$ 0.00	0.02 $\pm$ 0.00	0.00 $\pm$ 0.00
$\epsilon_{Pretag} * SF$	0.44 $\pm$ 0.03	0.48 $\pm$ 0.04	0.04 $\pm$ 0.01	0.02 $\pm$ 0.00	0.00 $\pm$ 0.00
ϵ_{pretag}				0.09 $\pm$ 0.01	
$\epsilon_{pretag} * SF$				0.07 $\pm$ 0.01	
Pretag	5.52 $\pm$ 0.54	6.07 $\pm$ 0.59	0.57 $\pm$ 0.08	0.21 $\pm$ 0.02	0.00 $\pm$ 0.00
$\geq$ 1+ Tag	0.54 $\pm$ 0.07	0.90 $\pm$ 0.11	0.09 $\pm$ 0.02	0.04 $\pm$ 0.01	0.00 $\pm$ 0.00
$\geq$ 2+ Tag	0.00 $\pm$ 0.00	0.10 $\pm$ 0.02	0.01 $\pm$ 0.00	0.00 $\pm$ 0.00	0.00 $\pm$ 0.00
CMX					
ϵ_{Pretag}	0.22 $\pm$ 0.01	0.25 $\pm$ 0.01	0.03 $\pm$ 0.00	0.01 $\pm$ 0.00	0.00 $\pm$ 0.00
$\epsilon_{Pretag} * SF$	0.20 $\pm$ 0.02	0.23 $\pm$ 0.02	0.02 $\pm$ 0.00	0.01 $\pm$ 0.00	0.00 $\pm$ 0.00
ϵ_{pretag}				0.04 $\pm$ 0.00	
$\epsilon_{pretag} * SF$				0.03 $\pm$ 0.00	
Pretag	2.37 $\pm$ 0.25	2.79 $\pm$ 0.29	0.30 $\pm$ 0.03	0.08 $\pm$ 0.01	0.00 $\pm$ 0.00
$\geq$ 1+ Tag	0.23 $\pm$ 0.03	0.41 $\pm$ 0.05	0.05 $\pm$ 0.01	0.01 $\pm$ 0.00	0.00 $\pm$ 0.00
$\geq$ 2+ Tag	0.00 $\pm$ 0.00	0.05 $\pm$ 0.01	0.01 $\pm$ 0.00	0.00 $\pm$ 0.00	0.00 $\pm$ 0.00
Total					
Pretag	18.63 $\pm$ 1.79	21.03 $\pm$ 2.01	2.08 $\pm$ 0.22	0.62 $\pm$ 0.06	0.11 $\pm$ 0.01
$\geq$ 1 Tag	1.83 $\pm$ 0.23	3.10 $\pm$ 0.37	0.34 $\pm$ 0.05	0.11 $\pm$ 0.02	0.02 $\pm$ 0.01
$\geq$ 2 Tag	0.00 $\pm$ 0.00	0.35 $\pm$ 0.06	0.04 $\pm$ 0.01	0.01 $\pm$ 0.01	0.00 $\pm$ 0.00

Table 36: Summary table for WZ. See Table 33 for a description of the variables.

ZZ					
	1 jet	2 jets	3 jets	4 jets	$\geq$ 5 jets
$\epsilon_{b-jet}(\%)$	30.12 ± 5.04	46.86 ± 3.03	40.98 ± 6.30	33.33 ± 10.29	28.57 ± 17.07
$\epsilon_{c-jet}(\%)$	9.30 ± 3.13	7.01 ± 1.75	9.26 ± 3.94	10.53 ± 7.04	0.00 ± 0.00
$\epsilon_{b-jet} * SF(\%)$	27.38 ± 4.92	42.60 ± 3.94	37.25 ± 6.23	30.30 ± 9.56	25.97 ± 15.61
$\epsilon_{c-jet} * SF(\%)$	8.45 ± 3.06	6.37 ± 1.80	8.42 ± 3.75	9.57 ± 6.52	0.00 ± 0.00
$\Phi_e^{\geq 1}(\%)$	90.90 ± 9.84	92.39 ± 8.44	92.50 ± 8.57	92.73 ± 8.34	92.79 ± 6.51
$\Phi_e^{\geq 2}(\%)$	0.00 ± 0.00	82.63 ± 14.88	82.86 ± 14.94	82.75 ± 15.02	82.63 ± 14.77
$\epsilon_{\geq 1}(\%)$	4.98 ± 0.78	15.56 ± 1.29	14.84 ± 2.63	20.41 ± 5.76	12.50 ± 8.27
$\epsilon_{\geq 2}$ (%)	0.00 ± 0.00	3.57 ± 0.66	2.75 ± 1.21	2.04 ± 2.02	0.00 ± 0.00
$\epsilon_{\geq 1} * \Phi_e$ (%)	4.53 ± 0.86	14.38 ± 1.77	13.73 ± 2.75	18.93 ± 5.61	11.60 ± 7.72
$\epsilon_{\geq 2} * \Phi_e(\%)$	0.00 ± 0.00	2.95 ± 0.76	2.28 ± 1.08	1.69 ± 1.70	0.00 ± 0.00
$\epsilon_{bjet}(\%)$				38.20 ± 5.15	
$\epsilon_{cjet}(\%)$				8.97 ± 3.24	
$\epsilon_{bjet} * SF(\%)$				34.72 ± 5.21	
$\epsilon_{cjet} * SF(\%)$				8.15 ± 3.14	
$\epsilon_{\geq 1}(\%)$				15.79 ± 2.32	
$\epsilon_{\geq 2}(\%)$				2.43 ± 0.98	
$\Phi_E^1(\%)$				92.59 ± 8.29	
$\Phi_E^2(\%)$				82.80 ± 14.94	
$\epsilon_{\geq 1}(\%) * \Phi_E^1$				14.62 ± 2.52	
$\epsilon_{\geq 2}(\%) * \Phi_E^2$				2.01 ± 0.89	
CEM					
ϵ_{Pretag}	0.07 ± 0.00	0.06 ± 0.00	0.02 ± 0.00	0.01 ± 0.00	0.00 ± 0.00
$\epsilon_{Pretag} * SF$	0.06 ± 0.00	0.06 ± 0.00	0.02 ± 0.00	0.01 ± 0.00	0.00 ± 0.00
ϵ_{pretag}				0.03 ± 0.00	
$\epsilon_{pretag} * SF$				0.02 ± 0.00	
Pretag	0.31 ± 0.03	0.30 ± 0.03	0.09 ± 0.01	0.03 ± 0.00	0.00 ± 0.00
$\geq$ 1+ Tag	0.01 ± 0.00	0.04 ± 0.01	0.01 ± 0.00	0.00 ± 0.00	0.00 ± 0.00
$\geq$ 2+ Tag	0.00 ± 0.00	0.01 ± 0.00	0.00 ± 0.00	0.00 ± 0.00	0.00 ± 0.00
CMUP					
ϵ_{Pretag}	0.08 ± 0.00	0.07 ± 0.00	0.02 ± 0.00	0.01 ± 0.00	0.00 ± 0.00
$\epsilon_{Pretag} * SF$	0.06 ± 0.00	0.06 ± 0.00	0.01 ± 0.00	0.00 ± 0.00	0.00 ± 0.00
ϵ_{pretag}				0.02 ± 0.00	
$\epsilon_{pretag} * SF$				0.02 ± 0.00	
Pretag	0.29 ± 0.03	0.28 ± 0.03	0.06 ± 0.01	0.02 ± 0.00	0.00 ± 0.00
$\geq$ 1+ Tag	0.01 ± 0.00	0.04 ± 0.01	0.01 ± 0.00	0.00 ± 0.00	0.00 ± 0.00
$\geq$ 2+ Tag	0.00 ± 0.00	0.01 ± 0.00	0.00 ± 0.00	0.00 ± 0.00	0.00 ± 0.00
CMX					
ϵ_{Pretag}	0.03 ± 0.00	0.03 ± 0.00	0.01 ± 0.00	0.00 ± 0.00	0.00 ± 0.00
$\epsilon_{Pretag} * SF$	0.03 ± 0.00	0.03 ± 0.00	0.00 ± 0.00	0.00 ± 0.00	0.00 ± 0.00
ϵ_{pretag}				0.01 ± 0.00	
$\epsilon_{pretag} * SF$				0.00 ± 0.00	
Pretag	0.13 ± 0.01	0.12 ± 0.01	0.02 ± 0.00	0.00 ± 0.00	0.00 ± 0.00
$\geq$ 1+ Tag	0.01 ± 0.00	0.02 ± 0.00	0.00 ± 0.00	0.00 ± 0.00	0.00 ± 0.00
$\geq$ 2+ Tag	0.00 ± 0.00	0.00 ± 0.00	0.00 ± 0.00	0.00 ± 0.00	0.00 ± 0.00
Total					
Pretag	0.73 ± 0.07	0.70 ± 0.07	0.17 ± 0.02	0.05 ± 0.01	0.00 ± 0.00
$\geq$ 1 Tag	0.03 ± 0.01	0.10 ± 0.02	0.02 ± 0.01	0.01 ± 0.00	0.00 ± 0.00
$\geq$ 2 Tag	0.00 ± 0.00	0.02 ± 0.01	0.00 ± 0.00	0.00 ± 0.00	0.00 ± 0.00

Table 37: Summary table for ZZ. See Table 33 for a description of the variables.

$Z \to \tau\tau$					
	1 jet	2 jets	3 jets	4 jets	$\geq$ 5 jets
$\epsilon_{b-jet}(\%)$	47.62 ± 10.90	40.00 ± 10.95	0.00 ± 0.00	0.00 ± 0.00	0.00 ± 0.00
$\epsilon_{c-jet}(\%)$	6.98 ± 3.88	10.00 ± 5.48	14.29 ± 13.23	0.00 ± 0.00	0.00 ± 0.00
$\epsilon_{b-jet} * SF(\%)$	43.29 ± 10.31	36.36 ± 10.24	0.00 ± 0.00	0.00 ± 0.00	0.00 ± 0.00
$\epsilon_{c-jet} * SF(\%)$	6.34 ± 3.63	9.09 ± 5.12	12.99 ± 12.15	0.00 ± 0.00	0.00 ± 0.00
$\Phi_e^{\geq 1}(\%)$	90.90 ± 22.66	91.49 ± 20.78	92.15 ± 23.39	0.00 ± 0.00	0.00 ± 0.00
$\Phi_e^{\geq 2}(\%)$	0.00 ± 0.00	82.63 ± 32.97	82.63 ± 34.20	0.00 ± 0.00	0.00 ± 0.00
$\epsilon_{\geq 1}(\%)$	2.02 ± 0.33	3.86 ± 0.89	11.11 ± 6.05	0.00 ± 0.00	0.00 ± 0.00
$\epsilon_{\geq 2}$ (%)	0.00 ± 0.00	0.00 ± 0.00	0.00 ± 0.00	0.00 ± 0.00	0.00 ± 0.00
$\epsilon_{\geq 1} * \Phi_e$ (%)	1.84 ± 0.55	3.53 ± 1.14	10.24 ± 6.15	0.00 ± 0.00	0.00 ± 0.00
$\epsilon_{\geq 2} * \Phi_e(\%)$	0.00 ± 0.00	0.00 ± 0.00	0.00 ± 0.00	0.00 ± 0.00	0.00 ± 0.00
$\epsilon_{bjet}(\%)$			0.00 ± 0.00		
$\epsilon_{cjet}(\%)$			14.29 ± 13.23		
$\epsilon_{bjet} * SF(\%)$			0.00 ± 0.00		
$\epsilon_{cjet} * SF(\%)$			12.99 ± 12.15		
$\epsilon_{\geq 1}(\%)$			9.38 ± 5.15		
$\epsilon_{\geq 2}(\%)$			0.00 ± 0.00		
$\Phi_E^1(\%)$			92.15 ± 23.39		
$\Phi_E^2(\%)$			82.63 ± 34.20		
$\epsilon_{\geq 1}(\%) * \Phi_E^1$			8.64 ± 5.23		
$\epsilon_{\geq 2}(\%) * \Phi_E^2$			0.00 ± 0.00		
CEM					
ϵ_{Pretag}	0.09 ± 0.00	0.02 ± 0.00	0.00 ± 0.00	0.00 ± 0.00	0.00 ± 0.00
$\epsilon_{Pretag} * SF$	0.08 ± 0.01	0.02 ± 0.00	0.00 ± 0.00	0.00 ± 0.00	0.00 ± 0.00
ϵ_{pretag}			0.00 ± 0.00		
$\epsilon_{pretag} * SF$			0.00 ± 0.00		
Pretag	3.24 ± 0.49	0.75 ± 0.11	0.08 ± 0.02	0.00 ± 0.00	0.00 ± 0.00
$\geq$ 1+ Tag	0.06 ± 0.02	0.03 ± 0.01	0.01 ± 0.01	0.00 ± 0.00	0.00 ± 0.00
$\geq$ 2+ Tag	0.00 ± 0.00	0.00 ± 0.00	0.00 ± 0.00	0.00 ± 0.00	0.00 ± 0.00
CMUP					
ϵ_{Pretag}	0.05 ± 0.00	0.01 ± 0.00	0.00 ± 0.00	0.00 ± 0.00	0.00 ± 0.00
$\epsilon_{Pretag} * SF$	0.04 ± 0.00	0.01 ± 0.00	0.00 ± 0.00	0.00 ± 0.00	0.00 ± 0.00
ϵ_{pretag}			0.00 ± 0.00		
$\epsilon_{pretag} * SF$			0.00 ± 0.00		
Pretag	1.46 ± 0.22	0.41 ± 0.06	0.00 ± 0.00	0.00 ± 0.00	0.00 ± 0.00
$\geq$ 1+ Tag	0.03 ± 0.01	0.01 ± 0.01	0.00 ± 0.00	0.00 ± 0.00	0.00 ± 0.00
$\geq$ 2+ Tag	0.00 ± 0.00	0.00 ± 0.00	0.00 ± 0.00	0.00 ± 0.00	0.00 ± 0.00
CMX					
ϵ_{Pretag}	0.02 ± 0.00	0.01 ± 0.00	0.00 ± 0.00	0.00 ± 0.00	0.00 ± 0.00
$\epsilon_{Pretag} * SF$	0.02 ± 0.00	0.01 ± 0.00	0.00 ± 0.00	0.00 ± 0.00	0.00 ± 0.00
ϵ_{pretag}			0.00 ± 0.00		
$\epsilon_{pretag} * SF$			0.00 ± 0.00		
Pretag	0.84 ± 0.13	0.24 ± 0.04	0.00 ± 0.00	0.00 ± 0.00	0.00 ± 0.00
$\geq$ 1+ Tag	0.02 ± 0.01	0.01 ± 0.00	0.00 ± 0.00	0.00 ± 0.00	0.00 ± 0.00
$\geq$ 2+ Tag	0.00 ± 0.00	0.00 ± 0.00	0.00 ± 0.00	0.00 ± 0.00	0.00 ± 0.00
Total					
Pretag	5.55 ± 0.67	1.39 ± 0.17	0.08 ± 0.02	0.00 ± 0.00	0.00 ± 0.00
$\geq$ 1 Tag	0.10 ± 0.03	0.05 ± 0.02	0.01 ± 0.01	0.00 ± 0.00	0.00 ± 0.00
$\geq$ 2 Tag	0.00 ± 0.00	0.00 ± 0.00	0.00 ± 0.00	0.00 ± 0.00	0.00 ± 0.00

Table 38: Summary table for $Z \to \tau\tau$. See Table 33 for a description of the variables.

Single top, t-channel					
	1 jet	2 jets	3 jets	4 jets	$\geq$ 5 jets
$\epsilon_{b-jet}(\%)$	46.29 ± 0.41	45.95 ± 0.37	45.54 ± 0.92	42.44 ± 1.81	44.44 ± 4.14
$\epsilon_{c-jet}(\%)$	7.77 ± 1.93	6.88 ± 0.86	13.46 ± 3.35	9.76 ± 4.63	0.00 ± 0.00
$\epsilon_{b-jet} * SF(\%)$	42.08 ± 2.80	41.77 ± 2.78	41.40 ± 2.86	38.58 ± 3.03	40.40 ± 4.61
$\epsilon_{c-jet} * SF(\%)$	7.06 ± 1.99	6.25 ± 1.14	12.24 ± 3.45	8.87 ± 4.37	0.00 ± 0.00
$\Phi_e^{\geq 1}(\%)$	90.90 ± 6.04	91.23 ± 5.87	92.49 ± 5.11	93.02 ± 4.83	93.29 ± 4.78
$\Phi_e^{\geq 2}(\%)$	0.00 ± 0.00	82.63 ± 11.57	82.70 ± 11.03	82.80 ± 11.00	83.07 ± 10.83
$\epsilon_{\geq 1}(\%)$	39.53 ± 0.37	47.11 ± 0.38	58.55 ± 1.12	61.08 ± 2.37	63.16 ± 5.53
$\epsilon_{\geq 2}$ (%)	0.00 ± 0.00	1.80 ± 0.10	11.86 ± 0.73	15.09 ± 1.74	21.05 ± 4.68
$\epsilon_{\geq 1} * \Phi_e$ (%)	35.93 ± 2.41	42.98 ± 2.79	54.15 ± 3.17	56.82 ± 3.68	58.92 ± 5.98
$\epsilon_{\geq 2} * \Phi_e(\%)$	0.00 ± 0.00	1.49 ± 0.22	9.81 ± 1.44	12.49 ± 2.20	17.49 ± 4.51
$\epsilon_{bjet}(\%)$				44.90 ± 0.80	
$\epsilon_{cjet}(\%)$				11.61 ± 2.57	
$\epsilon_{bjet} * SF(\%)$				40.81 ± 2.79	
$\epsilon_{cjet} * SF(\%)$				10.55 ± 2.72	
$\epsilon_{\geq 1}(\%)$				59.13 ± 0.99	
$\epsilon_{\geq 2}(\%)$				12.71 ± 0.67	
$\Phi_E^1(\%)$				92.65 ± 5.03	
$\Phi_E^2(\%)$				82.75 ± 11.01	
$\epsilon_{\geq 1}(\%) * \Phi_E^1$				54.78 ± 3.11	
$\epsilon_{\geq 2}(\%) * \Phi_E^2$				10.52 ± 1.51	
CEM					
ϵ_{Pretag}	4.37 ± 0.05	4.47 ± 0.05	0.50 ± 0.01	0.10 ± 0.01	0.02 ± 0.00
$\epsilon_{Pretag} * SF$	3.99 ± 0.30	4.08 ± 0.31	0.45 ± 0.04	0.09 ± 0.01	0.02 ± 0.00
ϵ_{pretag}				0.62 ± 0.01	
$\epsilon_{pretag} * SF$				0.57 ± 0.05	
Pretag	8.38 ± 3.48	8.57 ± 3.56	0.96 ± 0.40	0.20 ± 0.08	0.04 ± 0.01
$\geq$ 1+ Tag	3.01 ± 1.27	3.68 ± 1.55	0.52 ± 0.22	0.11 ± 0.05	0.02 ± 0.01
$\geq$ 2+ Tag	0.00 ± 0.00	0.13 ± 0.06	0.09 ± 0.04	0.02 ± 0.01	0.01 ± 0.00
CMUP					
ϵ_{Pretag}	2.56 ± 0.04	2.67 ± 0.04	0.29 ± 0.01	0.07 ± 0.01	0.01 ± 0.00
$\epsilon_{Pretag} * SF$	1.93 ± 0.15	2.02 ± 0.15	0.22 ± 0.02	0.05 ± 0.01	0.01 ± 0.00
ϵ_{pretag}				0.36 ± 0.01	
$\epsilon_{pretag} * SF$				0.27 ± 0.02	
Pretag	4.06 ± 1.69	4.24 ± 1.76	0.46 ± 0.19	0.11 ± 0.05	0.01 ± 0.01
$\geq$ 1+ Tag	1.46 ± 0.61	1.82 ± 0.77	0.25 ± 0.11	0.06 ± 0.03	0.01 ± 0.00
$\geq$ 2+ Tag	0.00 ± 0.00	0.06 ± 0.03	0.05 ± 0.02	0.01 ± 0.01	0.00 ± 0.00
CMX					
ϵ_{Pretag}	0.94 ± 0.02	0.89 ± 0.02	0.10 ± 0.01	0.02 ± 0.00	0.00 ± 0.00
$\epsilon_{Pretag} * SF$	0.85 ± 0.07	0.81 ± 0.06	0.09 ± 0.01	0.02 ± 0.00	0.00 ± 0.00
ϵ_{pretag}				0.13 ± 0.01	
$\epsilon_{pretag} * SF$				0.12 ± 0.01	
Pretag	1.71 ± 0.71	1.63 ± 0.68	0.19 ± 0.08	0.04 ± 0.02	0.00 ± 0.00
$\geq$ 1+ Tag	0.62 ± 0.26	0.70 ± 0.30	0.10 ± 0.04	0.02 ± 0.01	0.00 ± 0.00
$\geq$ 2+ Tag	0.00 ± 0.00	0.02 ± 0.01	0.02 ± 0.01	0.01 ± 0.00	0.00 ± 0.00
Total					
Pretag	14.15 ± 4.05	14.44 ± 4.15	1.61 ± 0.46	0.36 ± 0.10	0.05 ± 0.02
$\geq$ 1 Tag	5.08 ± 1.50	6.21 ± 1.83	0.87 ± 0.26	0.20 ± 0.06	0.03 ± 0.01
$\geq$ 2 Tag	0.00 ± 0.00	0.21 ± 0.07	0.16 ± 0.05	0.04 ± 0.02	0.01 ± 0.00

Table 39: Summary table for single top (t-channel). See Table 33 for a description of the variables.

Single top, s-channel					
	1 jet	2 jets	3 jets	4 jets	$\geq$ 5 jets
$\epsilon_{b-jet}(\%)$	44.69 ± 0.47	44.34 ± 0.24	45.96 ± 0.66	42.96 ± 1.47	38.54 ± 3.40
$\epsilon_{c-jet}(\%)$	0.00 ± 0.00	4.91 ± 1.69	11.81 ± 2.86	0.00 ± 0.00	0.00 ± 0.00
$\epsilon_{b-jet} * SF(\%)$	40.62 ± 2.72	40.31 ± 2.67	41.78 ± 2.82	39.05 ± 2.90	35.03 ± 3.86
$\epsilon_{c-jet} * SF(\%)$	0.00 ± 0.00	4.46 ± 1.65	10.74 ± 2.96	0.00 ± 0.00	0.00 ± 0.00
$\Phi_e^{\geq 1}(\%)$	90.90 ± 6.02	93.07 ± 4.73	93.21 ± 4.70	93.23 ± 4.74	93.40 ± 4.86
$\Phi_e^{\geq 2}(\%)$	0.00 ± 0.00	82.63 ± 10.95	82.76 ± 10.92	82.91 ± 10.89	83.39 ± 10.70
$\epsilon_{\geq 1}(\%)$	42.62 ± 0.46	64.85 ± 0.32	68.30 ± 0.85	66.72 ± 1.96	61.39 ± 4.84
$\epsilon_{\geq 2}$ (%)	0.00 ± 0.00	18.11 ± 0.26	21.56 ± 0.75	17.59 ± 1.58	18.81 ± 3.89
$\epsilon_{\geq 1} * \Phi_e$ (%)	38.74 ± 2.60	60.36 ± 3.08	63.66 ± 3.31	62.20 ± 3.65	57.34 ± 5.42
$\epsilon_{\geq 2} * \Phi_e(\%)$	0.00 ± 0.00	14.96 ± 1.99	17.84 ± 2.43	14.58 ± 2.32	15.69 ± 3.82
$\epsilon_{bjet}(\%)$				45.27 ± 0.59	
$\epsilon_{cjet}(\%)$				7.85 ± 1.95	
$\epsilon_{bjet} * SF(\%)$				41.15 ± 2.77	
$\epsilon_{cjet} * SF(\%)$				7.14 ± 2.01	
$\epsilon_{\geq 1}(\%)$				67.86 ± 0.77	
$\epsilon_{\geq 2}(\%)$				20.85 ± 0.67	
$\Phi_E^1(\%)$				93.22 ± 4.72	
$\Phi_E^2(\%)$				82.82 ± 10.91	
$\epsilon_{\geq 1}(\%) * \Phi_E^1$				63.26 ± 3.28	
$\epsilon_{\geq 2}(\%) * \Phi_E^2$				17.27 ± 2.34	
CEM					
ϵ_{Pretag}	3.02 ± 0.04	5.93 ± 0.06	0.80 ± 0.02	0.16 ± 0.01	0.03 ± 0.00
$\epsilon_{Pretag} * SF$	2.76 ± 0.21	5.41 ± 0.41	0.73 ± 0.06	0.14 ± 0.01	0.03 ± 0.00
ϵ_{pretag}				0.99 ± 0.02	
$\epsilon_{pretag} * SF$				0.90 ± 0.07	
Pretag	2.57 ± 0.29	5.05 ± 0.56	0.68 ± 0.08	0.13 ± 0.02	0.03 ± 0.00
$\geq$ 1+ Tag	1.00 ± 0.13	3.05 ± 0.37	0.44 ± 0.06	0.08 ± 0.01	0.01 ± 0.00
$\geq$ 2+ Tag	0.00 ± 0.00	0.76 ± 0.13	0.12 ± 0.02	0.02 ± 0.00	0.00 ± 0.00
CMUP					
ϵ_{Pretag}	1.71 ± 0.03	3.46 ± 0.04	0.47 ± 0.01	0.09 ± 0.01	0.01 ± 0.00
$\epsilon_{Pretag} * SF$	1.29 ± 0.10	2.61 ± 0.20	0.35 ± 0.03	0.07 ± 0.01	0.01 ± 0.00
ϵ_{pretag}				0.58 ± 0.01	
$\epsilon_{pretag} * SF$				0.44 ± 0.04	
Pretag	1.20 ± 0.14	2.44 ± 0.27	0.33 ± 0.04	0.06 ± 0.01	0.01 ± 0.00
$\geq$ 1+ Tag	0.47 ± 0.06	1.47 ± 0.18	0.21 ± 0.03	0.04 ± 0.01	0.00 ± 0.00
$\geq$ 2+ Tag	0.00 ± 0.00	0.37 ± 0.06	0.06 ± 0.01	0.01 ± 0.00	0.00 ± 0.00
CMX					
ϵ_{Pretag}	0.63 ± 0.02	1.18 ± 0.03	0.15 ± 0.01	0.03 ± 0.00	0.01 ± 0.00
$\epsilon_{Pretag} * SF$	0.57 ± 0.05	1.07 ± 0.08	0.13 ± 0.01	0.03 ± 0.00	0.01 ± 0.00
ϵ_{pretag}				0.19 ± 0.01	
$\epsilon_{pretag} * SF$				0.17 ± 0.01	
Pretag	0.51 ± 0.06	0.96 ± 0.11	0.12 ± 0.01	0.03 ± 0.00	0.01 ± 0.00
$\geq$ 1+ Tag	0.20 ± 0.03	0.58 ± 0.07	0.08 ± 0.01	0.02 ± 0.00	0.00 ± 0.00
$\geq$ 2+ Tag	0.00 ± 0.00	0.14 ± 0.03	0.02 ± 0.00	0.00 ± 0.00	0.00 ± 0.00
Total					
Pretag	4.29 ± 0.44	8.45 ± 0.86	1.13 ± 0.12	0.23 ± 0.03	0.04 ± 0.00
$\geq$ 1 Tag	1.66 ± 0.20	5.10 ± 0.58	0.72 ± 0.08	0.14 ± 0.02	0.02 ± 0.00
$\geq$ 2 Tag	0.00 ± 0.00	1.26 ± 0.21	0.20 ± 0.03	0.03 ± 0.01	0.01 ± 0.00

Table 40: Summary table for single top (s-channel). See Table 33 for a description of the variables.

W + LF Mistags					
	1 jet	2 jets	3 jets	4 jets	$\geq$ 5 jets
CEM					
(+) Pred	257.35 ± 4.40	99.18 ± 0.78	16.56 ± 0.63	10.05 ± 0.09	2.33 ± 0.04
(-) Pred	64.18 ± 4.25	31.38 ± 0.73	7.00 ± 0.62	4.20 ± 0.06	0.94 ± 0.02
(+,-) Pred	0.00 ± 0.00	0.91 ± 0.13	1.07 ± 0.04	1.04 ± 0.05	0.35 ± 0.03
(-,-) Pred	0.00 ± 0.00	0.00 ± 0.00	0.00 ± 0.00	0.00 ± 0.00	0.00 ± 0.00
CMUP					
(+) Pred	118.56 ± 2.16	42.42 ± 0.59	6.30 ± 0.08	4.12 ± 0.05	1.42 ± 0.03
(-) Pred	28.86 ± 2.08	12.67 ± 0.55	2.52 ± 0.06	1.81 ± 0.04	0.62 ± 0.02
(+,-) Pred	0.00 ± 0.00	0.36 ± 0.07	0.24 ± 0.02	0.87 ± 0.06	0.26 ± 0.03
(-,-) Pred	0.00 ± 0.00	0.00 ± 0.00	0.00 ± 0.00	0.00 ± 0.00	0.00 ± 0.00
CMX					
(+) Pred	64.45 ± 1.53	23.10 ± 0.28	3.20 ± 0.10	1.68 ± 0.02	0.76 ± 0.03
(-) Pred	14.92 ± 1.47	6.79 ± 0.26	1.32 ± 0.09	0.57 ± 0.01	0.32 ± 0.02
(+,-) Pred	0.00 ± 0.00	0.17 ± 0.02	0.20 ± 0.02	0.16 ± 0.02	0.13 ± 0.02
(-,-) Pred	0.00 ± 0.00	0.00 ± 0.00	0.00 ± 0.00	0.00 ± 0.00	0.00 ± 0.00
Total					
(+) Pred	440.36 ± 5.13	164.69 ± 1.02	26.06 ± 0.64	15.85 ± 0.10	4.51 ± 0.06
(-) Pred	107.95 ± 4.95	50.84 ± 0.94	10.84 ± 0.63	6.59 ± 0.07	1.87 ± 0.04
(+,-) Pred	0.00 ± 0.00	1.45 ± 0.15	1.50 ± 0.05	2.07 ± 0.08	0.74 ± 0.05
(-,-) Pred	0.00 ± 0.00	0.00 ± 0.00	0.00 ± 0.00	0.00 ± 0.00	0.00 ± 0.00
CEM					
Pretag	17448.00 ± 0.00	2780.00 ± 0.00	197.00 ± 0.00	95.00 ± 0.00	18.00 ± 0.00
$\geq$ 1+ Tag	53.89 ± 11.35	22.77 ± 4.58	3.73 ± 0.82	1.43 ± 0.29	0.06 ± 0.01
$\geq$ 2+ Tag	0.00 ± 0.00	0.30 ± 0.07	0.14 ± 0.03	0.06 ± 0.01	-0.06 ± 0.01
CMUP					
Pretag	8383.00 ± 0.00	1219.00 ± 0.00	86.00 ± 0.00	34.00 ± 0.00	10.00 ± 0.00
$\geq$ 1+ Tag	25.38 ± 5.39	9.80 ± 2.00	1.28 ± 0.26	0.32 ± 0.06	0.09 ± 0.02
$\geq$ 2+ Tag	0.00 ± 0.00	0.11 ± 0.03	-0.06 ± 0.01	0.11 ± 0.02	0.05 ± 0.01
CMX					
Pretag	4452.00 ± 0.00	677.00 ± 0.00	41.00 ± 0.00	13.00 ± 0.00	6.00 ± 0.00
$\geq$ 1+ Tag	13.81 ± 3.08	5.66 ± 1.15	0.78 ± 0.16	0.11 ± 0.02	0.13 ± 0.03
$\geq$ 2+ Tag	0.00 ± 0.00	0.07 ± 0.02	0.02 ± 0.00	-0.00 ± 0.00	0.07 ± 0.02
Total					
Pretag	30283.00 ± 0.00	4676.00 ± 0.00	324.00 ± 0.00	142.00 ± 0.00	34.00 ± 0.00
$\geq$ 1 Tag	93.08 ± 19.09	38.23 ± 7.68	5.80 ± 1.21	1.86 ± 0.37	0.28 ± 0.06
$\geq$ 2 Tag	0.00 ± 0.00	0.48 ± 0.11	0.10 ± 0.04	0.17 ± 0.04	0.05 ± 0.04

Table 41: Summary table for mistag background. N_{+}^{pred} is the positive tag matrix prediction over the pretag data, N_{-}^{pred} is the negative tag matrix prediction over the pretag data, $N_{+,-}^{pred}$ is the positive tag matrix prediction over the $\geq$ 1 tag data, $N_{-,-}^{pred}$ is the negative tag matrix prediction over the $\geq$ 1 negative data, and the results are given corrected for other backgrounds and the light flavor asymmetry.

$W + c$					
	1 jet	2 jets	3 jets	4 jets	≥ 5 jets
$\epsilon_{b-jet}(\%)$	28.57 $\pm$ 12.07	20.00 $\pm$ 6.32	35.71 $\pm$ 12.81	66.67 $\pm$ 27.22	0.00 $\pm$ 0.00
$\epsilon_{c-jet}(\%)$	9.56 $\pm$ 0.33	9.50 $\pm$ 0.50	9.43 $\pm$ 1.26	12.89 $\pm$ 1.98	10.29 $\pm$ 3.69
$\epsilon_{b-jet} * SF(\%)$	25.97 $\pm$ 11.10	18.18 $\pm$ 5.87	32.46 $\pm$ 11.84	60.60 $\pm$ 25.06	0.00 $\pm$ 0.00
$\epsilon_{c-jet} * SF(\%)$	8.69 $\pm$ 1.19	8.64 $\pm$ 1.23	8.57 $\pm$ 1.61	11.72 $\pm$ 2.37	9.35 $\pm$ 3.57
F_{1c} (%)	4.30 $\pm$ 0.90	6.00 $\pm$ 1.30	6.00 $\pm$ 1.30	5.90 $\pm$ 1.30	5.90 $\pm$ 1.30
F_{2c} (%)	0.00 $\pm$ 0.00	0.00 $\pm$ 0.00	0.00 $\pm$ 0.00	0.00 $\pm$ 0.00	0.00 $\pm$ 0.00
WCC, 1C, 1 Tag (%)	8.19 $\pm$ 1.10	8.86 $\pm$ 1.23	10.94 $\pm$ 2.10	14.37 $\pm$ 2.95	8.26 $\pm$ 4.08
WCC, 2C, 1 Tag (%)	0.00 $\pm$ 0.00	0.00 $\pm$ 0.00	0.00 $\pm$ 0.00	21.39 $\pm$ 7.19	33.05 $\pm$ 13.88
WCC, 2C, 2 Tag (%)	0.00 $\pm$ 0.00	0.00 $\pm$ 0.00	0.00 $\pm$ 0.00	0.00 $\pm$ 0.00	0.00 $\pm$ 0.00
$\Phi_e^{\geq 1}(\%)$	90.90 $\pm$ 12.00	90.90 $\pm$ 12.00	90.90 $\pm$ 12.00	90.90 $\pm$ 12.00	90.90 $\pm$ 12.00
$\Phi_e^{\geq 2}(\%)$	0.00 $\pm$ 0.00	0.00 $\pm$ 0.00	0.00 $\pm$ 0.00	0.00 $\pm$ 0.00	0.00 $\pm$ 0.00
$\epsilon_{\geq 1}(\%)$	0.00 $\pm$ 0.00	0.00 $\pm$ 0.00	0.00 $\pm$ 0.00	0.00 $\pm$ 0.00	0.00 $\pm$ 0.00
$\epsilon_{\geq 2}$ (%)	0.00 $\pm$ 0.00	0.00 $\pm$ 0.00	0.00 $\pm$ 0.00	0.00 $\pm$ 0.00	0.00 $\pm$ 0.00
$\epsilon_{\geq 1} * \Phi_e$ (%)	0.35 $\pm$ 0.09	0.51 $\pm$ 0.13	0.61 $\pm$ 0.15	0.78 $\pm$ 0.20	0.43 $\pm$ 0.11
$\epsilon_{\geq 2} * \Phi_e(\%)$	0.00 $\pm$ 0.00	0.00 $\pm$ 0.00	0.00 $\pm$ 0.00	0.00 $\pm$ 0.00	0.00 $\pm$ 0.00
$\epsilon_{bjet}(\%)$			0.00 $\pm$ 0.00		
$\epsilon_{cjet}(\%)$			0.00 $\pm$ 0.00		
$\epsilon_{bjet} * SF(\%)$			0.00 $\pm$ 0.00		
$\epsilon_{cjet} * SF(\%)$			0.00 $\pm$ 0.00		
$\epsilon_{\geq 1}(\%)$			0.00 $\pm$ 0.00		
$\epsilon_{\geq 2}(\%)$			0.00 $\pm$ 0.00		
$\Phi_E^1(\%)$			100.00 $\pm$ 0.00		
$\Phi_E^2(\%)$			100.00 $\pm$ 0.00		
$\epsilon_{\geq 1}(\%) * \Phi_E^1$			100.00 $\pm$ 0.00		
$\epsilon_{\geq 2}(\%) * \Phi_E^2$			100.00 $\pm$ 0.00		
CEM					
Pretag	676.67 $\pm$ 159.34	139.08 $\pm$ 35.90	7.63 $\pm$ 2.20	2.33 $\pm$ 0.89	0.09 $\pm$ 0.13
$\geq$ 1+ Tag	55.42 $\pm$ 15.16	11.89 $\pm$ 3.51	0.78 $\pm$ 0.25	0.31 $\pm$ 0.13	0.01 $\pm$ 0.01
$\geq$ 2+ Tag	0.00 $\pm$ 0.00	0.00 $\pm$ 0.00	0.00 $\pm$ 0.00	0.00 $\pm$ 0.00	0.00 $\pm$ 0.00
CMUP					
Pretag	340.53 $\pm$ 75.91	65.01 $\pm$ 15.53	3.18 $\pm$ 0.92	0.43 $\pm$ 0.26	0.10 $\pm$ 0.08
$\geq$ 1+ Tag	27.89 $\pm$ 7.28	5.56 $\pm$ 1.53	0.32 $\pm$ 0.11	0.06 $\pm$ 0.04	0.01 $\pm$ 0.01
$\geq$ 2+ Tag	0.00 $\pm$ 0.00	0.00 $\pm$ 0.00	0.00 $\pm$ 0.00	0.00 $\pm$ 0.00	0.00 $\pm$ 0.00
CMX					
Pretag	190.39 $\pm$ 39.95	38.94 $\pm$ 8.59	1.76 $\pm$ 0.45	0.18 $\pm$ 0.10	0.17 $\pm$ 0.06
$\geq$ 1+ Tag	15.59 $\pm$ 3.87	3.33 $\pm$ 0.86	0.18 $\pm$ 0.05	0.02 $\pm$ 0.01	0.01 $\pm$ 0.00
$\geq$ 2+ Tag	0.00 $\pm$ 0.00	0.00 $\pm$ 0.00	0.00 $\pm$ 0.00	0.00 $\pm$ 0.00	0.00 $\pm$ 0.00
Total					
Pretag	1207.59 $\pm$ 275.18	243.04 $\pm$ 60.01	12.57 $\pm$ 3.56	2.94 $\pm$ 1.25	0.37 $\pm$ 0.25
$\geq$ 1 Tag	98.90 $\pm$ 26.31	20.78 $\pm$ 5.90	1.28 $\pm$ 0.41	0.39 $\pm$ 0.18	0.03 $\pm$ 0.02
$\geq$ 2 Tag	0.00 $\pm$ 0.00	0.00 $\pm$ 0.00	0.00 $\pm$ 0.00	0.00 $\pm$ 0.00	0.00 $\pm$ 0.00

Table 42: Summary table for the W+C background. F_{ic} is the heavy flavor fraction measured from [10], and the efficiencies given are the event tag rates in Monte Carlo. Φ_E is the ratio of event efficiencies with and without the b-tagging scale factor using the full binomial expression.

$W + c\bar{c}$					
	1 jet	2 jets	3 jets	4 jets	$\geq$ 5 jets
$\epsilon_{b-jet}(\%)$	50.00 ± 35.36	0.00 ± 0.00	33.33 ± 27.22	0.00 ± 0.00	0.00 ± 0.00
$\epsilon_{c-jet}(\%)$	8.94 ± 0.77	10.04 ± 1.03	13.33 ± 3.58	13.25 ± 2.63	4.00 ± 2.77
$\epsilon_{b-jet} * SF(\%)$	45.45 ± 32.28	0.00 ± 0.00	30.30 ± 24.82	0.00 ± 0.00	0.00 ± 0.00
$\epsilon_{c-jet} * SF(\%)$	8.13 ± 1.28	9.13 ± 1.53	12.12 ± 3.63	12.04 ± 2.87	3.64 ± 2.56
F_{1c} (%)	1.60 ± 0.40	2.40 ± 0.60	3.80 ± 1.00	3.50 ± 1.00	3.50 ± 1.00
F_{2c} (%)	0.00 ± 0.00	1.80 ± 0.50	2.90 ± 0.80	3.70 ± 1.00	3.70 ± 1.00
WCC, 1C, 1 Tag (%)	7.40 ± 1.03	8.91 ± 1.38	13.63 ± 2.79	15.22 ± 5.99	0.00 ± 0.00
WCC, 2C, 1 Tag (%)	0.00 ± 0.00	15.44 ± 2.39	18.71 ± 4.65	26.30 ± 6.33	8.67 ± 5.94
WCC, 2C, 2 Tag (%)	0.00 ± 0.00	0.33 ± 0.18	0.15 ± 0.15	0.00 ± 0.00	0.00 ± 0.00
$\Phi_e^{\geq 1}(\%)$	90.90 ± 12.00	91.15 ± 11.71	91.20 ± 11.64	91.29 ± 11.54	91.07 ± 11.80
$\Phi_e^{\geq 2}(\%)$	0.00 ± 0.00	82.63 ± 21.82	82.63 ± 21.82	0.00 ± 0.00	0.00 ± 0.00
$\epsilon_{\geq 1}(\%)$	0.00 ± 0.00	0.00 ± 0.00	0.00 ± 0.00	0.00 ± 0.00	0.00 ± 0.00
$\epsilon_{\geq 2}$ (%)	0.00 ± 0.00	0.00 ± 0.00	0.00 ± 0.00	0.00 ± 0.00	0.00 ± 0.00
$\epsilon_{\geq 1} * \Phi_e$ (%)	0.12 ± 0.03	0.49 ± 0.15	1.06 ± 0.32	1.44 ± 0.44	0.32 ± 0.10
$\epsilon_{\geq 2} * \Phi_e(\%)$	0.00 ± 0.00	0.01 ± 0.00	0.00 ± 0.00	0.00 ± 0.00	0.00 ± 0.00
$\epsilon_{bjet}(\%)$				0.00 ± 0.00	
$\epsilon_{cjet}(\%)$				0.00 ± 0.00	
$\epsilon_{bjet} * SF(\%)$				0.00 ± 0.00	
$\epsilon_{cjet} * SF(\%)$				0.00 ± 0.00	
$\epsilon_{\geq 1}(\%)$				0.00 ± 0.00	
$\epsilon_{\geq 2}(\%)$				0.00 ± 0.00	
$\Phi_E^1(\%)$				100.00 ± 0.00	
$\Phi_E^2(\%)$				100.00 ± 0.00	
$\epsilon_{\geq 1}(\%) * \Phi_E^1$				100.00 ± 0.00	
$\epsilon_{\geq 2}(\%) * \Phi_E^2$				100.00 ± 0.00	
CEM					
Pretag	251.78 ± 69.54	97.36 ± 29.53	8.52 ± 2.90	2.84 ± 1.25	0.11 ± 0.16
$\geq$ 1+ Tag	18.63 ± 5.75	11.40 ± 3.84	1.35 ± 0.50	0.57 ± 0.27	0.00 ± 0.01
$\geq$ 2+ Tag	0.00 ± 0.00	0.14 ± 0.06	0.01 ± 0.00	0.00 ± 0.00	0.00 ± 0.00
CMUP					
Pretag	126.71 ± 33.40	45.51 ± 12.93	3.55 ± 1.21	0.53 ± 0.35	0.13 ± 0.10
$\geq$ 1+ Tag	9.38 ± 2.78	5.33 ± 1.69	0.56 ± 0.21	0.11 ± 0.07	0.01 ± 0.00
$\geq$ 2+ Tag	0.00 ± 0.00	0.06 ± 0.03	0.00 ± 0.00	0.00 ± 0.00	0.00 ± 0.00
CMX					
Pretag	70.84 ± 17.75	27.26 ± 7.25	1.97 ± 0.60	0.22 ± 0.13	0.21 ± 0.08
$\geq$ 1+ Tag	5.24 ± 1.48	3.19 ± 0.96	0.31 ± 0.10	0.04 ± 0.03	0.01 ± 0.00
$\geq$ 2+ Tag	0.00 ± 0.00	0.04 ± 0.01	0.00 ± 0.00	0.00 ± 0.00	0.00 ± 0.00
Total					
Pretag	449.33 ± 120.68	170.13 ± 49.70	14.04 ± 4.71	3.58 ± 1.73	0.45 ± 0.34
$\geq$ 1 Tag	33.25 ± 10.02	19.92 ± 6.49	2.22 ± 0.81	0.72 ± 0.36	0.02 ± 0.02
$\geq$ 2 Tag	0.00 ± 0.00	0.24 ± 0.10	0.01 ± 0.00	0.00 ± 0.00	0.00 ± 0.00

Table 43: Summary table for the W+CC background. F_{ic} is the heavy flavor fraction measured from [10], and the efficiencies given are the event tag rates in Monte Carlo. Φ_E is the ratio of event efficiencies with and without the b-tagging scale factor using the full binomial expression.

$W + \mathrm{bb}$					
	1 jet	2 jets	3 jets	4 jets	$\geq$ 5 jets
$\epsilon_{b-jet}(\%)$	37.19 ± 0.56	40.58 ± 0.64	41.26 ± 1.10	43.17 ± 1.46	40.19 ± 2.88
$\epsilon_{c-jet}(\%)$	5.61 ± 3.16	0.00 ± 0.00	7.35 ± 3.16	6.17 ± 2.70	11.89 ± 5.62
$\epsilon_{b-jet} * SF(\%)$	33.81 ± 2.29	36.89 ± 2.50	37.50 ± 2.67	39.24 ± 2.91	36.53 ± 3.56
$\epsilon_{c-jet} * SF(\%)$	5.10 ± 2.95	0.00 ± 0.00	6.68 ± 3.01	5.61 ± 2.57	10.81 ± 5.31
$F_{1b}(\%)$	1.00 ± 0.30	1.40 ± 0.40	2.40 ± 0.60	2.20 ± 0.60	2.20 ± 0.60
$F_{2b}(\%)$	0.00 ± 0.00	1.40 ± 0.40	2.30 ± 0.60	2.60 ± 0.70	2.60 ± 0.70
WBB, 1B, 1 Tag (%)	34.94 ± 2.35	38.07 ± 2.34	45.77 ± 4.50	43.58 ± 3.65	40.54 ± 7.39
WBB, 2B, 1 Tag (%)	0.00 ± 0.00	57.90 ± 3.51	62.78 ± 4.82	62.23 ± 4.06	62.13 ± 5.22
WBB, 2B, 2 Tag (%)	0.00 ± 0.00	14.12 ± 1.93	18.17 ± 2.80	18.24 ± 3.02	15.06 ± 3.60
$\Phi_e^{\geq 1}(\%)$	90.90 ± 6.00	92.17 ± 5.25	92.12 ± 5.27	92.33 ± 5.15	92.24 ± 5.20
$\Phi_e^{\geq 2}(\%)$	0.00 ± 0.00	82.63 ± 10.91	82.79 ± 11.07	83.16 ± 11.43	83.52 ± 11.83
$\epsilon_{\geq 1}(\%)$	0.00 ± 0.00	0.00 ± 0.00	0.00 ± 0.00	0.00 ± 0.00	0.00 ± 0.00
$\epsilon_{\geq 2}$ (%)	0.00 ± 0.00	0.00 ± 0.00	0.00 ± 0.00	0.00 ± 0.00	0.00 ± 0.00
$\epsilon_{\geq 1} * \Phi_e$ (%)	0.35 ± 0.11	1.34 ± 0.39	2.54 ± 0.67	2.57 ± 0.71	2.48 ± 0.69
$\epsilon_{\geq 2} * \Phi_e(\%)$	0.00 ± 0.00	0.20 ± 0.06	0.42 ± 0.12	0.47 ± 0.14	0.39 ± 0.12
$\epsilon_{bjet}(\%)$				0.00 ± 0.00	
$\epsilon_{cjet}(\%)$				0.00 ± 0.00	
$\epsilon_{bjet} * SF(\%)$				0.00 ± 0.00	
$\epsilon_{cjet} * SF(\%)$				0.00 ± 0.00	
$\epsilon_{\geq 1}(\%)$				0.00 ± 0.00	
$\epsilon_{\geq 2}(\%)$				0.00 ± 0.00	
$\Phi_E^1(\%)$				100.00 ± 0.00	
$\Phi_E^2(\%)$				100.00 ± 0.00	
$\epsilon_{\geq 1}(\%) * \Phi_E^1$				100.00 ± 0.00	
$\epsilon_{\geq 2}(\%) * \Phi_E^2$				100.00 ± 0.00	
CEM					
Pretag	157.36 ± 51.33	64.91 ± 21.23	5.98 ± 1.95	1.89 ± 0.82	0.07 ± 0.11
$\geq$ 1+ Tag	54.99 ± 18.33	31.12 ± 10.36	3.23 ± 1.08	1.01 ± 0.45	0.04 ± 0.06
$\geq$ 2+ Tag	0.00 ± 0.00	4.58 ± 1.63	0.53 ± 0.19	0.19 ± 0.09	0.01 ± 0.01
CMUP					
Pretag	79.19 ± 24.83	30.34 ± 9.34	2.49 ± 0.81	0.35 ± 0.23	0.08 ± 0.07
$\geq$ 1+ Tag	27.67 ± 8.88	14.55 ± 4.56	1.35 ± 0.45	0.19 ± 0.12	0.04 ± 0.03
$\geq$ 2+ Tag	0.00 ± 0.00	2.14 ± 0.72	0.22 ± 0.08	0.03 ± 0.02	0.01 ± 0.01
CMX					
Pretag	44.28 ± 13.31	18.17 ± 5.27	1.38 ± 0.40	0.15 ± 0.09	0.14 ± 0.05
$\geq$ 1+ Tag	15.47 ± 4.76	8.71 ± 2.57	0.75 ± 0.22	0.08 ± 0.05	0.07 ± 0.03
$\geq$ 2+ Tag	0.00 ± 0.00	1.28 ± 0.41	0.12 ± 0.04	0.01 ± 0.01	0.01 ± 0.00
Total					
Pretag	280.83 ± 89.47	113.42 ± 35.84	9.85 ± 3.17	2.39 ± 1.13	0.30 ± 0.22
$\geq$ 1 Tag	98.13 ± 31.97	54.39 ± 17.49	5.32 ± 1.75	1.28 ± 0.61	0.15 ± 0.12
$\geq$ 2 Tag	0.00 ± 0.00	8.01 ± 2.76	0.88 ± 0.32	0.24 ± 0.12	0.02 ± 0.02

Table 44: Summary table for the W+BB background. F_{ib} is the heavy flavor fraction measured from [10], and the efficiencies given are the event tag rates in Monte Carlo. Φ_E is the ratio of event efficiencies with and without the b-tagging scale factor using the full binomial expression.

Non-W : Raw Counts					
	1 jet	2 jets	3 jets	4 jets	$\geq$ 5 jets
Electrons					
N_A^{pre}	51191	5955	887	95	16
N_B^{pre}	35939	3317	396	54	10
N_C^{pre}	2290	605	38	17	3
N_D^{pre}	17443	2779	198	94	18
N_A^{+}	1477	320	74	13	2
N_B^{+}	585	110	32	9	1
N_C^{+}	115	52	11	3	2
N_D^{+}	246	136	40	34	8
N_A^{++}	0	10	2	1	0
N_B^{++}	0	1	4	3	0
N_C^{++}	0	1	2	1	0
N_D^{++}	0	9	10	6	1
F_{Non-W} (%)	9.22 $\pm$ 2.31	12.13 $\pm$ 3.09	8.62 $\pm$ 2.53		
N_+^B/N_+^A (%)	39.61 $\pm$ 1.93	34.38 $\pm$ 3.80	47.19 $\pm$ 8.83		
$N_+^{tagmethod}$	45.55 $\pm$ 15.78	17.88 $\pm$ 6.70	5.19 $\pm$ 2.52	1.42 $\pm$ 0.98	0.94 $\pm$ 0.76
R_+^B (%)	1.63 $\pm$ 0.33	3.32 $\pm$ 0.74	8.08 $\pm$ 2.19	16.67 $\pm$ 6.86	10.00 $\pm$ 10.68
$N_+^{pretagmethod}$	26.18 $\pm$ 8.47	11.18 $\pm$ 3.78	1.37 $\pm$ 0.55	1.37 $\pm$ 0.69	0.16 $\pm$ 0.17
R_{++}^B (%)	0.00 $\pm$ 0.00	0.03 $\pm$ 0.03	1.01 $\pm$ 0.55	5.56 $\pm$ 3.48	0.00 $\pm$ 0.00
$N_{++}^{pretagmethod}$	0.00 $\pm$ 0.00	0.10 $\pm$ 0.11	0.17 $\pm$ 0.11	0.46 $\pm$ 0.31	0.00 $\pm$ 0.00
Muons					
N_A^{pre}	15286	1977	285	41	11
N_B^{pre}	6223	532	67	8	2
N_C^{pre}	1009	266	18	7	6
N_D^{pre}	12831	1870	124	46	15
N_A^{+}	859	194	30	8	3
N_B^{+}	109	25	8	4	1
N_C^{+}	50	28	2	1	1
N_D^{+}	180	95	22	24	10
N_A^{++}	0	5	1	0	0
N_B^{++}	0	0	2	0	1
N_C^{++}	0	3	0	0	0
N_D^{++}	0	5	5	9	2
F_{Non-W} (%)	3.20 $\pm$ 0.81	3.83 $\pm$ 1.01	3.83 $\pm$ 1.30		
N_+^B/N_+^A (%)	12.69 $\pm$ 1.29	12.89 $\pm$ 2.74	31.71 $\pm$ 10.09		
$N_+^{tagmethod}$	6.34 $\pm$ 2.37	3.61 $\pm$ 1.57	0.63 $\pm$ 0.53	0.32 $\pm$ 0.35	0.32 $\pm$ 0.35
R_+^B (%)	1.75 $\pm$ 0.39	4.70 $\pm$ 1.34	11.94 $\pm$ 5.06	50.00 $\pm$ 32.21	50.00 $\pm$ 62.05
$N_+^{pretagmethod}$	7.20 $\pm$ 2.42	3.41 $\pm$ 1.33	0.58 $\pm$ 0.32	0.90 $\pm$ 0.66	0.31 $\pm$ 0.39
R_{++}^B (%)	0.00 $\pm$ 0.00	0.00 $\pm$ 0.00	2.99 $\pm$ 2.22	0.00 $\pm$ 0.00	50.00 $\pm$ 62.05
$N_{++}^{pretagmethod}$	0.00 $\pm$ 0.00	0.00 $\pm$ 0.00	0.15 $\pm$ 0.12	0.00 $\pm$ 0.00	0.31 $\pm$ 0.39
Electrons					
Pretag	1608.17 $\pm$ 403.78	337.11 $\pm$ 85.94	16.99 $\pm$ 4.99	8.19 $\pm$ 2.40	1.55 $\pm$ 0.46
$\geq$ 1+ Tag	30.51 $\pm$ 7.42	12.80 $\pm$ 3.26	1.55 $\pm$ 0.53	1.38 $\pm$ 0.55	0.19 $\pm$ 0.17
$\geq$ 2+ Tag	0.00 $\pm$ 0.00	0.10 $\pm$ 0.11	0.17 $\pm$ 0.11	0.46 $\pm$ 0.31	0.00 $\pm$ 0.00
Muons					
Pretag	410.90 $\pm$ 103.78	72.57 $\pm$ 19.09	4.86 $\pm$ 1.66	1.80 $\pm$ 0.61	0.61 $\pm$ 0.21
$\geq$ 1+ Tag	6.76 $\pm$ 1.67	3.49 $\pm$ 1.01	0.59 $\pm$ 0.27	0.45 $\pm$ 0.31	0.31 $\pm$ 0.26
$\geq$ 2+ Tag	0.00 $\pm$ 0.00	0.00 $\pm$ 0.00	0.15 $\pm$ 0.12	0.00 $\pm$ 0.00	0.31 $\pm$ 0.39

Table 45: Raw event counts for Non-W backgrounds.

$t\bar{t}$ (8.7 pb)					
	1 jet	2 jets	3 jets	4 jets	$\geq$ 5 jets
Electrons					
N_A^{pre}	0.03 $\pm$ 0.00	0.18 $\pm$ 0.02	0.51 $\pm$ 0.05	0.67 $\pm$ 0.06	0.62 $\pm$ 0.06
N_B^{pre}	0.27 $\pm$ 0.03	1.49 $\pm$ 0.14	3.51 $\pm$ 0.33	3.23 $\pm$ 0.31	1.12 $\pm$ 0.11
N_C^{pre}	0.85 $\pm$ 0.08	3.22 $\pm$ 0.31	3.64 $\pm$ 0.35	2.36 $\pm$ 0.22	1.17 $\pm$ 0.11
N_D^{pre}	5.19 $\pm$ 0.49	27.05 $\pm$ 2.58	45.60 $\pm$ 4.33	46.15 $\pm$ 4.39	14.65 $\pm$ 1.41
N_A^{+}	0.01 $\pm$ 0.00	0.08 $\pm$ 0.01	0.21 $\pm$ 0.02	0.27 $\pm$ 0.03	0.26 $\pm$ 0.03
N_B^{+}	0.09 $\pm$ 0.01	0.79 $\pm$ 0.09	2.00 $\pm$ 0.22	2.02 $\pm$ 0.22	0.70 $\pm$ 0.08
N_C^{+}	0.27 $\pm$ 0.03	1.40 $\pm$ 0.16	1.93 $\pm$ 0.21	1.32 $\pm$ 0.14	0.68 $\pm$ 0.07
N_D^{+}	1.74 $\pm$ 0.20	13.77 $\pm$ 1.53	26.60 $\pm$ 2.90	28.97 $\pm$ 3.12	9.26 $\pm$ 1.01
N_A^{++}	0.00 $\pm$ 0.00	0.01 $\pm$ 0.00	0.03 $\pm$ 0.01	0.03 $\pm$ 0.00	0.03 $\pm$ 0.01
N_B^{++}	0.00 $\pm$ 0.00	0.16 $\pm$ 0.03	0.49 $\pm$ 0.08	0.56 $\pm$ 0.09	0.21 $\pm$ 0.03
N_C^{++}	0.00 $\pm$ 0.00	0.12 $\pm$ 0.02	0.41 $\pm$ 0.07	0.32 $\pm$ 0.05	0.13 $\pm$ 0.02
N_D^{++}	0.00 $\pm$ 0.00	2.54 $\pm$ 0.43	6.33 $\pm$ 1.06	8.29 $\pm$ 1.37	2.79 $\pm$ 0.46
Muons					
N_A^{pre}	0.02 $\pm$ 0.00	0.17 $\pm$ 0.02	0.45 $\pm$ 0.04	0.63 $\pm$ 0.06	0.48 $\pm$ 0.05
N_B^{pre}	0.16 $\pm$ 0.02	1.19 $\pm$ 0.11	2.74 $\pm$ 0.26	2.73 $\pm$ 0.26	0.77 $\pm$ 0.07
N_C^{pre}	0.67 $\pm$ 0.06	2.61 $\pm$ 0.25	3.21 $\pm$ 0.30	2.31 $\pm$ 0.22	0.96 $\pm$ 0.09
N_D^{pre}	3.61 $\pm$ 0.34	20.08 $\pm$ 1.91	34.07 $\pm$ 3.24	33.33 $\pm$ 3.17	10.51 $\pm$ 1.02
N_A^{+}	0.01 $\pm$ 0.00	0.07 $\pm$ 0.01	0.21 $\pm$ 0.02	0.29 $\pm$ 0.03	0.22 $\pm$ 0.02
N_B^{+}	0.05 $\pm$ 0.01	0.59 $\pm$ 0.06	1.62 $\pm$ 0.18	1.67 $\pm$ 0.18	0.47 $\pm$ 0.05
N_C^{+}	0.22 $\pm$ 0.03	1.17 $\pm$ 0.13	1.78 $\pm$ 0.19	1.34 $\pm$ 0.14	0.58 $\pm$ 0.06
N_D^{+}	1.21 $\pm$ 0.14	10.22 $\pm$ 1.13	19.87 $\pm$ 2.17	20.92 $\pm$ 2.26	6.64 $\pm$ 0.73
N_A^{++}	0.00 $\pm$ 0.00	0.01 $\pm$ 0.00	0.04 $\pm$ 0.01	0.04 $\pm$ 0.01	0.02 $\pm$ 0.00
N_B^{++}	0.00 $\pm$ 0.00	0.11 $\pm$ 0.02	0.42 $\pm$ 0.07	0.50 $\pm$ 0.08	0.14 $\pm$ 0.02
N_C^{++}	0.00 $\pm$ 0.00	0.17 $\pm$ 0.03	0.40 $\pm$ 0.07	0.30 $\pm$ 0.05	0.15 $\pm$ 0.03
N_D^{++}	0.00 $\pm$ 0.00	1.88 $\pm$ 0.32	4.73 $\pm$ 0.79	5.99 $\pm$ 0.99	2.00 $\pm$ 0.33

Table 46: Expectation of $t\bar{t}$ in Non-W sideband regions.

Non-W					
	1 jet	2 jets	3 jets	4 jets	$\geq$ 5 jets
Electrons					
N_A^{pre}	51190.97 $\pm$ 226.25	5954.82 $\pm$ 77.17	886.49 $\pm$ 29.78	94.33 $\pm$ 9.75	15.38 $\pm$ 4.00
N_B^{pre}	35938.73 $\pm$ 189.58	3315.51 $\pm$ 57.59	392.49 $\pm$ 19.90	50.77 $\pm$ 7.35	8.88 $\pm$ 3.16
N_C^{pre}	2289.15 $\pm$ 47.85	601.78 $\pm$ 24.60	34.36 $\pm$ 6.17	14.64 $\pm$ 4.13	1.83 $\pm$ 1.74
N_D^{pre}	17443.00 $\pm$ 132.07	2779.00 $\pm$ 52.72	198.00 $\pm$ 14.07	94.00 $\pm$ 9.70	18.00 $\pm$ 4.24
N_A^{+}	1476.99 $\pm$ 38.43	319.92 $\pm$ 17.89	73.79 $\pm$ 8.60	12.73 $\pm$ 3.61	1.74 $\pm$ 1.41
N_B^{+}	584.91 $\pm$ 24.19	109.21 $\pm$ 10.49	30.00 $\pm$ 5.66	6.98 $\pm$ 3.01	0.30 $\pm$ 1.00
N_C^{+}	114.73 $\pm$ 10.72	50.60 $\pm$ 7.21	9.07 $\pm$ 3.32	1.68 $\pm$ 1.74	1.32 $\pm$ 1.42
N_D^{+}	244.26 $\pm$ 15.69	122.23 $\pm$ 11.76	13.40 $\pm$ 6.96	5.03 $\pm$ 6.61	-1.26 $\pm$ 3.00
N_A^{++}	0.00 $\pm$ 0.00	10.29 $\pm$ 3.52	2.47 $\pm$ 1.75	1.54 $\pm$ 1.19	0.62 $\pm$ 0.62
N_B^{++}	0.00 $\pm$ 0.00	1.41 $\pm$ 1.18	4.07 $\pm$ 2.22	2.75 $\pm$ 1.99	0.53 $\pm$ 0.53
N_C^{++}	0.00 $\pm$ 0.00	1.45 $\pm$ 1.18	2.17 $\pm$ 1.67	1.26 $\pm$ 1.18	0.58 $\pm$ 0.58
N_D^{++}	0.00 $\pm$ 0.00	7.03 $\pm$ 3.23	4.25 $\pm$ 3.22	0.73 $\pm$ 0.73	0.27 $\pm$ 0.27
F_{Non-W} (%)	9.21 $\pm$ 2.31	12.06 $\pm$ 3.08	7.44 $\pm$ 2.34		
N_+^B/N_+^A (%)	39.60 $\pm$ 1.93	34.14 $\pm$ 3.79	42.24 $\pm$ 8.64		
$N_+^{tagmethod}$	45.43 $\pm$ 15.75	17.27 $\pm$ 6.56	3.83 $\pm$ 2.13	0.71 $\pm$ 0.80	0.56 $\pm$ 0.65
R_+^B (%)	1.63 $\pm$ 0.33	3.29 $\pm$ 0.74	7.64 $\pm$ 2.17	13.75 $\pm$ 6.96	3.39 $\pm$ 11.42
$N_+^{pretagmethod}$	26.16 $\pm$ 8.47	11.04 $\pm$ 3.75	1.12 $\pm$ 0.48	0.97 $\pm$ 0.59	0.05 $\pm$ 0.15
R_{++}^B (%)	0.00 $\pm$ 0.00	0.04 $\pm$ 0.04	1.04 $\pm$ 0.60	5.43 $\pm$ 4.14	5.99 $\pm$ 6.49
$N_{++}^{pretagmethod}$	0.00 $\pm$ 0.00	0.14 $\pm$ 0.13	0.15 $\pm$ 0.10	0.38 $\pm$ 0.32	0.08 $\pm$ 0.09
Muons					
N_A^{pre}	15285.98 $\pm$ 123.64	1976.83 $\pm$ 44.46	284.55 $\pm$ 16.88	40.37 $\pm$ 6.40	10.52 $\pm$ 3.32
N_B^{pre}	6222.84 $\pm$ 78.89	530.81 $\pm$ 23.07	64.26 $\pm$ 8.19	5.27 $\pm$ 2.84	1.23 $\pm$ 1.42
N_C^{pre}	1008.33 $\pm$ 31.76	263.39 $\pm$ 16.31	14.79 $\pm$ 4.25	4.69 $\pm$ 2.65	5.04 $\pm$ 2.45
N_D^{pre}	12831.00 $\pm$ 113.27	1870.00 $\pm$ 43.24	124.00 $\pm$ 11.14	46.00 $\pm$ 6.78	15.00 $\pm$ 3.87
N_A^{+}	858.99 $\pm$ 29.31	193.93 $\pm$ 13.93	29.79 $\pm$ 5.48	7.71 $\pm$ 2.83	2.78 $\pm$ 1.73
N_B^{+}	108.95 $\pm$ 10.44	24.41 $\pm$ 5.00	6.38 $\pm$ 2.83	2.33 $\pm$ 2.01	0.53 $\pm$ 1.00
N_C^{+}	49.78 $\pm$ 7.07	26.83 $\pm$ 5.29	0.22 $\pm$ 1.43	-0.34 $\pm$ 1.01	0.42 $\pm$ 1.00
N_D^{+}	178.79 $\pm$ 13.42	84.78 $\pm$ 9.81	2.13 $\pm$ 5.17	3.08 $\pm$ 5.39	3.36 $\pm$ 3.24
N_A^{++}	0.00 $\pm$ 0.00	6.12 $\pm$ 2.52	2.17 $\pm$ 1.34	1.26 $\pm$ 0.89	1.27 $\pm$ 0.90
N_B^{++}	0.00 $\pm$ 0.00	1.23 $\pm$ 0.87	2.83 $\pm$ 1.79	1.02 $\pm$ 0.73	2.12 $\pm$ 1.32
N_C^{++}	0.00 $\pm$ 0.00	3.91 $\pm$ 2.11	1.08 $\pm$ 0.77	1.13 $\pm$ 0.80	1.20 $\pm$ 0.85
N_D^{++}	0.00 $\pm$ 0.00	4.33 $\pm$ 2.54	2.42 $\pm$ 1.84	4.56 $\pm$ 2.90	1.80 $\pm$ 1.47
F_{Non-W} (%)	3.20 $\pm$ 0.81	3.78 $\pm$ 1.00	2.80 $\pm$ 1.10		
N_+^B/N_+^A (%)	12.68 $\pm$ 1.29	12.59 $\pm$ 2.73	22.93 $\pm$ 9.71		
$N_+^{tagmethod}$	6.31 $\pm$ 2.36	3.38 $\pm$ 1.51	0.05 $\pm$ 0.33	-0.08 $\pm$ 0.24	0.10 $\pm$ 0.24
R_+^B (%)	1.75 $\pm$ 0.39	4.60 $\pm$ 1.34	9.92 $\pm$ 5.09	44.27 $\pm$ 45.90	42.95 $\pm$ 95.94
$N_+^{pretagmethod}$	7.19 $\pm$ 2.42	3.30 $\pm$ 1.30	0.35 $\pm$ 0.23	0.58 $\pm$ 0.65	0.19 $\pm$ 0.44
R_{++}^B (%)	0.00 $\pm$ 0.00	0.23 $\pm$ 0.17	4.40 $\pm$ 2.98	19.45 $\pm$ 18.00	172.44 $\pm$ 230.49
$N_{++}^{pretagmethod}$	0.00 $\pm$ 0.00	0.17 $\pm$ 0.13	0.16 $\pm$ 0.12	0.26 $\pm$ 0.26	0.77 $\pm$ 1.08
Electrons					
Pretag	1607.56 $\pm$ 403.69	335.18 $\pm$ 85.63	14.66 $\pm$ 4.61	7.07 $\pm$ 2.22	1.34 $\pm$ 0.42
$\geq$ 1+ Tag	30.49 $\pm$ 7.41	12.58 $\pm$ 3.23	1.25 $\pm$ 0.47	0.88 $\pm$ 0.46	0.07 $\pm$ 0.15
$\geq$ 2+ Tag	0.00 $\pm$ 0.00	0.14 $\pm$ 0.13	0.15 $\pm$ 0.10	0.38 $\pm$ 0.32	0.07 $\pm$ 0.09
Muons					
Pretag	410.61 $\pm$ 103.74	71.71 $\pm$ 18.95	3.55 $\pm$ 1.40	1.31 $\pm$ 0.52	0.45 $\pm$ 0.18
$\geq$ 1+ Tag	6.74 $\pm$ 1.66	3.33 $\pm$ 0.98	0.25 $\pm$ 0.17	0.00 $\pm$ 0.22	0.12 $\pm$ 0.21
$\geq$ 2+ Tag	0.00 $\pm$ 0.00	0.17 $\pm$ 0.13	0.16 $\pm$ 0.12	0.00 $\pm$ 0.26	0.12 $\pm$ 1.08

Table 47: Non-W expectation, removing $t\bar{t}$.

D Cross Check: $W \to l\nu$ Cross Section

As a cross-check to the $t\bar{t} \to Wl\nu b\bar{b}qq$ analysis, we calculate the $W \to l\nu X$ cross section in the ≥ 0 jet bins. We do this in a rough and approximate way in order to be sure there are no major problems.

We perform the analysis in two ways. First, we examine the effect of using the same background fractions as the Gen4 analysis outlined in Ref [12]. This is not strictly correct because the electron analysis had higher E_T and $\not{E}_T$ cuts than we do (they use 25 GeV for both, we use 20 for both).

Then, we calculate the backgrounds for our analysis cuts. The method we have used is to calculate the electroweak backgrounds using Monte Carlo predictions and scale factors, along with the theoretical cross sections. The Non-W backgrounds are estimated in the same $\not{E}_T$ vs iso method as the $t\bar{t}$ analysis.

The Monte Carlo samples used are $W \to l\nu$ (for electrons, muons, and taus) and $Z \to l^+l^-$ (for electrons and muons), all generated with PYTHIA. We then require the events to pass the event selection for the $t\bar{t}$ analysis, except that we examine ≥ 0 jets.

Our results are summarized in Table 48. We notice that the electron and muon results are not consistent with each other. This has been seen in the dilepton channel, and was attributed to a poor modelling of the track χ^2 probability of muons.

We have repeated the analysis using a cut on the COT χ^2 probability of $P < 1 \times 10^{-8}$. The results are outlined in Table 49. In this table, the ratio of cross sections for the electron and muon channels are consistent within statistical errors (the dominant systematic is the luminosity, which is correlated between the two measurements).

The effect on the $t\bar{t}$ cross section is lessened because of the optimization cuts. Most of the sample is $t\bar{t}$ anyway, so the effect of fake muons is smaller than the W cross section. Using this cut, the optimized cross sections change by 0.0 pb for the ≥ 1 tag, and +0.1 pb for ≥ 2 tags. The unoptimized cross sections change by -0.3 pb for the ≥ 1 tag, and +0.1 pb for ≥ 2 tags. The fit result changes by -0.2 pb.

We have not used this cut because the effect is small.

	CEM	CMUP	CMX
Pretag Efficiency	0.2328 ± 0.0000	0.1313 ± 0.0000	0.0586 ± 0.0000
Lepton ID SF	0.959 ± 0.015	0.794 ± 0.015	0.954 ± 0.016
Luminosity (pb^{-1})	318.5	318.5	305.2

	Electron	Muon
$\epsilon \int \mathcal{L}dt$	71.1 ± 4.4	51.4 ± 4.6
$N_{observed}$	198940	158498
Using Gen4 Background Fractions		
F_{BKG}, Gen4	0.045 ± 0.008	0.095 ± 0.005
Cross Section (pb)	2672 ± 6 (stat) ± 166 (sys)	2788 ± 7 (stat) ± 247 (sys)
Using Gen5 Background Fractions		
F_{Non-W}	0.029 ± 0.007	0.014 ± 0.003
$F_{Z\rightarrow l^+l^-}$	0.0030 ± 0.0002	0.038 ± 0.002
$F_{W\rightarrow\tau\nu}$	0.036 ± 0.002	0.029 ± 0.002
F_{BKG}, Gen5	0.068 ± 0.006	0.081 ± 0.011
Cross Section (pb)	2607 ± 6 (stat) ± 173 (sys)	2833 ± 7 (stat) ± 255 (sys)

Table 48: Summary for W cross section calculation, *without* additional χ^2 probability cut on muons.

	CEM	CMUP	CMX
Pretag Efficiency	0.2328 ± 0.0000	0.1313 ± 0.0000	0.0586 ± 0.0000
Lepton ID SF	0.959 ± 0.015	0.794 ± 0.015	0.954 ± 0.016
Muon χ^2 Prob SF	-	0.987 ± 0.013	0.987 ± 0.013
Luminosity (pb^{-1})	318.5	318.5	305.2

	Electron	Muon
$\epsilon \int \mathcal{L}dt$	71.1 ± 4.4	51.4 ± 4.6
$N_{observed}$	198940	143980
Using Gen4 Background Fractions		
F_{BKG}, Gen4	0.045 ± 0.008	0.095 ± 0.005
Cross Section (pb)	2672 ± 6 (stat) ± 166 (sys)	2566 ± 6 (stat) ± 234 (sys)
Using Gen5 Background Fractions		
F_{Non-W}	0.029 ± 0.007	0.012 ± 0.003
$F_{Z\rightarrow l^+l^-}$	0.0030 ± 0.0002	0.038 ± 0.002
$F_{W\rightarrow\tau\nu}$	0.036 ± 0.002	0.029 ± 0.002
F_{BKG}, Gen5	0.068 ± 0.006	0.081 ± 0.011
Cross Section (pb)	2607 ± 6 (stat) ± 173 (sys)	2596 ± 6 (stat) ± 242 (sys)

Table 49: Summary for W cross section calculation, *with* additional χ^2 probability cut on muons.

References

[1] A. Foland, M. Franklin, J. ao Guimarães da Costa, and S. Rappoccio, Method 2 Backgrounds For Top Pair Production in Lepton Plus Jets Events with ≥ 1 `SecVtx` Tags for Winter 2005, CDF Note 7486. 4, 6, 8, 14, 30

[2] J. ao Guimarães da Costa, S. Rappoccio, and D. Sherman, Measurement of the SecVtx Mistag Asymmetry in 5.3.3, CDF Note 7585. 6

[3] H. Bachacou *et al.*, Preliminary Background Estimate of the SECVTX-tagged Lepton + Jets Sample, CDF Note 7562. 8

[4] H. Bachacou *et al.*, Combining the SecVtx B-Tagging Scale Factors for 5.3.3 Analyses, CDF Note 7480. 13

[5] F. Canelli and A. Bhatti, Generic Jet Corrections for Run II, CDF Note 7358. 13

[6] R. Erbacher and Y. Ishizawa and B. Kilminster and K. Lannon and P. Lujan and T. Maki and B. Mohr and J. Nielsen and E. Palencia and S. Rappoccio and R. Rossin and M. Soderberg and V. Sorin and K. Yorita, Preliminary Event Selection and t-tbar Signal Acceptance for the Winter 2005 Top Lepton + Jets Sample, CDF Note 7372. 13

[7] Daniel Jeans, Offline track studies, CDF Note 7105. 13

[8] M. C. et al., THE T ANTI-T CROSS-SECTION AT 1.8-TEV AND 1.96-TEV: A STUDY OF THE SYSTEMATICS DUE TO PARTON DENSITIES AND SCALE DEPENDENCE., JHEP 0404:068 (2004). 15, 32

[9] H. Bachacou, J. Nielsen, and W. Yao, Optimized Measurement of the t-tbar Production Cross Section with SECVTX, CDF Note 6902. 15, 26

[10] H. Bachacou, C. Ferretti, J. Nielsen, and W. Yao, Heavy Flavor Contributions to the SECVTX-tagged W + Jets Sample, CDF Note 7007. 26, 41, 75, 76, 77

[11] H. Bachacou, J. Nielsen, and W. Yao, Optimized Measurement of the t-tbar Production Cross Section with SECVTX, CDF Note 6902. 32

[12] D. Amidei *et al.*, First Measurements of Inclusive W and Z Cross Sections from Run II of the Tevatron Collider, CDF Note 7014. 81